Lithos 262 (2016) 169–191

Contents lists available at ScienceDirect

Lithos

journal homepage: www.elsevier.com/locate/lithos

Synthesis paper

The role of changing geodynamics in the progressive contamination of Late Cretaceous to Late Miocene arc magmas in the southern Central Andes

Rosemary E. Jones [a,b,*], Linda A. Kirstein [a], Simone A. Kasemann [c], Vanesa D. Litvak [d], Stella Poma [e], Ricardo N. Alonso [f], Richard Hinton [a], EIMF [g]

[a] School of GeoSciences, University of Edinburgh, The King's Buildings, James Hutton Road, Edinburgh EH9 3FE, UK
[b] Department of Earth Sciences, University of Oxford, South Parks Road, Oxford OX1 3AN, UK
[c] Faculty of Geosciences & MARUM, Centre for Marine Environmental Sciences, University of Bremen, 28334 Bremen, Germany
[d] Universidad de Buenos Aires. CONICET. Instituto de Estudios Andinos Don Pablo Groeber (IDEAN). Facultad de Ciencias Exactas y Naturales. Buenos Aires, Argentina
[e] Universidad de Buenos Aires. CONICET. Instituto de Geociencias Básicas y Aplicadas de Buenos Aires (IGEBA). Facultad de Ciencias Exactas y Naturales. Buenos Aires, Argentina
[f] Departamento de Geología, Universidad Nacional de Salta, CONICET, 4400 Salta, Argentina
[g] Edinburgh Ion Microprobe Facility, School of GeoSciences, University of Edinburgh, West Mains Road, Edinburgh EH9 3JW, UK

ARTICLE INFO

Article history:
Received 4 April 2016
Accepted 1 July 2016
Available online 14 July 2016

Keywords:
Central Andes
Geochronology
Arc magma petrogenesis
Crustal contamination
Geodynamics

ABSTRACT

The tectonic and geodynamic setting of the southern Central Andean convergent margin changed significantly between the Late Cretaceous and the Late Miocene, influencing magmatic activity and its geochemical composition. Here we investigate how these changes, which include changing slab-dip angle and convergence angles and rates, have influenced the contamination of the arc magmas with crustal material. Whole rock geochemical data for a suite of Late Cretaceous to Late Miocene arc rocks from the Pampean flat-slab segment (29–31 °S) of the southern Central Andes is presented alongside petrographic observations and high resolution age dating. In-situ U–Pb dating of magmatic zircon, combined with Ar–Ar dating of plagioclase, has led to an improved regional stratigraphy and provides an accurate temporal constraint for the geochemical data.

A generally higher content of incompatible trace elements (e.g. Nb/Zr ratios from 0.019 to 0.083 and Nb/Yb from 1.5 to 16.4) is observed between the Late Cretaceous (~72 Ma), when the southern Central Andean margin is suggested to have been in extension, and the Miocene when the thickness of the continental crust increased and the angle of the subducting Nazca plate shallowed. Trace and rare earth element compositions obtained for the Late Cretaceous to Late Eocene arc magmatic rocks from the Principal Cordillera of Chile, combined with a lack of zircon inheritance, suggest limited assimilation of the overlying continental crust by arc magmas derived from the mantle wedge. A general increase in incompatible, fluid-mobile/immobile (e.g., Ba/Nb) and fluid-immobile/immobile (e.g., Nb/Zr) trace element ratios is attributed to the influence of the subducting slab on the melt source region and/or the influx of asthenospheric mantle.

The Late Oligocene (~26 Ma) to Early Miocene (~17 Ma), and Late Miocene (~6 Ma) arc magmatic rocks present in the Frontal Cordillera show evidence for the bulk assimilation of the Permian–Triassic (P–T) basement, both on the basis of their trace and rare earth element compositions and the presence of P–T inherited zircon cores. Crustal reworking is also identified in the Argentinean Precordillera; Late Miocene (12–9 Ma) arc magmatic rocks display distinct trace element signatures (specifically low Th, U and REE concentrations) and contain inherited zircon cores with Proterozoic and P–T ages, suggesting the assimilation of both the P–T basement and a Grenville-aged basement. We conclude that changing geodynamics play an important role in determining the geochemical evolution of magmatic rocks at convergent margins and should be given due consideration when evaluating the petrogenesis of arc magmas.

1. Introduction

Subduction zones are the principal sites for the production of new continental crust through the production of arc magmas. Determining the relative contributions to arc magmas from the mantle, subducting

* Corresponding author at: Department of Earth Sciences, University of Oxford, South Parks Road, Oxford OX1 3AN, UK. Tel.: +44 1865 272000.
E-mail address: Rosie.Jones@earth.ox.ac.uk (R.E. Jones).

http://dx.doi.org/10.1016/j.lithos.2016.07.002
0024-4937/

components (e.g., sediments, oceanic crust) and pre-existing crust, are key to quantifying rates of crustal growth and recycling over time. Crustal material can either be incorporated into arc magmas in the melt source region, due to the subduction of sediments/subduction erosion of overriding lithosphere, and/or due to the assimilation of the overlying crust as arc magmas migrate towards the surface. The Andean margin has been an important site for continental crust production throughout the Cenozoic and is a type locality of an ocean-continent convergent margin.

The recycling of crustal material to Andean arc magmas has been long identified, however the mode of recycling is widely debated. Although most authors agree that there is an increase in the contributions to Central Andean arc magmas from crustal derived material over the course of the Cenozoic, the origin (i.e., subducted crustal material or the overlying Andean crust) of these crustal signatures remains unresolved. The contamination of the melt source region with subducted sediments (e.g., Kilian and Behrmann, 2003; Lucassen et al., 2010; Sigmarsson et al., 1990), crustal material from subduction erosion (e.g., Goss et al., 2013; Kay et al., 2005; Stern, 1991), melts derived from the subducting oceanic plate (e.g., Reich et al., 2003; Stern and Kilian, 1996), as well as the contamination of arc magmas during ascent through the continental crust (e.g., Davidson et al., 1991; Hildreth and Moorbath, 1988; James, 1982; Wörner et al., 1992), has all previously been invoked to explain the petrological and geochemical characteristics of arc magmatic rocks from the Andean margin.

The Andean margin is segmented along its length, with different segments being influenced by different tectonic regimes and geodynamic settings (e.g., Jordan et al., 1983; Pilger, 1981). The geodynamic setting of the southern Central Andean margin has changed significantly over the course of the Cenozoic. Specifically, the angle at which the Nazca plate subducted beneath the South American continent shallowed during the Miocene (e.g., Cahill and Isacks, 1992; Yañez et al., 2001, 2002). This resulted in the margin developing from the extensional regime in existence during the Late Cretaceous (~75 Ma) to a highly compressive regime during the latter part of the Miocene (Jordan et al., 1983). Consequently the thickness of the continental crust increased from ~30 km to >50 km over the latter part of the Cenozoic (Allmendinger et al., 1990; Chulick et al., 2013; Fromm et al., 2004; McGlashan et al., 2008).

The shallowing of the subducting Nazca plate has been linked with the subduction of the Juan Fernandez Ridge (JFR), a hotspot-derived seamount chain which may have undergone significant hydration and serpentinisation (e.g., Gutscher et al., 2000b; Jones et al., 2014; Kay and Mpodozis, 2002; Kopp et al., 2004; Pilger, 1981; Yañez et al., 2001, 2002). The intersection and subduction of the JFR has also been associated with increased levels of subduction erosion of the fore-arc (e.g., Stern, 1991; Stern and Skewes, 1995; von Huene et al., 1997) and is thought to act as a barrier to sediment transport and the accumulation of sediments in the Chilean trench north of ~33 °S (Völker et al., 2013; von Huene et al., 1997).

These changes in tectonic and geodynamic setting over time make the southern Central Andes an interesting location at which to investigate changes in the contamination of arc magmas with crustal derived material. Previous studies into the petrogenesis of Cenozoic arc magmas in this region have primarily utilised whole rock geochemistry (e.g., Bissig et al., 2003; Kay and Abbruzzi, 1996; Kay et al., 1991; Litvak and Poma, 2010; Litvak et al., 2007; Parada, 1990; Winocur et al., 2015) and have tended to focus on narrow geological timeframes or geographical areas. In this study a variety of geochronological and geochemical techniques have been applied to both plutonic and volcanic arc rocks, which have been emplaced and erupted over a wide time frame (~73–6 Ma) and over a wide across-arc extent, from the Principal Cordillera of Chile (−70.8 °W) to the Argentinean Precordillera (−69.1 °W), allowing a more complete picture to be established.

A comprehensive new major, trace and rare earth element data set is presented alongside the results of high resolution U–Pb and Ar–Ar age dating. Prior to this study the majority of the age information available for the southern Central Andean arc stratigraphy has been derived from K–Ar dating (e.g., Limarino et al., 1999; Litvak and Page, 2002; Mpodozis and Cornejo, 1988; Nasi et al., 1990; Pineda and Calderón, 2008; Pineda and Emparan, 2006), combined with some Ar–Ar dating (Bissig et al., 2001) and limited U–Pb dating (Martin et al., 1997). Due to the variable effects of hydrothermal alteration on the arc magmatic rocks (e.g., Bissig et al., 2001; Litvak et al., 2007; Maksaev et al., 1984) some of the K–Ar ages have been found to be unreliable (Winocur et al., 2015). On this basis, this study conducted high resolution in-situ U–Pb dating of magmatic zircon and Ar–Ar dating of plagioclase in order to improve the regional stratigraphy and to provide an accurate temporal constraint for the geochemical data. In addition, in-situ U–Pb dating has the potential to reveal inherited zircon cores and therefore can be used to identify the age of the continental crust being assimilated (e.g., Beard et al., 2005). Finally, the results obtained have been used to investigate the growth and evolution of the Andean continental crust and to refine geodynamic models of the evolution of the Pampean flat-slab segment.

2. The geological and geodynamic setting

The study area is located within the Pampean (Chilean) flat-slab segment (between 29 and 31 °S) of the southern Central Andes and spans the Principal Cordillera, Frontal Cordillera and Precordillera of Chile and Argentina (Fig. 1). Subduction of oceanic crust beneath the South American continent has been active since the Jurassic and has produced a series of volcanic arcs (e.g., Charrier et al., 2007; Ramos et al., 2002; Stern, 2004). From the Cretaceous through to the Late Oligocene the southern Central Andes is considered to have been in extension (e.g., Charrier et al., 2007 and references therein). At ~25 Ma the oceanic Farallón plate divided into the Nazca and Cocos plates (Lonsdale, 2005). This caused an increase in convergence rates (from ~8 cm/yr to ~15 cm/yr) and a change from oblique (NE–SW) to orthogonal (ENE–WSW) convergence (Pardo Casas and Molnar, 1987; Somoza, 1998; Somoza and Ghidella, 2012). The westward migration of the South American plate is also thought to have been initiated after ~30 Ma (Silver et al., 1998). After this time the Andean margin became more compressional and the reconfiguration of the subducting oceanic plates has been linked to a period of major uplift, increased magmatic activity, and a broadening and eastward migration of the magmatic arc (Pilger, 1984). Increased convergence rates (~15 cm/yr) are thought to have been sustained up until ~20 Ma, followed by a gradual decline to present day values (~7 cm/yr) (Pilger, 1984; Somoza and Ghidella, 2012).

There is currently no active volcanism in the Pampean flat-slab segment due to the low angle at which the oceanic Nazca plate subducts beneath the South American continent (e.g., Cahill and Isacks, 1992). The JFR began intersecting the Andean continental margin during the early Miocene (~18 Ma at ~30 °S) and is thought to have led to the shallowing of the subduction angle (Gutscher et al., 2000b; Jones et al., 2014; Kirby et al., 1996; Nur and Ben-Avraham, 1981; Pilger, 1981, 1984; Yañez et al., 2001, 2002). This shallowing led to a broadening and eastward migration of the magmatic arc, a reduction in magma volume, and the eventual cessation of arc magmatism in the late Miocene (~6 Ma) (Bissig et al., 2001; Kay et al., 1987; Litvak et al., 2007; Ramos et al., 1989).

3. Cenozoic arc magmatism and stratigraphy

In the southern Central Andes the Cenozoic plutonic and volcanic arc rocks occur as north–south trending belts which lie to the east of the Coastal Batholith, which is primarily late Paleozoic to early Cretaceous in age. The older, more continuous western belt was intruded in the Paleocene–Eocene and the younger more eastern belt is of Oligocene–Miocene age, demonstrating an eastward migration of magmatism with time (Parada et al., 2007) (Fig. 1). There is a geographical gap between the two belts which corresponds with a widespread lull in

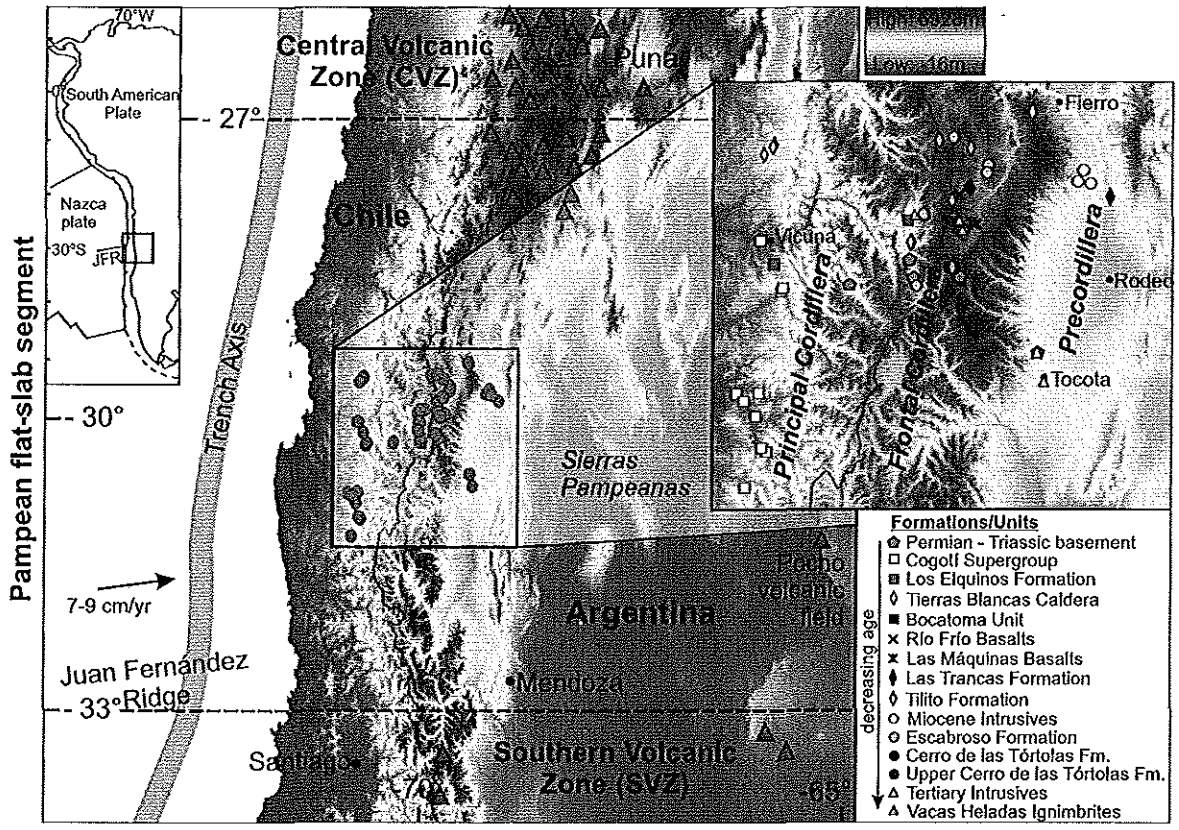

Fig. 1. Map of the study area showing the main features of the present day southern Central Andean margin. In the main map the sample locations are highlighted as blue circles and primary active volcanoes as brown triangles. In the expanded region the samples are identified by assigned geological formation/unit. Digital elevation data from Jarvis et al. (2008).

magmatic activity between ~39 and 26 Ma (Parada et al., 1988, 2007). In order to provide a context for the geochemical data, the Cenozoic arc stratigraphy for the southern Central Andes is outlined below and in Fig. 2.

The Paleocene–Eocene belt is located in the Chilean Principal Cordillera (Fig. 1) and is primarily composed of epizonal plutons which have been assembled into the Cogotí Supergroup (Parada et al., 1988). Granitoids of the Cogotí Supergroup have K–Ar ages between 67 ± 2 Ma and 38 ± 1 Ma (Parada et al., 1988 and references therein). However, Parada et al. (1988) note there is evidence of partial Ar loss, suggesting the Cogotí Supergroup is likely to be Late Cretaceous to Paleocene in age. Coeval to the Cogotí Supergroup is the extrusive Los Elquinos Formation (69.8 ± 0.9 Ma to 57.6 ± 2.5 Ma (Pineda and Emparan, 2006)) which consists of basaltic to rhyolitic lavas, tuffs and breccias (Charrier et al., 2007). During the Paleocene a number of calderas, including the Tierras Blancas Caldera (Emparan and Pineda, 1999), also formed along the margin between 26 and 30 °S (Charrier et al., 2007). To the east of the volcanic arc, mafic, intra-plate volcanism was concurrent with the emplacement of the Cogotí Supergroup (Litvak and Poma, 2010). The Río Frío Basalts were erupted in what is now the Argentinean Frontal Cordillera and have been K–Ar dated at 55.9 ± 1.9 Ma (Litvak and Page, 2002).

A general reduction in magmatic activity has been identified between ~39 and 26 Ma in the southern Central Andes (Parada et al., 1988), however, some arc magmatism continued during this time interval. The Bocatoma Unit has been dated as Eocene to Early Oligocene with reported Ar–Ar and K–Ar ages ranging between 39.5 and 30 ± 1.9 Ma (Bissig et al., 2001; Martin et al., 1995; Mpodozis and Cornejo, 1988; Nasi et al., 1990). This primarily intrusive unit consists of fine grained to coarsely porphyritic diorites and granodiorites, and some andesitic porphyries (Bissig et al., 2001; Maksaev et al., 1984). A number of dacitic and rhyolitic ignimbrites and lava flows located in the Valle del Cura region (Frontal Cordillera, Argentina) have been K–Ar dated between 44 ± 2 and 34 ± 1 Ma and have been assigned to the Valle del Cura Formation (Limarino et al., 1999; Litvak and Poma, 2005). However, it has recently been suggested that these Eocene to early Oligocene K–Ar ages may be unreliable due to the high levels of hydrothermal alteration evident in these units and new Ar–Ar dating suggests these volcanic sequences are Oligocene to Early Miocene in age (Winocur et al., 2015).

Following the break-up of the Farallón plate and reconfiguration of the margin at ~25 Ma (Lonsdale, 2005), the extensive Doña Ana Group was erupted at and near the arc front, spanning either side of the current Chilean–Argentine border. The Group consists of two formations; the Tilito Formation (27–23 Ma), composed of high-K calc-alkaline andesite lavas and dacitic to rhyolitic ignimbrites, which have been intruded by basic to intermediate dykes; and the Escabroso Formation (21–18 Ma), composed of medium-K, pyroxene bearing, calc-alkaline basaltic and andesitic lavas (Kay et al., 1987, 1991; Maksaev et al., 1984; Martin et al., 1997). The Tilito Formation is thought to be derived from a long lived volcanic centre and the volcanic rocks have undergone significant hydrothermal alteration and mineralisation (Bissig et al., 2001; Litvak et al., 2007; Syracuse et al., 2010). The Tilito and Escabroso formations are separated by a major unconformity (Martin et al., 1995) which has been attributed to a period of deformation at ~20 Ma (Kay and Mpodozis, 2002).

During the production of the calc-alkaline Doña Ana Group at the arc front, the Las Máquinas basalts were being erupted in the back-arc region. These alkaline basalts have been K–Ar dated between 22.8 ± 1.1 Ma and 22.0 ± 0.8 Ma and their trace element geochemistry suggests they were erupted in an extensional setting with influence from the subducting slab (Kay et al., 1991; Litvak et al., 2005). The volcanic

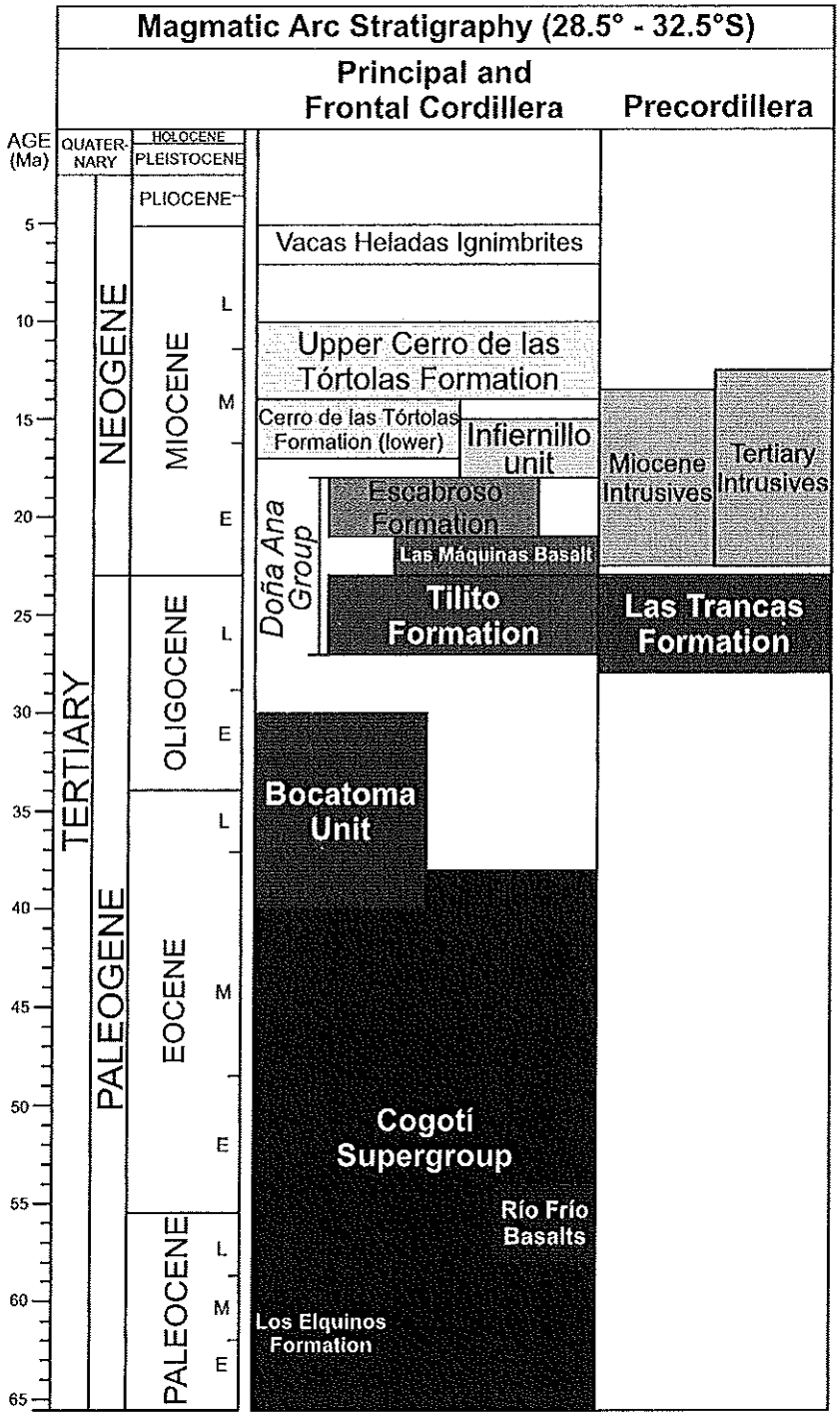

Fig. 2. The Cenozoic magmatic arc stratigraphy of the Principal Cordillera, Frontal Cordillera and Precordillera in the southern Central Andes. References are outlined in the text.

Las Trancas Formation, which outcrops in the Argentinean Precordillera and consists of andesitic to rhyolitic proximal block-and-ash pyroclastic flow deposits, ignimbrites, tuffs and dacitic lava flows, has also been identified as coeval with the Tilito Formation (Poma et al., 2005).

The volcanic Cerro de las Tórtolas Formation also appears on either side of the current Chilean–Argentinean border (Fig. 1). These lavas were erupted during the middle Miocene and are primarily composed of amphibole bearing, medium- to high- K calc-alkaline andesites and dacites. Litvak et al. (2007) and Ramos et al. (1989) identify two separate sequences; an older (17–14 Ma) andesitic to basaltic andesitic lower section which appears to have been erupted through a normal thickness of crust (30–35 km) and a younger (13–10 Ma) dacitic upper sequence.

The Infiernillo unit (18–15 Ma) is thought to be the subvolcanic equivalent of the Cerro de Las Tórtolas Formation and is composed of high-K calc-alkaline, shallow level, intermediate intrusives (Kay et al., 1987) (Fig. 2). A number of sub-volcanic outcrops identified in the Precordillera have been correlated with the Infiernillo Unit and are referred to as the Miocene Intrusives and Tertiary Intrusives (Cardó and Díaz, 1999; Cardó et al., 2007). The Miocene Intrusives which primarily

consist of granitoids and have been dated between 22.4 ± 0.1 and 21.2 ± 0.1 Ma (Llambias et al., 1990). Ages as young as 13.5 ± 7 Ma have been obtained for other deposits (JICA-MMAJ, 1999) and these have also been grouped into the Miocene Intrusives (Cardó et al., 2007). The Tertiary Intrusives consist of sub-volcanic andesites and dacites, and K–Ar dating has given ages of 18.3 ± 2.5 Ma and 17.5 ± 5 Ma (Cardó and Díaz, 1999; Leveratto, 1976), as well as a younger age of 8.8 ± 0.3 Ma (Wetten, 2005).

The Late Miocene, Vacas Heladas Ignimbrites represent the last significant volcanic activity in the region with a reported K–Ar age of 6.0 ± 0.4 Ma (Ramos et al., 1989). These high-K rhyolitic and dacitic tuffs lie unconformably over the Oligocene–Miocene sequences and have been correlated with the Vallecito Formation in Chile, which yields the same age (Bissig et al., 2001; Maksaev et al., 1984). These ignimbrites are isotopically enriched and contain the highest proportion of crustal components (e.g., Litvak et al., 2007).

4. The southern Central Andean basement

The basement present in the Principal and Frontal Cordillera's is primarily composed of Paleozoic marine sedimentary deposits and meta-sediments which have been intruded, and unconformably overlain by Late Paleozoic to Mesozoic plutonic complexes and volcanic deposits (Kay et al., 1989; Martin et al., 1999). In Chile, Late Paleozoic–Mesozoic plutonic complexes range in composition from gabbros to granites with two 'super-units' identified according to age: the Late Carboniferous–Early Permian, Elqui Complex and the Permian–Early Jurassic, Ingaguás Superunit (Mpodozis and Cornejo, 1988; Mpodozis and Kay, 1990, 1992; Nasi et al., 1990).The Colangüil Batholith is the age equivalent in Argentina (e.g., Llambías and Sato, 1990, 1995; Sato et al., 2015). There are also extensive deposits of Permian–Early Jurassic silicic, volcanic rocks (e.g., the Choiyoi Group and the Pastos Blancos Group) (Martin et al., 1999; Nasi et al., 1985). All the aforementioned Late Paleozoic–Mesozoic plutonic and volcanic rocks are suggested to have formed in the late stages of Carboniferous to Early Permian subduction along the western margin of Gondwana, and in a more extensional tectonic setting after the cessation of subduction in the Early Permian (Martin et al., 1999; Mpodozis and Kay, 1992).

The basement in the Argentinean Precordillera is composed of Grenville-aged crust (ages between ~1300 and ~950 Ma that are contemporaneous with the North American Grenville province) overlain by Cambrian to Ordovician strata. Although no Grenville-aged basement is exposed at the surface its presence has been identified by various geochemical studies and through the presence of xenoliths and xenocrystic zircon grains in Miocene volcanic rocks (e.g., Abbruzzi et al., 1993; Jones et al., 2015; Kay et al., 1996). It has been suggested that the basement of the Precordillera is a rifted fragment of Laurentian crust which was accreted onto the western margin of Gondwana during the Ordovician (e.g., Astini et al., 1995; Kay et al., 1996; Thomas and Astini, 2003; Thomas et al., 2004), although the origin and the exact timing of rifting and accretion remains widely debated (e.g., Finney, 2007; Keller, 1999; Rapela et al., 1998).

5. Sample preparation and analytical methods

5.1. Sample collection

Representative samples (based on the published maps and formation descriptions of Cardó and Díaz (1999), Cardó et al. (2007), Emparan and Pineda (1999), Mpodozis and Cornejo (1988), Nasi et al. (1990), Pineda and Emparan (2006), Pineda and Calderón (2008)) were collected from each of the major intrusive/extrusive Late Cretaceous to Late Miocene arc formations (detailed in Section 3) present between 29 and 31 °S (Figs. 1 and 2). Due to the eastward migration and expansion of the magmatic arc activity during this time interval, the sample locations form an W–E transect across the Andean Cordillera from Chile into Argentina (Fig. 1). Late Cretaceous to Late Miocene plutonic and volcanic rocks in the southern Central Andes are typically evolved, but where possible mafic samples were collected in order to evaluate source compositions and processes. A number of Late Paleozoic–Early Mesozoic basement samples were also collected in order to assess their potential role in the contamination of the Late Cretaceous to Late Miocene arc magmas.

5.2. U–Pb dating

In order to obtain zircon grains for U–Pb dating ~5 kg of each sample was crushed using a tungsten carbide jaw crusher. Zircons were then separated from 42 crushed samples using a combination of density and magnetic separation (Section 1, Supplementary Material). Individual zircon grains were hand-picked under a binocular microscope and mounted in epoxy resin accompanied by zircon Geostandards 91500 and/or GJ-1. These epoxy mounts were then ground and polished to expose the interior of the zircons at the surface.

Prior to analysis individual zircon grains were imaged and characterised using a Philips XL30CP Scanning Electron Microscope (SEM) at the University of Edinburgh in order to determine the presence or absence of multiple growth phases, xenocrystic cores, inclusions, and cracks. Imaging was carried out in both secondary electron (SE) and backscatter electron (BSE) modes, and suitable, representative zircons and specific locations for analysis were identified. U–Th–Pb analysis of zircons was performed on a Cameca ims 1270 secondary ion mass spectrometer (SIMS) at the NERC Edinburgh Ion Microprobe Facility (EIMF) using analytical procedures similar to those described by Kelly et al. (2008). Full details of analytical methods, applied corrections and data reduction are outlined in the Supplementary Material. Subsequent to analysis all analysed zircons were imaged on a SEM in both cathodoluminescence (CL) and SE modes to check the exact position of analysis, and to ensure the absence of cracks and inclusions at the bottom of the analysis pits (Fig. 3). Data from any problematic analysis locations (i.e. cracks present) was rejected. A total of 313 successful U–Th–Pb analyses were made and in most cases at least 8 successful analyses of separate zircon grains were made per sample. Multiple analyses (core and rim) were made on selected zircon grains in order to obtain information on growth history and inheritance (Fig. 3).

5.3. Ar–Ar dating

Due to the lack of magmatic zircon in some of the more basic to intermediate samples Ar–Ar dating of plagioclase was conducted on two samples (RJ1111 and AM0887). Plagioclase phenocrysts were separated from the crushed rock samples using similar mineral separation techniques to those used to separate zircon. Plagioclase crystals were hand-picked under a binocular microscope and sent to the Ar–Ar Research Laboratory at the Open University for analysis. Full details are presented in Section 3 of the Supplementary Material.

5.4. Whole-rock major, trace and rare earth element analysis

Sample blocks weighing ~50 g were cleaned and trimmed of any weathered surfaces, veins and xenoliths. These blocks were then crushed into chips using a tungsten carbide jaw crusher. The chips were also checked to ensure they contained no signs of alteration, veins, xenocrystic and xenolithic material, and then powdered in a tungsten carbide TEMA mill to obtain fine, homogeneous powders for analysis by X-ray florescence spectrometry (XRF) and inductively-coupled plasma mass spectrometry (ICP-MS). Details are presented in Section 4 of the Supplementary Material.

XRF analyses were carried out in the School of GeoSciences, University of Edinburgh following the analytical methods outlined in Fitton and Godard (2004) and Fitton et al. (1998). Major, minor and selected trace element (TE) compositions of 56 samples were analysed on a

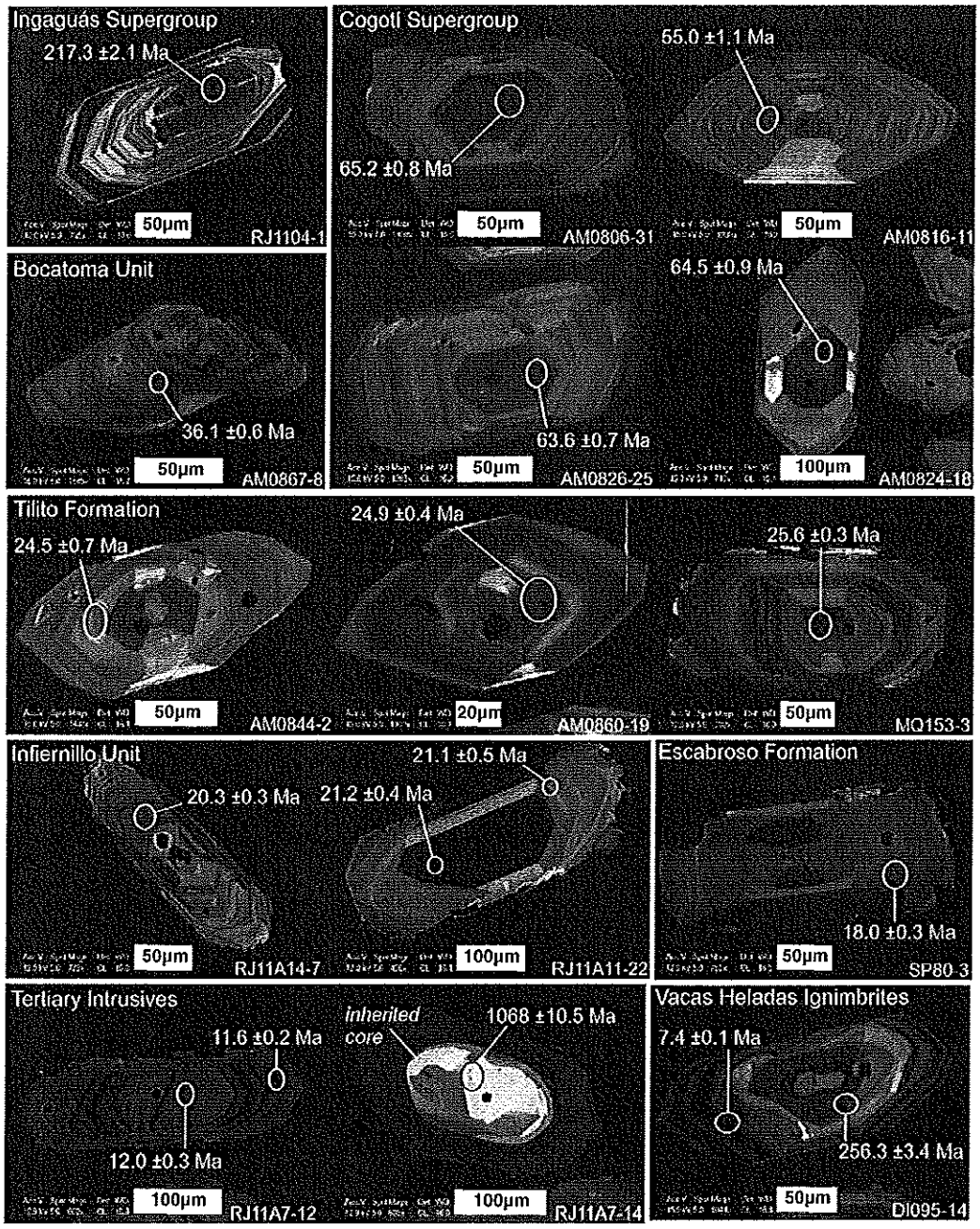

Fig. 3. Cathodoluminescence (CL) images of representative zircon grains from select samples, highlighting the presence of internal growth zoning, inherited cores and the location of SIMS analysis. The U–Pb ages are presented as the $^{206}Pb/^{238}U$ ages for the individual zircon grains and the errors are quoted at the 1σ level.

Philips PW2404 wavelength-dispersive sequential X-ray spectrometer with a 4 kW Rh-anode end-window X-ray tube. Major element oxide totals were generally within ±0.9% of 100% and have been recalculated to a 100% volatile free basis. Based on the repeated analysis of an individual sample prepared and analysed five times the precision for the major element analysis is determined as always being <1.1% (1σ) (Table A4, Supplementary Material). The accuracy of the measurements, based on repeated analysis of standard BHVO-1 (basalt) compared to the published values, is <3.5% relative (1σ) for all major elements, apart from P_2O_5 where accuracy is 5.5% relative (1σ) (Table A2, Supplementary Material). Precision for the TE and REE concentrations determined by XRF analysis is <4% (1σ) apart from for Ni where the precision is much lower. This may be a result of the low concentrations of Ni present in the analysed sample (average = 2.7 ppm). Precision for Ni, based on the repeated analysis of BHVO-1 (117.5 ppm Ni) gave a precision of 0.5% (1σ) (Table A3, Supplementary Material). A full evaluation of the accuracy of the TE and REE analysis is presented in Table A3, Supplementary Material, but is generally determined to be better than 10% relative (1σ).

A subgroup of 39 samples representing each of the major volcanic and plutonic formations were selected for REE analysis via ICP-MS. Select samples were also analysed for U, Th, Pb and Hf concentrations. Sample powders were dissolved using a tri-acid digestion procedure and analysis was carried out on an Agilent 7500ce ICP-MS at the Scottish Universities Environmental Research Centre (SUERC), East Kilbride. Based on the repeated analysis of international standard BCR-2 the

precision of the analysis is <4% (1σ) and the accuracy is <7% relative (1σ) for all elements apart from Pb, where precision and accuracy are much lower (7.3 and 30.9% respectively) (Table A6, Supplementary Material). On this basis the use of Pb in the interpretations will be limited. A good agreement has been found between the TE and REE concentrations produced by XRF and ICP-MS analysis (Figs. A5–A7,

Table 1
The results of U–Pb and Ar–Ar dating and assigned geological unit (determined based on sample location, the new age determinations, and the results of whole rock geochemical analysis). The two sample ages which are displayed in italics and underlined are those obtained by Ar–Ar dating of plagioclase. Sample age calculations have been made using computer program ISOPLOT v3.7 (Ludwig, 2008). The age range ($^{206}Pb/^{238}U$ ages) of inherited zircon grains/cores are also presented where identified. The large uncertainty on the U–Pb age obtained for sample AM0890 reflects the limited number of zircon grains obtained from this sample (Supplementary Material). However, the U–Pb age is very similar to the Ar–Ar age produced for sample RJ1111 (61.2 ± 1.0 Ma), which is from the same formation (Los Elquinos Formation).

Sample	Rock type	Age (Ma)	±2σ or 95% conf.	Assigned geological unit	Age range ($^{206}Pb/^{238}U$, Ma (±1σ)) of inherited zircon cores/grains
RJ11A18	Granodiorite	**280.2**	3.5	Plutón Tocota (Colangüil Batholith)	
MQ39	Rhyolite	**269.7**	2.6	Choiyoi Group	
RJ11A20	Rhyolite	**269.6**	7	Choiyoi Group	
AM0862	Rhyolite	**269.3**	5.2	Choiyoi Group	
AM0853	Rhyolite	**261.0**	6	Pastos Blancos Group	
AM0855	Rhyolite	**248.6**	5.5	Pastos Blancos Group	
AM0856	Rhyolite			Pastos Blancos Group	
RJ1104	Granite	**221.0**	4.4	El León Unit (Ingaguás Supergroup)	
AM0812	Diorite	**72.6**	0.77	Cogotí Supergroup	
AM0823	Granodiorite	**69.8**	0.73	Cogotí Supergroup	
AM0824	Syeno-diorite	**64.6**	0.65	Cogotí Supergroup	
AM0806	Granite	**64.4**	0.66	Cogotí Supergroup	
RJ1103	Syeno-diorite	**64.3**	0.59	Cogotí Supergroup	
AM0826	Granite	**64.2**	0.69	Cogotí Supergroup	
AM0819	Diorite			Cogotí Supergroup	
AM0822	Granodiorite	**57.3**	1.7	Cogotí Supergroup	
AM0814	Diorite			Cogotí Supergroup	
AM0815	Granodiorite	**55.0**	1.7	Cogotí Supergroup	
AM0816	Granodiorite	**54.1**	0.76	Cogotí Supergroup	
RJ1101	Granite	**38.9**	0.99	Cogotí Supergroup	
RJ1109	Diorite			Cogotí Supergroup	
AM0890	Basaltic andesite	**61.9**	9.11	Los Elquinos Formation	
RJ1111	Basaltic andesite	***61.2***	*1*	Los Elquinos Formation	
RF17	Basaltic-Trachyandesite			Río Frío Basalts	
RJ1105	Diorite	**40.2**	1.2	Tierras Blancas Caldera	
RJ1106	Diorite			Tierras Blancas Caldera	
RJ1107	Basalt			Tierras Blancas Caldera	
AM0867	Andesite	**35.6**	0.78	Bocatoma Unit	171.8 (±4.1)
AM0866	Andesite			Bocatoma Unit	
AM0870	Trachy-andesite			Bocatoma Unit	
AM0846	Rhyolite	**26.1**	1.6	Tilito Formation (Lower Doña Ana Group)	158.0 (±2.4)
MQ153	Andesite	**25.2**	0.26	Tilito Formation (Lower Doña Ana Group)	
AM0847	Rhyolite			Tilito Formation (Lower Doña Ana Group)	
AM0845	Rhyolite	**24.9**	0.32	Tilito Formation (Lower Doña Ana Group)	276.7 (±2.9)–278.5 (±2.9)
AM0860	Dacite	**24.9**	0.4	Tilito Formation (Lower Doña Ana Group)	
ZN122	Andesite	**24.8**	0.37	Tilito Formation (Lower Doña Ana Group)	
AM0844	Rhyolite	**24.7**	0.28	Tilito Formation (Lower Doña Ana Group)	241.0 ± 2.7
AM0849	Rhyolite	**24.7**	0.43	Tilito Formation (Lower Doña Ana Group)	
RF64	Rhyolite	**24.3**	0.7	Tilito Formation (Lower Doña Ana Group)	388.1 (±5.3)
PC14	Rhyolite	**23.6**	0.21	Tilito Formation (Lower Doña Ana Group)	
Z27	Dacite	**23.2**	0.3	Tilito Formation (Lower Doña Ana Group)	
MQ8	Basalt			Las Máquinas Basalts	
MQ145	Basalt			Las Máquinas Basalts	
RJ11A5	Rhyolite	**22.6**	0.33	Las Trancas Formation	257.5 (±2.9)–273.1 (±3.6)
RJ11A10	Granite	**22.2**	0.23	Miocene Intrusives	
RJ11A11	Granite	**21.4**	0.29	Miocene Intrusives	
RJ11A14	Granodiorite	**20.4**	0.31	Miocene Intrusives	138.1 (±2.6)
AM0887	Andesite	***19.3***	*0.3*	Escabroso Formation (Upper Doña Ana Group)	
1026	Andesite-Trachyandesite	**18.2**	0.28	Escabroso Formation (Upper Doña Ana Group)	
SP80	Andesite	**18.1**	0.37	Escabroso Formation (Upper Doña Ana Group)	
AM0886	Andesite			Escabroso Formation (Upper Doña Ana Group)	
MQ158	Basaltic andesite			Escabroso Formation (Upper Doña Ana Group)	
AM0871	Basaltic andesite			Escabroso Formation (Upper Doña Ana Group)	
AM0872	Dacite			Escabroso Formation (Upper Doña Ana Group)	
RF62	Trachyandesite	**17.1**	0.63	Cerro de las Tórtolas Formation	
RF65	Andesite			Cerro de las Tórtolas Formation	
MQ28	Trachyandesite			Upper Cerro de las Tórtolas Formation	
MQ30	Trachyandesite			Upper Cerro de las Tórtolas Formation	
RJ11A7	Trachyandesite	**11.7**	0.21	Tertiary Intrusives	1068.1 (±10.5)–1249 (±10.9)
RJ11A17	Dacite	**9.5**	0.18	Tertiary Intrusives	239.7 (±3.0)–1066.0 (±13.7)
RJ11A15	Trachydacite	**9.4**	0.18	Tertiary Intrusives	249.0 (±2.6)–1225.7 (±11.7)
MQ33	Rhyolite	**6.2**	0.19	Vacas Heladas Ignimbrites	15.1 (±0.2)–255.7 (±2.7)
DI095	Rhyolite	**6.2**	0.3	Vacas Heladas Ignimbrites	256.3 (±3.4)–270.7 (±3.0)
MQ32	Rhyolite			Vacas Heladas Ignimbrites	
AM0889	Rhyolite			Vacas Heladas Ignimbrites	

Supplementary Material). Therefore, select REE concentrations determined for certain samples by XRF analysis is included alongside the REE concentrations determined by ICP-MS.

6. Results

Detailed sample information, including a summary of the petrology of each formation/unit (Table A7), and full results are presented in the Supplementary Material.

6.1. Geochronological results

The results of U–Pb dating and Ar–Ar dating for individual samples are presented in Table 1. In order to obtain overall U–Pb ages for the Late Cretaceous–Late Miocene samples the data has been plotted on Tera-Wasserburg plots, where the U–Pb data is uncorrected for common Pb and the mixing line is anchored to the $^{207}Pb/^{206}Pb$ ratio for modern day common Pb (0.84) (Section 2, Supplementary Material). The overall U–Pb ages for these samples are given by the intercept on the Tera-Wasserburg plot and uncertainties are quoted at the 2σ or 95% confidence level. The overall U–Pb ages presented for the samples of the P–T basement are concordia ages or intercept ages with uncertainties quoted at the 2σ or 95% confidence level (Section 2, Supplementary Material). For the two samples dated using the Ar–Ar dating technique the age determinations are plateau ages with uncertainties quoted at the 2σ level (Figs. A1 and A3, Supplementary Material). All of the plots and age calculations were made using computer program ISOPLOT v3.7 (Ludwig, 2008).

In the majority of cases the new U–Pb and Ar–Ar ages presented in this study confirm the previously reported age range of the sampled geological formations/units. However, in a few instances the ages obtained by this study are at odds with the previously reported ages and the geological maps of the region; these differences are outlined below.

A number of dacitic and rhyolitic ignimbrites and lava flows which outcrop in the Valle del Cura region (Frontal Cordillera, Argentina) have previously produced Eocene K–Ar ages ranging between 44 ± 2 and 34 ± 1 Ma, and have been assigned to the Valle del Cura Formation (Limarino et al., 1999; Litvak and Poma, 2005). Samples of the Valle del Cura Formation collected as part of this study have produced Late Oligocene to Early Miocene ages, ranging between 24.3 and 17.1 Ma (Table 1). Oligocene to Early Miocene ages have also been reported for the Valle del Cura Formation by Winocur et al. (2015). These authors propose that the units previously identified as the Valle del Cura Formation are part of the Doña Ana Group. The U–Pb dating presented by this study supports this inference and some of the samples of the Valle del Cura Formation collected as part of this study have been assigned to the Doña Ana Group. Other samples thought to be the Valle del Cura Formation have been assigned to the Cerro de las Tórtolas Formation due to the younger ages obtained (17.1 Ma) (Table 1, Fig. 2).

A number of intrusive units which crop out in the Precordillera of Argentina have been mapped as Miocene Intrusives and Tertiary Intrusives and correlated with the Infiernillo Unit found on the Chilean side of the border (Cardó and Díaz, 1999; Cardó et al., 2007). However, the U–Pb ages obtained in this study, as well as geochemical evidence, suggest these intrusive bodies are not related. U–Pb ages of between 22.2 ± 0.2 and 20.4 ± 0.3 Ma were obtained for the Miocene Intrusives present in the Llanos del Molle (Llambias et al., 1990) and mapped by Cardó et al. (2007). These ages are significantly older than the ages reported for the Infiernillo Unit on the Chilean side of the boarder (18–15 Ma, (Kay et al., 1987)). Conversely, much younger U–Pb ages (11.7 ± 0.2 to 9.4 ± 0.2 Ma) were obtained for the Tertiary Intrusives which outcrop in the Precordillera. Previously reported K–Ar ages for these sub-volcanic andesites and dacites range between 18.3 ± 2.5 Ma and 17.5 ± 5 Ma (Cardó and Díaz, 1999; Leveratto, 1976), perhaps explaining why these deposits have been linked with the Infiernillo Unit. The new U–Pb ages presented here are similar to the K–Ar age of 8.8 ± 0.3 Ma reported by Wetten (2005) for the same intrusive bodies, which this particular author refers to as the Cerro Bola Andesite. There is a variety of evidence to suggest that these intrusive bodies have been affected by hydrothermal alteration. On this basis we suggest that some of the K–Ar ages are likely to be unreliable and that the Tertiary Intrusives are Late Miocene in age and consequently distinct from the Infiernillo Unit.

6.2. Geochemical results

6.2.1. Major elements

The results of major oxide analysis are presented in Figs. 4 and 5. The Late Cretaceous to Late Miocene magmatic rocks primarily have medium- to high- K, calc-alkaline compositions. The intrusive samples range from gabbroic to granitic in composition, with SiO_2 contents ranging between 50.9 and 71.3 wt.% (Fig. 4a). The extrusive samples range from basalts to rhyolites with SiO_2 contents ranging between 49.7 and 75.3 wt.% (Fig. 4b). All samples plot within the sub-alkaline field on plots of total alkalis versus silica with the exception of the Paleocene Río Frío Basalt, which is alkaline in composition (Fig. 4b). All the samples are relatively evolved with an average Mg# of 41 and Ni concentration of 11 ppm. The P–T basement rocks have medium- to high-K calc-alkaline to shoshonitic compositions and are more felsic than the Late Cretaceous to Late Miocene arc rocks, with SiO_2 contents ranging between 68.7 and 76.7 wt.% (Fig. 4).

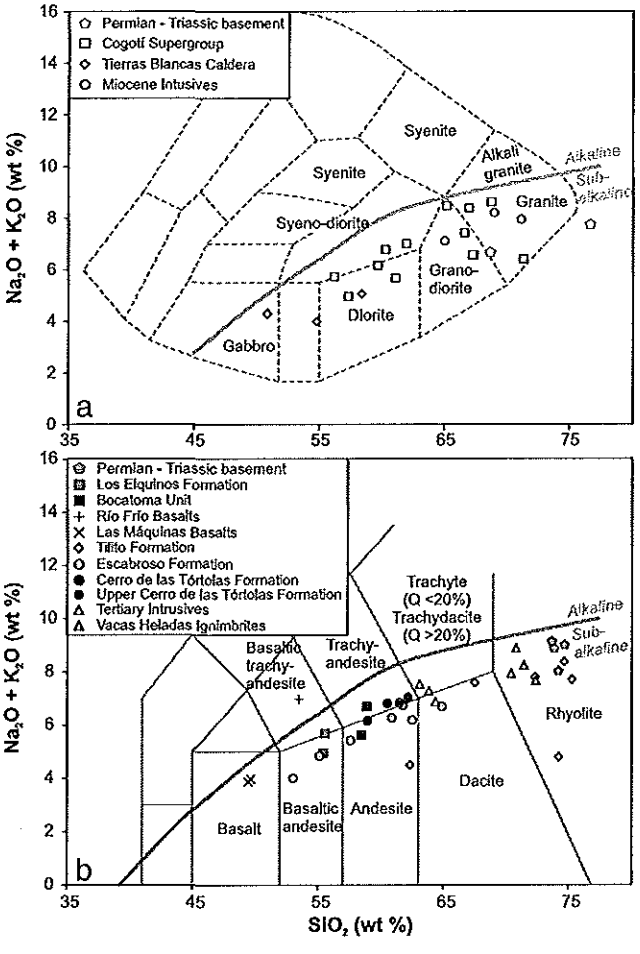

Fig. 4. Plots of total alkalis versus silica content for a) intrusive samples (fields from Wilson (1989)) and b) extrusive samples (fields from Le Maitre et al. (1989)). The alkaline/subalkaline fields are from Irvine and Baragar (1971).

Major elements, TiO_2, Al_2O_3, Fe_2O_3, MgO, CaO, and to a lesser extent MnO display typical negative correlations with SiO_2 content (Fig. 5), whereas K_2O shows a positive correlation (Fig. 5). The plot of P_2O_5 versus SiO_2 content shows a convex trend with a general positive correlation between P_2O_5 and SiO_2 content until SiO_2 reaches ~63 wt.%, after which a negative correlation is observed (Fig. 5). These overall trends are consistent with fractional crystallisation (FC) processes, for example the increased crystallisation of apatite after ~63 wt.% SiO_2. The alkali oxides, K_2O and Na_2O show the weakest correlations with SiO_2 (Fig. 5), suggesting that these elements may have been mobilised during alteration. The highest variation is observed in samples of the Cogotí Supergroup which shows a range of K_2O contents between 0.5 to 4.8%

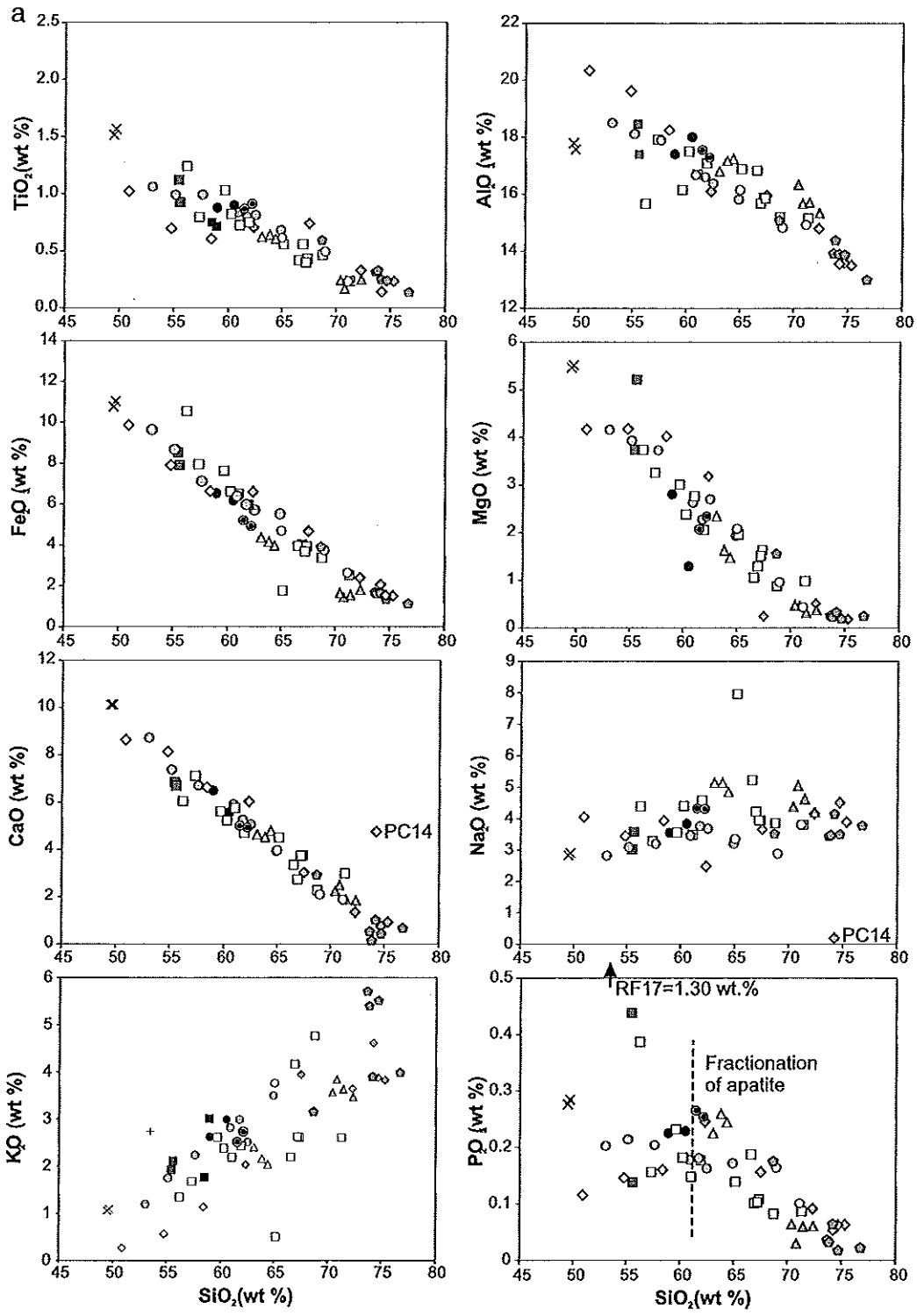

Fig. 5. Harker-type variation diagrams of major (wt.%) and minor (ppm) elements versus SiO_2 content for the Late Cretaceous to Late Miocene samples and the PT basement. Intrusive samples are plotted as open symbols and extrusive samples as filled symbols. The uncertainty on the data points is less than the size of the symbols.

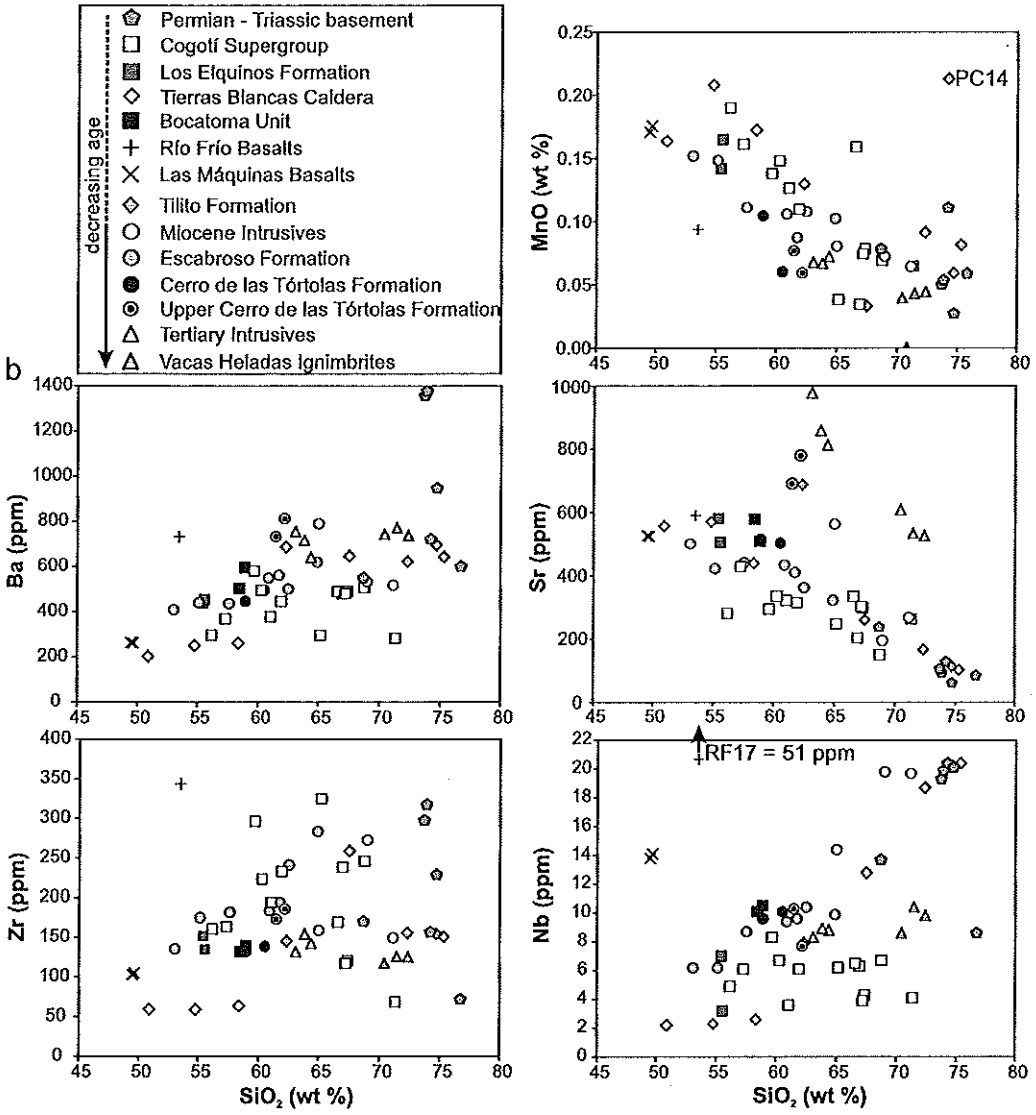

Fig. 5 (*continued*).

with a limited increase in SiO_2 content. Values for certain major element oxides, obtained for certain samples, also appear to sit away from the main data trends. For example, sample PC14 from the Tilito Formation appears to have lost all of its Na_2O and displays higher CaO and MnO contents (Fig. 5). This suggests leaching of Na, potentially from plagioclase, and replacement with carbonate minerals; this is confirmed by petrographic analysis (Fig. A8, Supplementary Material). Therefore, some variation in the data away from the main trends displayed on the Harker diagrams may be the result of alteration and replacement processes.

6.2.2. Trace elements (TE) and rare earth elements (REE)

The results of trace- and rare earth- element analysis are presented in Figs. 5 and 6 With the exception of the sample (RF17) of the Río Frío Basalts (Paleocene), all samples, including the Las Máquinas Basalts and those of the P–T basement, display typical subduction zone TE and REE signatures with enrichments in the large ion lithophile elements (LILE, e.g., Rb, K, Ba, Sr, Pb) and the light rare earth elements (LREE) relative to the high field strength elements (HFSE, e.g., Nb, Zr, Ti, Y) and heavy rare earth elements (HREE) (Fig. 6). As evident in Fig. 5, sample RF17 (Río Frío Basalts) has a distinct TE composition, with apparent enrichments in P, Nb and Zr. This sample is also alkaline in composition (Fig. 4b) and is clearly not co-genetic with other Paleocene arc formations (e.g., Cogotí Supergroup and Los Elquinos Formation), indicating that the Río Frío Basalts may have formed from a distinct mantle source.

The multi-element plots for all other samples exhibit prominent negative Nb anomalies and positive K and Pb anomalies (Fig. 6). With the exception of the most mafic sample (MQ8, Las Máquinas Basalts), all samples show negative Ti anomalies and depletions in HREE relative to N-MORB (Fig. 6). The Late Oligocene, Las Maquinas Basalts (MQ8) shows the least enrichment in the LILE, consistent with emplacement in a back-arc setting (e.g., Litvak and Poma, 2010). Samples of the Los Elquinos Formation (Paleocene), Tierras Blancas Caldera (Eocene) and Bocatoma Unit (Early Oligocene) display relatively limited enrichments in LILE, with the exception of Sr. These Paleocene–Early Oligocene samples, along with samples of the youngest (~13–6 Ma) arc formations (Upper Cerro de las Tórtolas Formation, Tertiary Intrusives and Vacas Heladas Ignimbrites), display positive Sr anomalies and limited negative Eu anomalies (Fig. 6). The youngest samples (~13–6 Ma) also have Sr contents which are significantly higher than the overall decreasing trend observed with increasing SiO_2 content (Fig. 5). In addition, these samples display relatively steeply dipping REE patterns with depletions

in the HREE, suggesting a change in the petrogenesis of the youngest arc magmas erupted and emplaced in the southern Central Andes (Fig. 6).

7. Discussion

7.1. Temporal variations in the contamination of southern Central Andean arc magmas

It is clear from many of the TE plots (e.g., Figs. 5b and 6) that there are significant variations in either the degree of melting or the composition of the source of the arc magmas, or in the level of interaction with the continental crust, over time. How the TE compositions have changed over time, due to what processes, and how this relates to the changing geodynamic setting of the southern Central Andean margin, is discussed below.

7.1.1. The Late Cretaceous to Eocene

Concentrations of incompatible, fluid-mobile (e.g., Ba, Pb, U) and fluid-immobile (e.g., Nb, Zr) elements, in the Late Cretaceous–Eocene samples of the Cogotí Supergroup, Los Elquinos Formation, Tierras Blancas Caldera and the Botacoma Unit, remain relatively constant with increasing differentiation (Fig. 5). There are limited correlations between certain TE ratios and SiO_2 content (Fig. 7) suggesting that these TE variations are not the result of FC. A number of lines of evidence support limited interaction of these arc magmas with the existing continental crust; no inherited zircon grains and cores are identified in these arc rocks (Table 1); 'mantle-like' $\delta^{18}O$ values have been obtained for zircons from these samples (Jones et al., 2015); and low $^{87}Sr/^{86}Sr$ isotope ratios have been reported for these the Late Cretaceous–Eocene magmatic belts (Parada et al., 1988). On this basis it is suggested that the observed enrichments in fluid-mobile, incompatible elements (e.g., LILE) and depletions in HFSE and HREE reflect processes occurring in the source region, rather than resulting from crustal contamination and/or differentiation processes.

Overall the fluid mobile/immobile TE ratios (e.g., Ba/Nb, U/Th) are highly variable for the Late Cretaceous–Eocene arc rocks (Fig. 7) suggesting that the source region has been variably influenced by slab-derived fluids. A general increase in these ratios is observed between the Late Cretaceous (~72 Ma) and the Eocene (~50 Ma) suggesting an increased influence of slab-derived fluids on the arc magmas with time (Fig. 8). With an increase in fluid flux from the subducting slab an increase in the amount of partial melting occurring in the mantle wedge might be expected. An increase in certain element ratios (e.g., Nb/Zr, Nb/Yb) between the Late Cretaceous and the Late Eocene

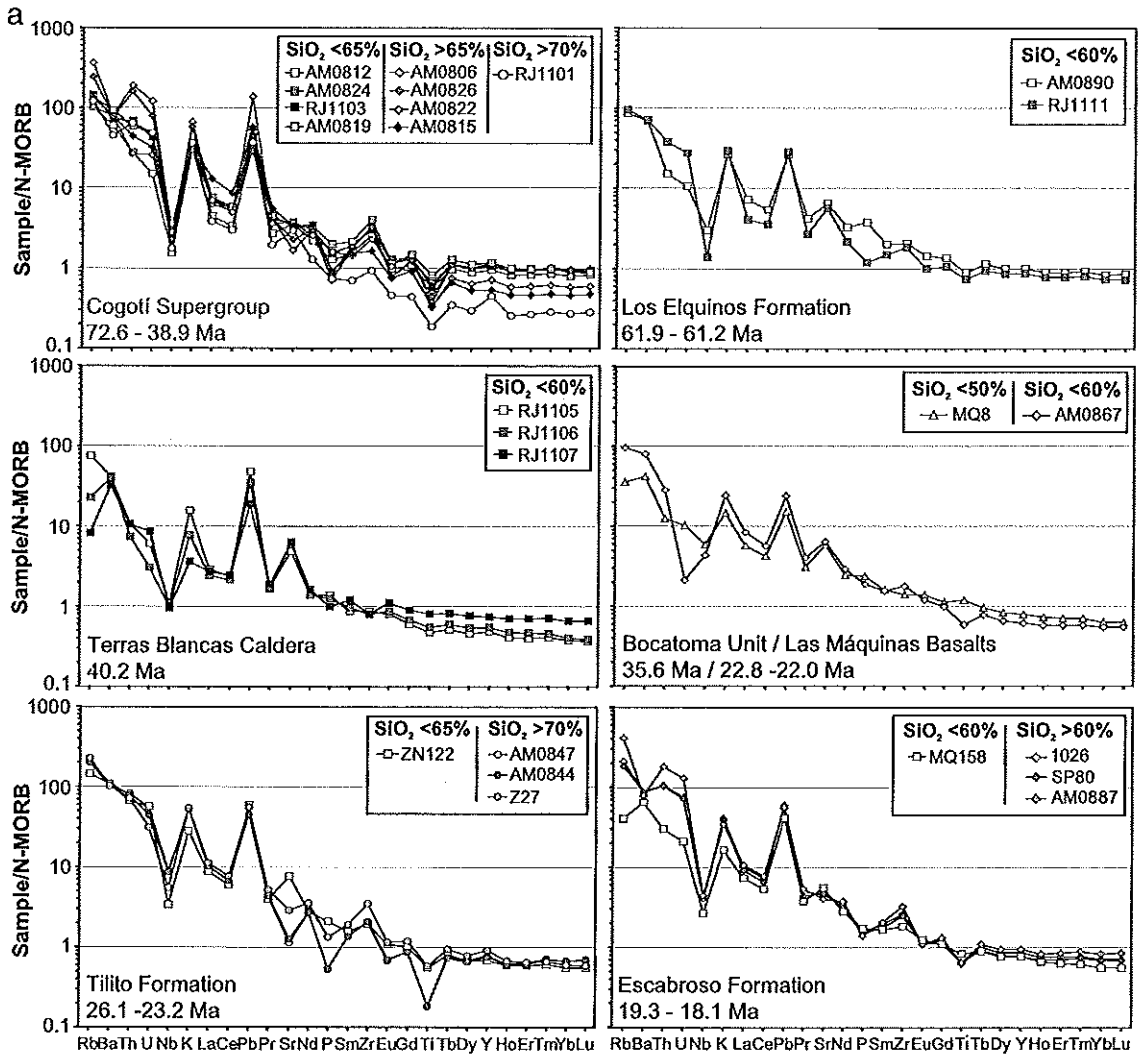

Fig. 6. Multi-element plots normalised to N-MORB values (Sun and McDonough, 1989) for each of the major Late Cretaceous to Late Miocene geological formations/units and the P–T basement.

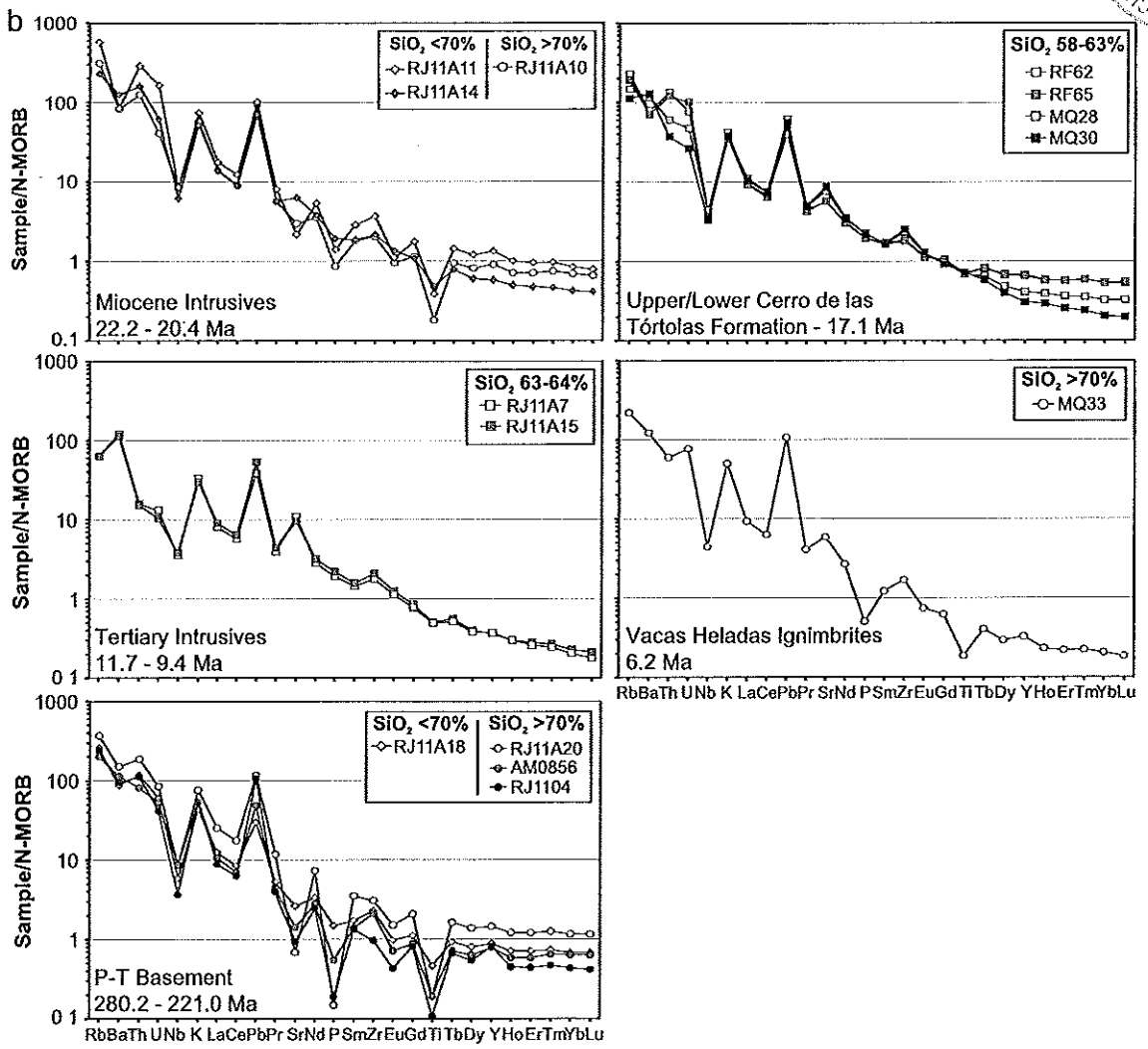

Fig. 6 (*continued*).

(Fig. 8) could be interpreted as an indication of a decrease in partial melting of the mantle over time. This is at odds with the evidence for an increase in fluid flux from the slab (e.g., increasing Ba/Nb and U/Th (Fig. 8)). Therefore, these element ratios are interpreted as representing an increase in the enrichment of the mantle wedge, either with subduction derived components (e.g., sediments) and/or due to an influx of asthenospheric mantle.

During this time interval magmatism was also occurring in a back-arc position, east of the main volcanic arc. These extension-related basalts (Río Frío Basalts 55.9 ± 1.9 Ma (Litvak and Page, 2002)) have a distinct composition to the magmas erupted in the main volcanic arc. These basalts exhibit high fluid immobile, incompatible TE ratios (e.g., Nb/Zr) and low fluid mobile, incompatible TE ratios (e.g., Ba/Nb), suggesting they represent small degree partial melts which received little influence from slab-derived fluids, as suggested by Litvak and Poma (2010).

7.1.2. The Late Oligocene to Early Miocene

After a period of reduced arc magmatism between the Mid Eocene and the Late Oligocene (Parada et al., 1988, 2007) the Doña Ana Group (Tilito and Escabroso Formations) was erupted at the arc front. The samples of the Tilito Formation (Lower Doña Ana Group) from closer to the trench, have quite distinct compositions from those collected farther to the east, despite their being of the same age (Late Oligocene). The more westerly rhyolitic ignimbrites (AM0844, AM0846 and AM0847) are highly evolved (SiO_2 > 72 wt.%), have high concentrations of Nb (>18 ppm) accounting for high Nb/Zr and Nb/Yb ratios (Figs. 8 and 9). The more easterly samples (ZN122 and Z27) are less evolved with andesitic–dacitic compositions.

The presence of inherited zircon cores with P–T ages (ranging between 278.5 ± 2.9 Ma and 241 ± 2.7 Ma, Table 1) in the samples of the Tilito Formation from the Chilean side of the margin, suggests bulk assimilation of the P–T basement (e.g., Beard et al., 2005). It has previously been suggested that the contamination of the Late Oligocene–Early Miocene arc magmas with P–T aged lower crust accounts for the relatively high $^{87}Sr/^{86}Sr$ ratios (0.705335) of the Doña Ana Group (e.g., Kay and Abbruzzi, 1996). The range of inherited zircon ages obtained by this study is within the range of U–Pb ages obtained for the Choiyoi Group and Pastos Blancos Group, which comprise part of the basement stratigraphy. These basement groups also appear adjacent to the Tilito Formation in outcrop and therefore it seems likely that the magmas of the Tilito Formation have assimilated this crust. The similar geochemical features (e.g., negative Eu, Ti and P anomalies, positive Y anomalies, high Nb/Zr ratios) observed in samples of the P–T basement and the rhyolitic samples of the Tilito Formation (Figs. 4, 5, and 7) support this suggestion. No inherited zircon cores were found in the

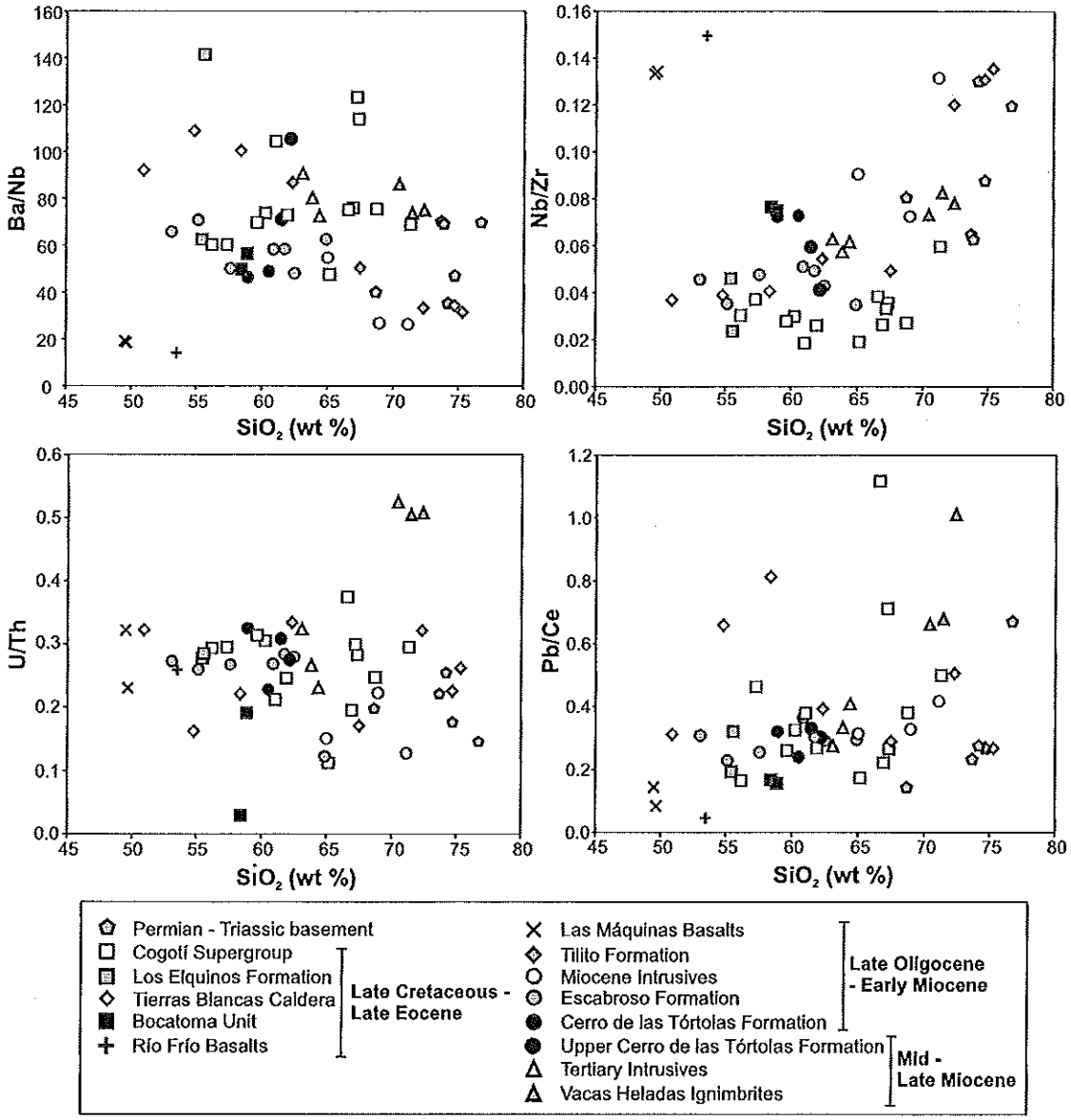

Fig. 7. Ratios of fluid-mobile/immobile incompatible TE (Ba/Nb, U/Th and Pb/Ce) and fluid-immobile/immobile incompatible TE (Nb/Zr) plotted against SiO_2 content.

more mafic samples erupted farther to the east, providing evidence for a more limited interaction between the arc magmas and the basement farther away from the trench.

Coeval with the eruption of the Tilito Formation, the Las Máquinas Basalts were emplaced to the east, on the Argentinean side of the margin. These basalts have high Nb/Zr (Fig. 9) and Nb/U ratios and low fluid mobile/immobile incompatible element ratios (e.g., Ba/Nb and Pb/Nb) (Fig. 7) suggesting a limited influence of fluids derived from the subducting slab and initially relatively small degrees of partial melting. This is consistent with these geological units representing back-arc volcanism (Kay and Abbruzzi, 1996; Kay et al., 1991; Litvak and Poma, 2010). On a plot of Nb/Yb vs. Th/Yb the Las Máquinas Basalt plots between the fields for E-MORB and OIB (Fig. 10) suggesting extraction of small degree melts from a relatively enriched mantle source. This might be expected for a region of the subcontinental mantle which has experienced less partial melting and melt extraction than the mantle situated beneath the main volcanic arc. These compositions are also similar to those of Holocene alkali basalts and trachy-basalts erupted in the back-arc region of the Southern Volcanic Zone (SVZ) (Jacques et al., 2013). These authors suggest that these back-arc basalts are formed from the melting of enriched Proterozoic subcontinental lithosphere.

The Miocene Intrusives, which consist of Early Miocene granitoids that cropout on the border between the Frontal Cordillera and the Precordillera, are highly enriched in incompatible elements such as Rb, Nb, Th, and Ce, which likely reflects their highly evolved nature. Ratios of fluid mobile/immobile incompatible element ratios are generally low, suggesting the limited influence of slab-derived fluids on the primary magmas (Figs. 7, 8 and 9). The U–Pb zircon ages presented here for the Miocene Intrusives (22.2 ± 0.23 to 20.43 ± 0.31 Ma) overlap with the ages obtained for the back-arc Las Máquinas Basalts (K/Ar dated between 22.8 ± 1.1 Ma to 22.0 ± 0.8 Ma (Kay et al., 1991; Litvak et al., 2005)). Like the Las Máquinas Basalts, the relatively high Nb/Zr ratios could be indicative of relatively small degree partial melting, which would be consistent with their generation relatively far away from the trench and therefore over a more dehydrated slab.

Geochemical modelling suggests that the compositions of the Miocene Intrusives can be generated from the composition of the Las Máquinas Basalts, by a combination of fractional crystallisation (FC),

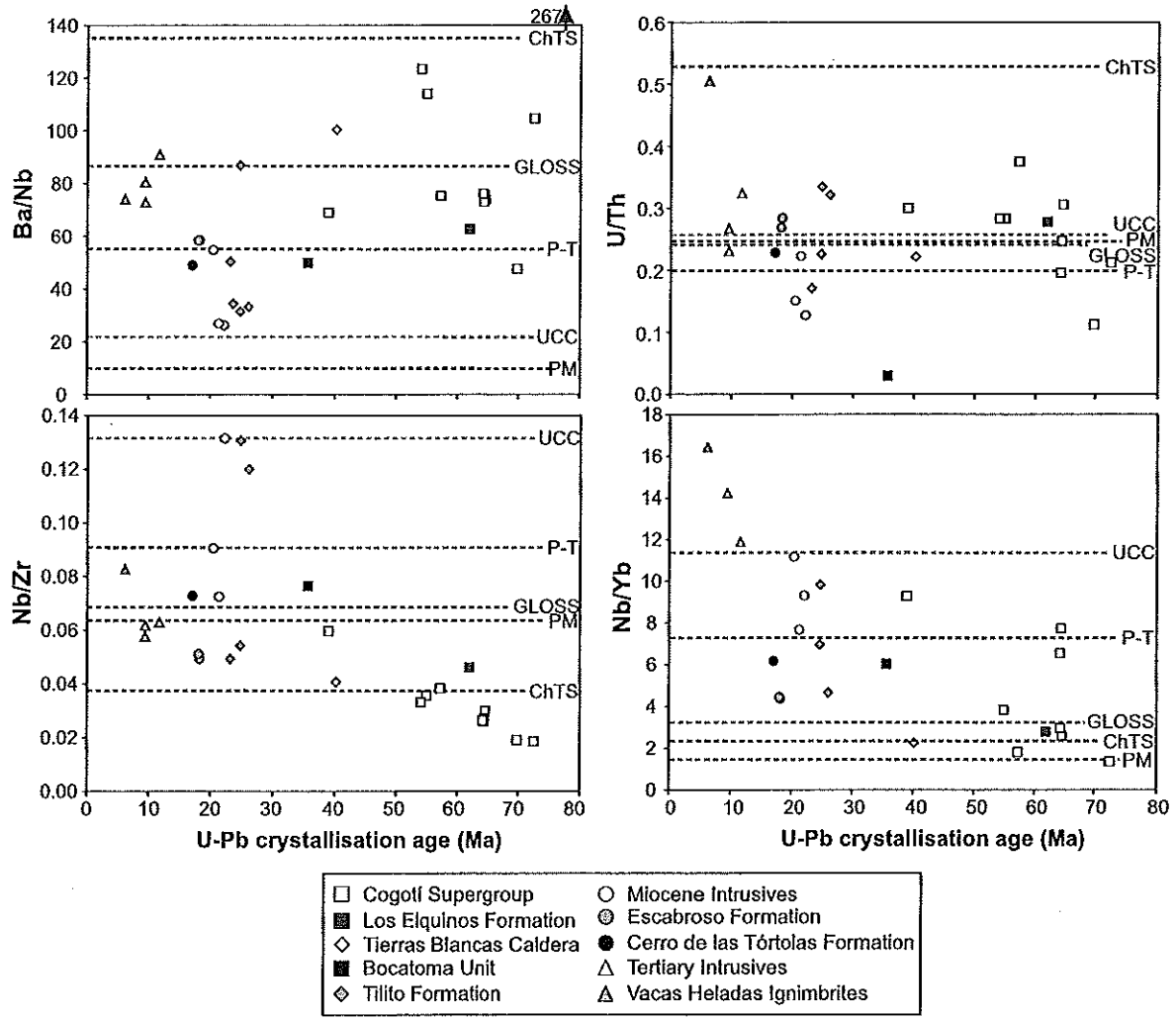

Fig. 8. Plots of fluid-mobile/immobile incompatible element ratios and immobile/immobile incompatible element ratios against corresponding U–Pb crystallisation ages. The values for primitive mantle (PM (Sun and McDonough, 1989)), upper continental crust (UCC (Taylor and McLennan, 1995)), global sediment composition (GLOSS (Plank and Langmuir, 1998)), the composition of sediment currently in the southern Chile trench (ChTS (Jacques et al., 2013)) and the average composition of the P–T basement (this study) are also shown.

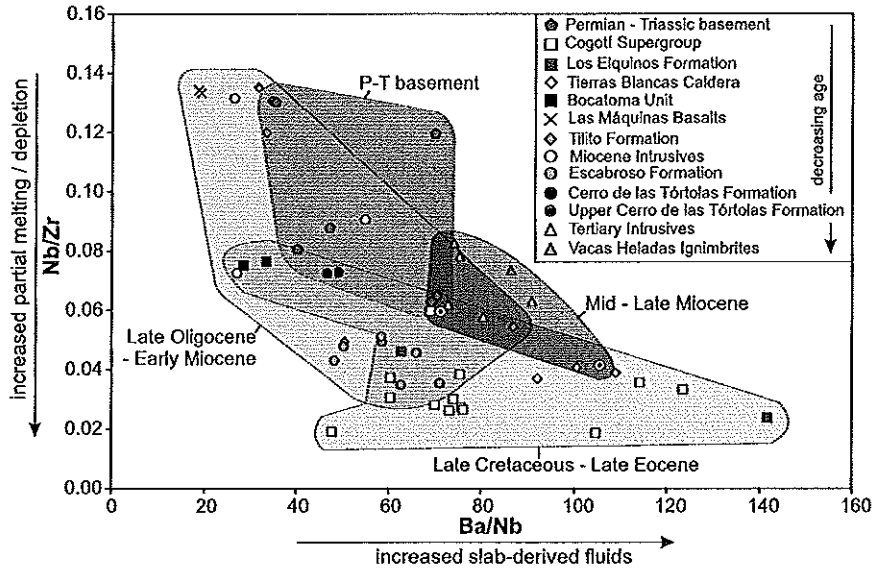

Fig. 9. A plot of Nb/Zr vs. Ba/Nb for the Late Cretaceous to Late Miocene arc magmatic rocks (both intrusive and extrusive), and samples of the P–T basement.

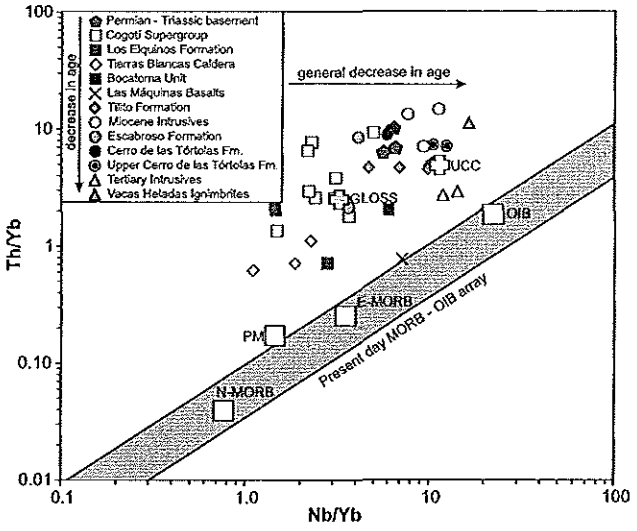

Fig. 10. Th/Yb vs. Nb/Yb discrimination diagram as defined by Pearce (2008). Values for N-MORB, P-MORB, OIB and primitive mantle (PM) from Sun and McDonough (1989), for GLOSS from Plank and Langmuir (1998) and upper continental crust (UCC) from Taylor and McLennan (1995).

and assimilation and fractional crystallisation (AFC) processes involving the P–T basement (Fig. 11), consistent with the presence of inherited zircon in sample RJ11A14 (Table 1). It is difficult to separate the effects of FC from AFC processes, as in this case the fractionating assemblage is virtually the same as the mineral assemblage found in the P–T basement. Evidence from O and Hf isotopic composition of zircon (Jones et al., 2015) suggests that the Miocene Intrusives have also interacted with an ancient, Grenville-aged basement, which is present in the Precordillera. The modelling supports the involvement of this ancient basement terrane, however it is apparent that the majority (~85%) of the assimilated crust must be the P–T basement (Fig. 11). Overall, this suggests that these granitoids, which are located farther away from the trench than the Las Máquinas Basalts, have formed through the differentiation and interaction of these back-arc basaltic melts with the pre-existing Andean crust.

The geochemical modelling also suggests that fractional crystallisation of these basaltic melts can account for the compositions of the less evolved sequences of the Tilito Formation, which outcrop further away from the trench (Tilito Formation – Argentina) (Fig. 11). The more evolved compositions closer to the trench (Tilito Formation – Chile) are more difficult to generate via FC or AFC processes when using the Las Máquinas Basalts as a starting composition. This suggests that the sequences for the Tilito Formation which are closer to the Chilean trench may be the result of decoupled assimilation and fractional crystallisation (i.e. FCA) (Cribb and Barton, 1996) and/or mixing processes involving the P–T basement (Fig. 11), as suggested by the presence of inherited zircon cores. Alternatively they may be derived from a different mantle source, which has received a greater influence from subduction related components.

The extrusive rocks of the younger Escabroso Formation (Upper Doña Ana Group) and Cerro de Las Tórtolas Formation (Early Miocene) are generally more mafic than the Late Oligocene samples of the Tilito Formation and Miocene Intrusives (Fig. 4) and have lower Nb/Zr and Nb/Yb ratios, and higher fluid mobile/immobile incompatible element ratios (e.g., Ba/Nb and U/Nb) (Figs. 7, 8 and 9). This suggests a higher degree of partial melting of the mantle wedge due to an increase in fluids derived from the subducting slab, alongside more limited FC and assimilation of the Andean crust. During the Early Miocene (~18 Ma) the JFR began intersecting the Andean margin in this region leading to the initiation of the shallowing of the subducting slab (e.g., Yañez et al., 2001, 2002). Therefore an increase in the influence of fluids derived from the subducting slab on the source of Early Miocene arc magmas might be expected.

These Early Miocene formations also lack any zircon inheritance (Table 1) providing further evidence for a reduction in the bulk assimilation of the Andean basement in comparison to the Late Oligocene, Tilito Formation and Miocene Intrusives. However, isotopic data still suggests the involvement of some radiogenic crustal components (e.g., Bissig et al., 2003; Jones et al., 2015; Kay and Abbruzzi, 1996; Kay et al., 1991).

7.1.3. The Mid to Late Miocene

During the Mid to Late Miocene the angle at which the Nazca plate was subducting shallowed and as a consequence arc magmatism migrated to the east. During this time interval the Tertiary Intrusives were emplaced in the eastern Frontal Cordillera and the Precordillera. These dacitic to trachydacitic units have relatively low Th, U and Rb concentrations, in addition to HREE depletions (Fig. 6). Kay and Abbruzzi (1996) also identified low Th, U and REE concentrations in the Precordilleran, Miocene arc magmatic rocks and also found them to have the least radiogenic Sr ($^{87}Sr/^{86}Sr$ = 0.7032–0.7038) and Pb ($^{206}Pb/^{204}Pb$ = 17.8–17.9, $^{207}Pb/^{204}Pb$ = 15.48–15.49, $^{208}Pb/^{204}Pb$ = 37.4–37.5) isotopic signatures of all the Cenozoic arc magmatic rocks in the Pampean flat-slab segment. They attribute this to the interaction of the Miocene arc magmas with the distinct, Grenville-aged basement present in the Argentinean Precordillera; xenoliths from this basement also yield low Th, U and REE concentrations and unradiogenic Pb isotopic ratios (Abbruzzi et al., 1993). This suggestion is supported by the identification of inherited zircon cores of Proterozoic age in all Tertiary Intrusives samples analysed as part of this study (Table 1).

Kay and Abbruzzi (1996) suggested that the more radiogenic Pb isotopic composition of the Precordilleran Miocene arc magmas in comparison to the Grenvillian xenoliths ($^{206}Pb/^{204}Pb$ = 17.1–17.8, $^{207}Pb/^{204}Pb$ = 15.42–15.49, $^{208}Pb/^{204}Pb$ = 36.6–37.4), requires the interaction of the magmas with an additional component, which has a Pb isotopic composition similar to that with which the Miocene arc magmas in the Frontal Cordillera have interacted. They proposed that this source of radiogenic Pb is derived from the sub-arc mantle wedge. However, in addition to Proterozoic aged inherited cores, this study identified P–T inherited zircon cores in samples of the Tertiary Intrusives (Table 1), thus, suggesting these magmas have also interacted with crust of this age. Radiogenic Pb isotope values (e.g., $^{206}Pb/^{204}Pb$ = 18.44–18.56, $^{207}Pb/^{204}Pb$ = 15.65–15.66, $^{208}Pb/^{204}Pb$ = 38.38–38.39 (Lucassen et al., 2002)) have been determined for the Late Palaeozoic Andean crust, and therefore we propose that the P–T basement may be the source of the radiogenic Pb.

In general as the subducting Nazca plate shallowed the volcanic front expanded and migrated to the east over the course of the Miocene. However, the youngest arc rocks in the region, the Vacas Heladas Ignimbrites occur in the Frontal Cordillera. During the same time interval magmatism was occurring at the Pocho volcanic field in the Sierra de Córdoba, situated directly to the east and 700 km away from the Chile trench. The Pocho volcanic rocks are thought to be associated with the arrival of the shallowly dipping subducting slab under this part of the South American continent (e.g., Kay and Gordillo, 1994). From this it can be inferred that very little of the mantle wedge must have remained under the Frontal Cordillera. Therefore, it is likely that the Vacas Heladas Ignimbrites represent small volume lower crustal melts, generated due the influence of heat and fluids derived from the subducting slab. These volcanic deposits have the highest fluid-immobile, incompatible TE ratios (e.g., Nb/Zr and Nb/Yb (Fig. 8)) of the Mid–Late Miocene arc formations (i.e., 15–6 Ma), suggesting they represent small degrees of partial melting, consistent with the small volumes of erupted magma. The high ratios of fluid-mobile/immobile incompatible TE (e.g., Ba/Nb, Pb/Ce) obtained from the Vacas Heladas Ignimbrites compared to the other Mid to Late Miocene arc magmas, are also indicative of a high

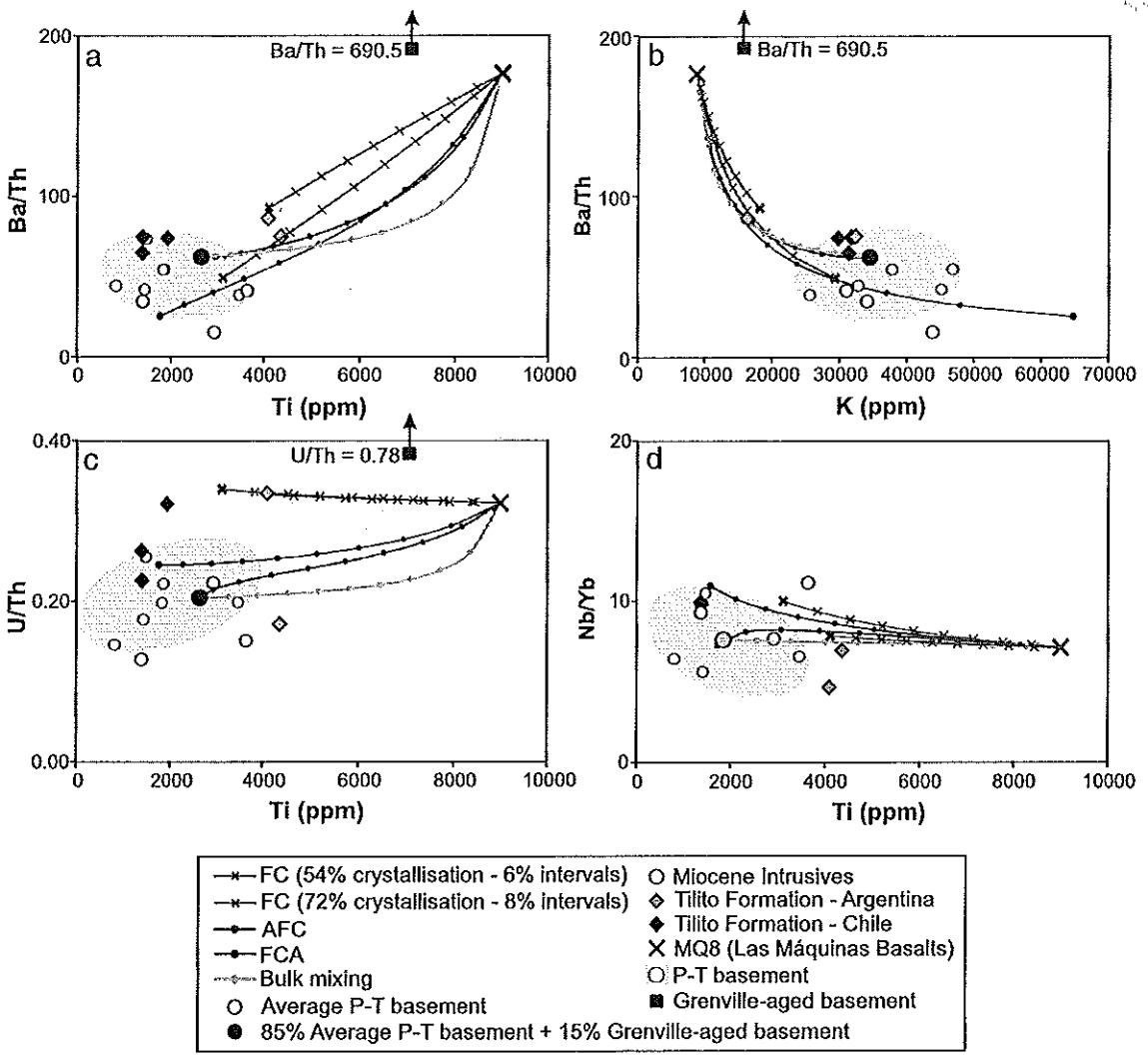

Fig. 11. Geochemical modelling conducted using the FC-AFC-FCA modeler of Ersoy and Helvacı (2010). The modelling uses the partition coefficients for intermediate melt compositions and an 'r' value of 0.3 (i.e., 30% assimilated material), as is supported by evidence from zircon isotope data (Jones et al., 2015). The starting composition used is sample MQ8 (Las Máquinas basalts) and is the least evolved sample from the region with a composition close to E-MORB (Fig. 10). The fractionating assemblage used to model the orange FC trend is plagioclase (35%), K-feldspar (15%), magnetite (20%), amphibole (5%), biotite (10%), clinopyroxene (10%) and olivine (5%); consistent with the minerals present in samples of the Las Máquinas Basalts and the more mafic samples for the Tilito Formation which outcrop in Argentina (i.e., further away from the trench) (Table A7, Supplementary Material). In this case increments represent 6% and crystallisation ends at 54%. The fractionating assemblage used to model the green FC trend is plagioclase (30%), K-feldspar (15%), magnetite (15%), amphibole (15%), biotite (13%), clinopyroxene (5%), olivine (5%), apatite (1%) and zircon (1%); consistent with the minerals present in samples of the Las Máquinas Basalts and Miocene Intrusives (Table A7, Supplementary Material). Increments on the green FC, AFC, FCA and mixing lines represent 8% and crystallisation ends at 72%, consistent with what might be expected for granitic (Miocene Intrusives) and rhyolitic rock types (Tilito Formation – Chile). The composition of the Grenville-aged basement is the average composition of xenoliths presented in Kay et al. (1996).

influence of slab-derived fluids on these magmas. These melts have subsequently been contaminated with the Late Paleozoic–Early Mesozoic basement and the older Cenozoic arc rocks, present in the upper crust. This is consistent with TE signatures obtained for the Vacas Heladas Ignimbrites; relatively high incompatible TE ratios (Figs. 7, 8, and 9) could be indicative of either relatively small degree partial melts and/or assimilation of the continental crust. This is also consistent with isotopic evidence; increasing $^{87}Sr/^{86}Sr$ ratios correlate with decreasing εNd values between the Late Oligocene and the Late Miocene, with the highest $^{87}Sr/^{86}Sr$ ratios (0.7055) and lowest εNd values (−2.0) reported for the Vacas Heladas Ignimbrites, suggesting an increase in crustal contamination with time (Kay and Abbruzzi, 1996; Kay et al., 1991; Litvak et al., 2007). Inherited zircon cores of P–T and Miocene age identify the crustal material being incorporated into the melts (Table 1).

The Mid to Late Miocene arc magmatic rocks also have adakitic signatures (Fig. 12a). Diagnostic geochemical features of adakites and their mode of formation remain controversial (e.g., Castillo, 2012). Originally it was proposed that adakites formed from the partial melting of young (<25 m.y.), basalt crust being subducted beneath volcanic arcs, where garnet and amphibole are residual phases (Defant and Drummond, 1990; Kay, 1978). Subsequently a number of other mechanisms of producing arc rocks with adakitic signatures have been outlined, including partial melting of a mafic lower crust (e.g., Chung et al., 2003; Kay et al., 1991, 2005), and high-pressure fractional crystallisation of hydrous mafic arc magmas (e.g., Castillo et al., 1999; Macpherson et al., 2006; Rodríguez et al., 2007; Rooney et al., 2011). To the south of the study area (~32 °S), Reich et al. (2003) propose that melting of young, hotspot-derived rocks associated with the JFR has resulted in the adakitic signatures of Late Miocene (~10 Ma) intrusions,

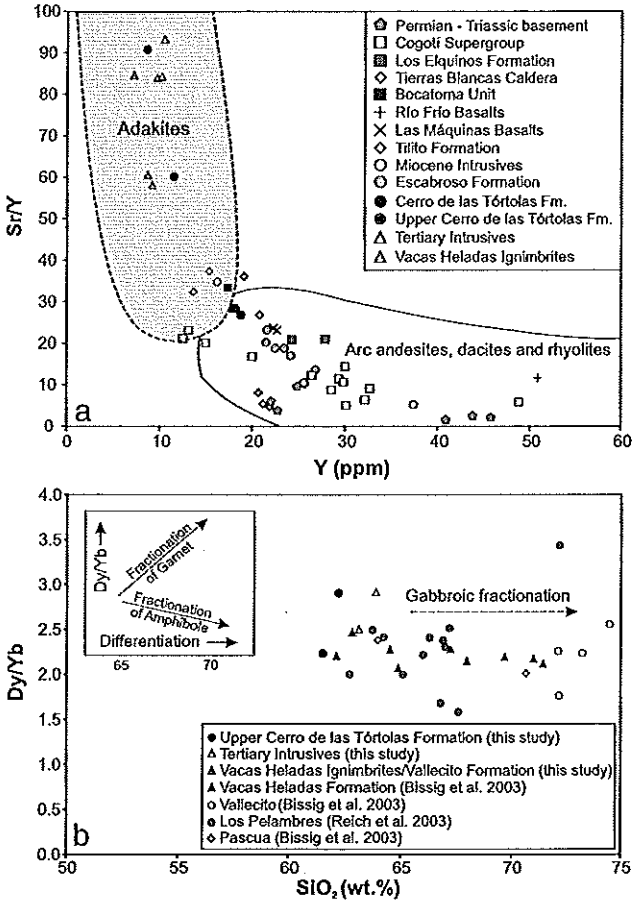

Fig. 12. a) Sr/Y vs. Y (boundaries are from Richards and Kerrich (2007)), typically used for distinguishing adakites as defined by Defant and Drummond (1990) and Drummond and Defant (1990), and b) Dy/Yb vs. SiO_2 (wt.%) for Mid to Late Miocene samples from the Central Andes. Data presented is from this study and from Bissig et al. (2003) and Reich et al. (2003).

on the basis of limited crustal thickness (<35 km at 10 Ma) at these latitudes, combined with the non-adakitic signatures of more recent arc rocks.

In the Pampean flat slab segment it is proposed that the adakitic signatures are the result of the arc magmas equilibrating with high pressure mineral assemblages, including garnet, in the lower crust (e.g., Bissig et al., 2003; Goss et al., 2011; Kay et al., 2005; Litvak et al., 2007). During this time interval the thickness of the continental crust is suggested to have increased to >45 km as a result of crustal shortening (e.g., Allmendinger et al., 1990; Kay et al., 1991). This increase of crustal thickness could have also resulted in the high-pressure fractional crystallisation of garnet or amphibole from the mafic arc magmas (e.g., Davidson et al., 2007; Macpherson et al., 2006). However, the relatively flat trend displayed on a plot of Dy/Yb against SiO_2 content (Fig. 12b) suggests these phases were not fractionated from the melts and that they underwent gabbroic fractionation, which has a limited effect on the shape of REE patterns. This provides further evidence to suggest that the Mid to Late Miocene arc magmas were equilibrating with high pressure mineral assemblages in the lower crust. Overall, the development of adakitic signatures in the Mid to Late Miocene suggests that over the course of the Late Cretaceous to Late Miocene the arc magmas generated were equilibrating with different residual mineral assemblages, with a development from lower pressure assemblages (i.e. pyroxene) to higher pressure assemblages (i.e. garnet), likely reflecting the significant increase in crustal thickness over time.

8. The geodynamic evolution of the southern Central Andes

The new geochronological and geochemical data obtained by this study provides new evidence with which to refine the tectonic and geodynamic models of the Pampean flat-slab segment. An updated evolutional model for the southern Central Andean margin between the Late Cretaceous and the Late Miocene is outlined below and in Fig. 13.

8.1. The Late Cretaceous–Early Eocene (~75–51 Ma)

During the Late Cretaceous–Early Eocene (~75–51 Ma) the magmatic arc along the western margin of South America was somewhat different to the compressional Andean arc now in existence (Fig. 13a). The oblique angle of subduction and the low convergence rates between the Farallón and South American plates are thought to have caused extension along the margin (Charrier et al., 2007; Pardo Casas and Molnar, 1987; Somoza, 1998). The Late Cretaceous to Early Eocene magmatic rocks, associated with extension, primarily consist of north–south trending plutonic belts. Volcanic rocks associated with these extensive plutonic belts are scarce and may have been removed by erosion.

TE signatures suggest the Late Cretaceous to Early Eocene arc magmas, emplaced in the Principal and Frontal Cordillera's, formed in a subduction zone setting from the partial melting of a metasomatised mantle wedge, which has been variably influenced by slab-derived fluids. Evidence from boron isotopic compositions suggests these fluids were primarily derived from the dehydration of altered oceanic crust and serpentinite (Jones et al., 2014). TE signatures, such as low overall Nb/Zr and Nb/Yb (Figs. 7 and 8), suggest significant partial melting of the mantle wedge took place during this time period. Whole-rock rare earth element geochemistry (e.g., La/Yb ratios) suggests the Late Cretaceous to Early Eocene mantle-derived melts underwent equilibration with/fractional crystallisation of a gabbroic assemblage, suggesting migration of the arc magmas through a crust of normal thickness (~30–35 km). A lack of zircon inheritance, 'mantle-like' oxygen isotope values and juvenile initial εHf values obtained for magmatic zircon (Jones et al., 2015), and low initial $^{87}Sr/^{86}Sr$ ratios reported for these plutonic belts (Parada et al., 1988), suggests minimal contamination by older continental crust. This combined evidence suggests that this time period represents a sustained period of upper crustal growth in the southern Central Andes (Fig. 13a).

8.2. The Early Eocene to Early Oligocene (~50–27 Ma)

This time period is characterised by a reduction in arc magmatism and a transition from the emplacement of primarily plutonic belts in the Principal Cordillera, to arc volcanism further away from the subduction zone trench in the Frontal Cordillera (Fig. 13b). During the Mid to Late Eocene granitoids and andesitic porphyries were emplaced in the Principal Cordillera, along with a number of intrusions related to caldera formation. In the Frontal Cordillera volcanic deposits were emplaced (e.g., the Botacoma Unit) and incompatible TE ratios (e.g., Ba/Nb, Nb/Zr) suggest these deposits were formed from small degree partial melting of the mantle wedge, with less influence from slab-derived fluids, in comparison to the plutonic belts present in the Principal Cordillera. The more limited influence of slab-derived fluids may reflect the position of this part of the arc further away from the trench, over a more dehydrated slab (Fig. 13b). An increase in the influence of crustally derived material on the compositions of these arc magmas is also identified between the intrusions emplaced in the Principal Cordillera, and the arc magmas erupted in the Frontal Cordillera. In particular, the presence of inherited zircon suggests that these Frontal Cordillera arc magmas assimilated Late Palaeozoic–Early Mesozoic basement.

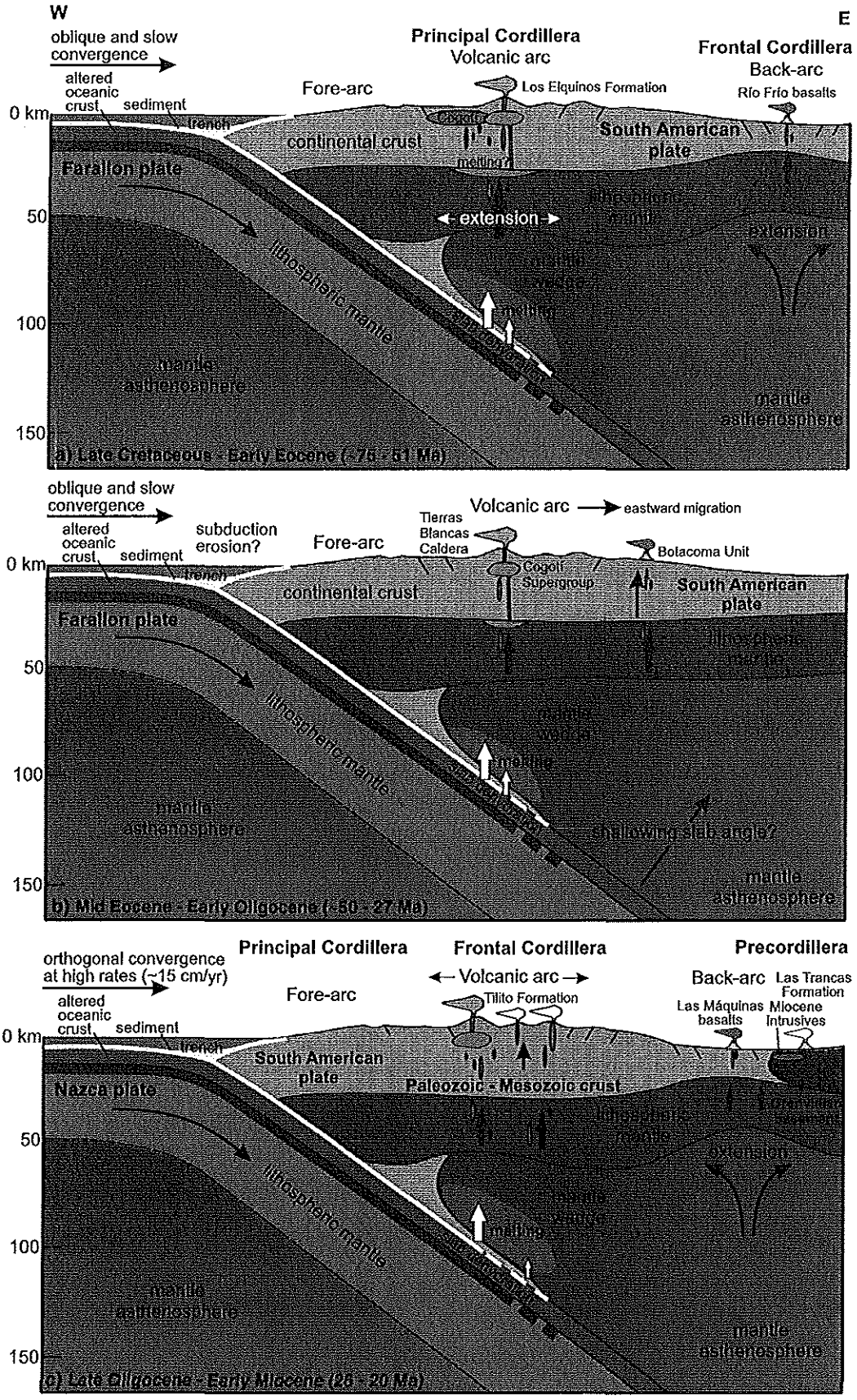

Fig. 13. Schematic cross sections of the southern Central Andean margin at approximately 29–31°S, showing the geodynamic evolution of the margin from the Late Cretaceous (~75 Ma) (a) through to the Late Miocene (6 Ma) (e).

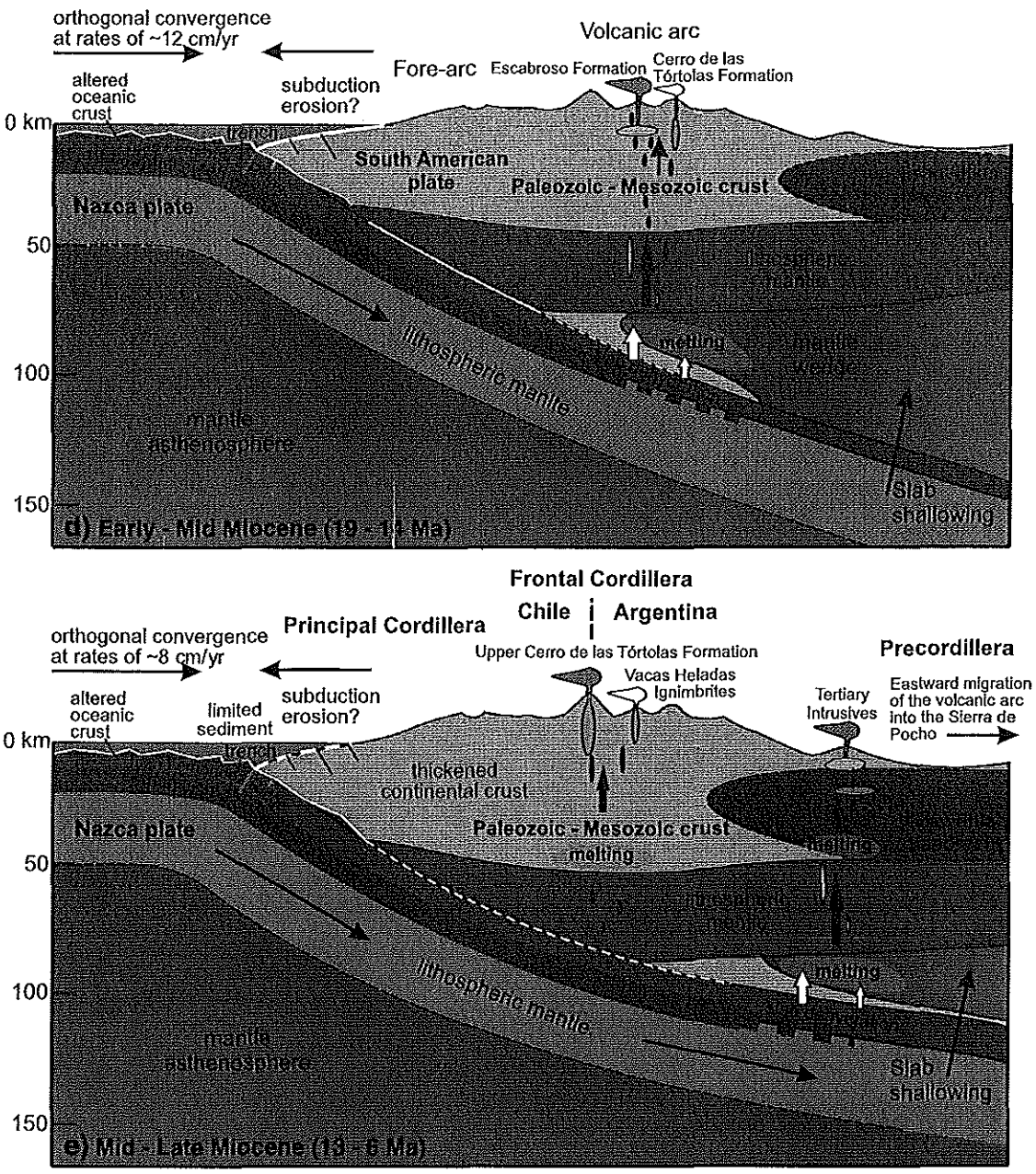

Fig. 13 (*continued*).

The poor development of the magmatic arc from 50 to 27 Ma may be related to the low convergence rates (~5–8 cm/yr) and oblique angle of subduction (NE direction) operating between the oceanic Farallón and the South American plate (e.g., Pardo Casas and Molnar, 1987; Somoza and Ghidella, 2012). The reduction in arc magmatism has previously been linked with an earlier period of flat-slab subduction along the Central Andean margin (e.g., O'Driscoll et al., 2012). The apparent eastward migration of the arc during this time interval supports the shallowing angle of subduction, however there is little other evidence to support flat-slab subduction during this time interval. For example, La/Yb ratios suggest that the ascending arc magmas were equilibrating with/fractionating a mineral assemblage which reflects a continental crust of normal thickness (~30–35 km), and that these melts were not derived from the melting of the subducting slab, which might result from flat-slab subduction (Gutscher et al., 2000a).

8.3. The Late Oligocene–Early Miocene (~26–20 Ma)

After the period of relative magmatic quiescence, this time interval is associated with a dramatic increase in magmatic activity and a broadening of the magmatic arc (Charrier et al., 2007 and references therein; Pilger, 1984). This has been related to a major change in plate configuration at ~25 Ma involving the break-up of the Farallón plate into the Cocos and Nazca plates (Lonsdale, 2005). This tectonic reconfiguration resulted in subduction becoming more normal to the margin (ENE direction) and convergence rates increasing from ~8 cm/yr to an average of ~15 cm/yr (Pardo Casas and Molnar, 1987; Somoza, 1998; Somoza and Ghidella, 2012).

In the southern Central Andes, this time period is characterised by the eruption of the Tilito Formation (Lower Doña Ana Group) in the main Andean arc, and extension related magmatism in the back-arc

region (Fig. 13c). The Tilito Formation (26.1–23.2 Ma) was erupted over a wide arc front, which is now situated in the Frontal Cordillera. An extensional regime operated to the east of the arc front, both during the late stages, and after the eruption of the Tilito Formation. This back-arc magmatism involved the eruption of the Las Máquinas Basalts (22.8–22.0 Ma (Kay et al., 1991; Litvak et al., 2005)) in the Frontal Cordillera, and the emplacement of high-K granitoids (Miocene Intrusives, 22.2–20.4 Ma) alongside dacitic to rhyolitic ignimbrites and lavas (Las Trancas Formation, 22.6 Ma), in the Argentinean Precordillera. Between ~23 and 21 Ma there is an apparent reduction in magmatism at the arc-front, with magmatic activity concentrated in the back-arc region.

TE signatures and the presence of inherited zircon grains/cores in the high- K, calc-alkaline rhyolites of the Tilito Formation erupted closest to the trench suggests the magmas bulk assimilated the Late Paleozoic–Early Mesozoic basement en route to the surface. The generally more mafic (andesitic) units of the Tilito Formation, erupted further away from the trench, show evidence for a more limited interaction with the Andean basement. The interaction of ascending mantle-derived melts with the overlying Andean continental crust is generally higher in the Late Oligocene to Early Miocene, than is evident earlier (i.e., Late Cretaceous–Mid Eocene). This evidence suggests the Late Oligocene to Early Miocene represented a period of significant crustal reworking and growth of the upper Andean continental crust due to both arc-related, and extension-related magmatism.

8.4. Early–Mid Miocene (~19–14 Ma)

After the apparent reduction in arc magmatism between ~23 and 21 Ma, arc magmatism at the arc-front was reinitiated with the eruption of the basaltic andesite and andesite lavas of the Escabroso Formation (Upper Doña Ana Group) and the Cerro de las Tórtolas Formation. An eastward migration of the arc-front is observed with the majority of arc volcanism occurring on the now Argentinean side of the margin (Fig. 13d). The REE compositions of the Escabroso and Cerro de las Tórtolas Formations (lower) indicate the arc magmas migrated through a continental crust of normal thickness and that the Andean crust had not yet undergone significant tectonic shortening related to increased compression.

The combination of higher fluid-mobile/immobile incompatible TE ratios and lower fluid-immobile incompatible TE ratios obtained for the Escabroso and Cerro de las Tórtolas Formations are indicative of an increased influence of slab-derived fluids on the melt source region, and a higher degree of partial melting, in comparison to the Late Oligocene. This is supported by boron isotopic compositions and concentrations obtained from melt inclusions (Jones et al., 2014). During this time interval subduction of the JFR began along the Andean margin. The JFR has been associated with hydrated and serpentinised oceanic lithosphere (Kopp et al., 2004), hence the subduction of this hydrated ridge may account for observed increase in the influence of slab-derived fluids on the melt source region.

8.5. Mid–Late Miocene (~13–6 Ma)

During the Mid to Late Miocene the angle of the subducting Nazca plate shallowed, causing the migration of arc magmatism to the east and an increase in compression along the margin, resulting in the main phase of uplift of the Andean range (e.g., Gregory-Wodzicki, 2000; Kurtz et al., 1997). In the Pampean flat-slab segment, arc magmatism during this time interval primarily consists of the eruption of trachyandesitic to dacitic lavas of the Upper Cerro de las Tórtolas Formation in the Frontal Cordillera, and the emplacement of shallow level, sub-volcanic andesites, dacites and trachydacites in the eastern Frontal Cordillera and the Precordillera. Subsequent to this, the last significant magmatic activity in this region is represented by the eruption of small volume, dacitic to rhyolitic ignimbrites, the Vacas Heladas Ignimbrites, in the Frontal Cordillera (Fig. 13e).

Zircon inheritance and the isotopic compositions (Jones et al., 2015; Kay et al., 1991) obtained for the Vacas Heladas Ignimbrites suggests the involvement of a Grenville-aged basement, the Late Paleozoic–Early Mesozoic Andean crust, as well as Cenozoic crust in the petrogenesis of these arc magmas. The interaction of these relatively young (~6 Ma) arc magmas, erupted in the Frontal Cordillera, with a Grenville-aged basement supports a number of structural models for the southern Central Andean margin (e.g., Gans et al., 2011; Gilbert et al., 2006; Ramos et al., 2004). These models suggest the Grenville-aged basement identified in the Argentinean Precordillera (e.g., Abbruzzi et al., 1993; Kay and Orrell, 1996; Rapela et al., 2010), has under-thrust the Frontal Cordillera as a result of crustal shortening.

A principal feature of the Mid to Late Miocene arc magmatic rocks is their adakitic signatures (Fig. 12). These have been interpreted as representing the melting and equilibration of arc magmas with a high pressure mineral assemblage, which includes garnet, in the lower crust. The occurrence of adakitic signatures in the Mid to Late Miocene is consistent with the timing of significant tectonic shortening in the region and the proposed timing of the main uplift of the Andean range (e.g., Gregory-Wodzicki, 2000; Kurtz et al., 1997; Vandervoort et al., 1995). This increase in crustal thickness has been linked to the increase in compression, in part due to the shallowing of the subducting slab (e.g., Jordan et al., 1983; Kay et al., 1991). The presence of adakitic signatures in the Tertiary Intrusives, emplaced in the Argentinean Precordillera, suggests the continental crust must have thickened to >50 km at this across-arc position (western Precordillera), as well as beneath the Frontal Cordillera.

9. Conclusions

The new age data and TE and REE compositions obtained for Late Cretaceous to Late Miocene arc magmatic rocks suggest progressive, yet variable contamination of the arc magmas over time. This study clearly demonstrates the link between the changing geodynamic setting in the southern Central Andes, specifically related to changes in the angle of the subducting slab and convergence angles and rates, and the compositions of the Late Cretaceous to Late Miocene arc magmas present in the Pampean flat-slab segment.

The TE geochemistry of the Late Cretaceous to Eocene arc rocks, combined with a lack of inherited zircon, provides evidence to suggest the Late Cretaceous to Late Eocene arc magmas had little interaction with the overlying Andean crust en route to the surface. This confirms previous evidence (e.g., Jones et al., 2015; Parada, 1990; Parada et al., 1988) and is in keeping with the more extensional regime and thinner continental crust in existence during this time period. The increased enrichment of arc magmas during this time interval is proposed to be a result of the gradual enrichment of the mantle wedge due to the increased influence of subducting components and/or the influx of asthenospheric mantle.

The TE and REE compositions of the Late Oligocene (~26 Ma) to Early Miocene (~17 Ma), and Late Miocene (~6 Ma) arc magmatic rocks present in the Frontal Cordillera, combined with the presence of P–T inherited zircon cores, provides evidence for the bulk assimilation of the P–T basement by these arc magmas. The distinct TE signatures (specifically low Th, U and REE concentrations) obtained for the Tertiary Intrusives (11.7–9.4 Ma), located in the Argentinean Precordillera, combined with the presence of inherited zircon cores of Proterozoic age, suggests these arc magmas have also interacted with the Grenville-aged basement present in the Precordillera.

The progressive enrichment of arc magmas in incompatible TE between the Late Oligocene (~26 Ma) and the Late Miocene (~6 Ma) is attributed to a combination of (1) the increased influence of subducting components on the melt source region, and (2) increased contamination of the arc magmas with existing continental crust en route to the surface. Both of these processes are linked with the shallowing angle of the

subducting Nazca plate, the increased compression along the margin, and the consequent increase in crustal thickness.

Acknowledgements

We are grateful to Nic Odling and Katarzyna Sokol for assistance in XRF analysis, and to Valerie Olive for expertise and guidance in ICP-MS analysis. James Malley and Sarah Sherlock are thanked for conducting the Ar–Ar dating, and Benjamin Heit, Dante Scatolon and Eduardo Campos for help with fieldwork logistics. We would also like to express our gratitude to Mike Hall and Robert McDonald for help with sample preparation and to Nicola Cayzer for guidance in SEM imaging. Godfrey Fitton, Alan Hastie, Cees-Jan de Hoog, Simon Harley and Jon Davidson are thanked for engaging discussions relating to the content of this manuscript. This work was funded by a NERC CASE studentship (NE/G524128/1) and the Derek and Maureen Moss Scholarship. SIMS analysis at the EIMF was supported by NERC (IMF425/1010). Linda Kirstein acknowledges support from the Carnegie Trust for the Universities of Scotland. The manuscript has benefited from thorough reviews from Pat Castillo and an anonymous reviewer.

Appendix A. Supplementary data

Supplementary data to this article can be found online at http://dx.doi.org/10.1016/j.lithos.2016.07.002.

References

Abbruzzi, J., Kay, S.M., Bickford, M.E., 1993. Implications for the nature of the Precordilleran basement from the geochemistry and age of Precambrian xenoliths in Miocene volcanic rocks, San Juan province. Actas 3, 331–339.

Allmendinger, R., Figueroa, D., Snyder, D., Beer, J., Mpodozis, C., Isacks, B., 1990. Foreland shortening and crustal balancing in the Andes at 30 S latitude. Tectonics 9, 789–809.

Astini, R.A., Benedetto, J.L., Vaccari, N.E., 1995. The early Paleozoic evolution of the Argentine Precordillera as a Laurentian rifted, drifted, and collided terrane: a geodynamic model. Geological Society of America Bulletin 107, 253–273.

Beard, J.S., Ragland, P.C., Crawford, M.L., 2005. Reactive bulk assimilation: a model for crust–mantle mixing in silicic magmas. Geology 33, 681–684.

Bissig, T., Lee, J.K.W., Clark, A.H., Heather, K.B., 2001. The Cenozoic History of Volcanism and Hydrothermal Alteration in the Central Andean Flat-Slab Region: new 40Ar–39Ar Constraints from the El Indio–Pascua Au (—Ag, Cu) Belt, 29°20′–30°30′ S. International Geology Review 43, 312–340.

Bissig, T., Clark, A.H., Lee, J.K., von Quadt, A., 2003. Petrogenetic and metallogenetic responses to Miocene slab flattening: new constraints from the El Indio-Pascua Au–Ag–Cu belt, Chile/Argentina. Mineralium Deposita 38, 844–862.

Cahill, T., Isacks, B.L., 1992. Seismicity and shape of the subducted Nazca plate. Journal of Geophysical Research: Solid Earth (1978–2012) 97, 17503–17529.

Cardó, R., Díaz, I.N., 1999. Hoja Geológica 3169-I, Rodeo, Provincias de San Juan. Instituto de Geología y Recursos Minerales, Servicio Geológico Minero Argentino, Buenos Aires.

Cardó, R., Díaz, I.N., Limarino, C.O., Litvak, V.D., Poma, S., Santamaria, G., 2007. Hoja Geológica 2969-III, Malimán, provincias de San Juan y La Rioja, Boletín 320 ed. Instituto de Geología y Recursos Minerales, Servicio Geológico Minero Argentino, Buenos Aires.

Castillo, P.R., 2012. Adakite petrogenesis. Lithos 134, 304–316.

Castillo, P.R., Janney, P.E., Solidum, R.U., 1999. Petrology and geochemistry of Camiguin Island, southern Philippines: insights to the source of adakites and other lavas in a complex arc setting. Contributions to Mineralogy and Petrology 134, 33–51.

Charrier, R., Pinto, L., Rodríguez, M.P., 2007. Tectonostratigraphic evolution of the Andean Orogen in Chile. In: Moreno, T., Gibbons, W. (Eds.), The Geology of Chile. The Geological Society, London, pp. 21–114.

Chulick, G.S., Detweiler, S., Mooney, W.D., 2013. Seismic structure of the crust and uppermost mantle of South America and surrounding oceanic basins. Journal of South American Earth Sciences 42, 260–276.

Chung, S.-L., Liu, D., Ji, J., Chu, M.-F., Lee, H.-Y., Wen, D.-J., Lo, C.-H., Lee, T.-Y., Qian, Q., Zhang, Q., 2003. Adakites from continental collision zones: melting of thickened lower crust beneath southern Tibet. Geology 31, 1021–1024.

Cribb, J.W., Barton, M., 1996. Geochemical effects of decoupled fractional crystallization and crustal assimilation. Lithos 37, 293–307.

Davidson, J.P., Harmon, R.S., Wörner, G., 1991. The source of central Andean magmas; some considerations. Geological Society of America Special Papers 265, 233–244.

Davidson, J., Turner, S., Handley, H., Macpherson, C., Dosseto, A., 2007. Amphibole "sponge" in arc crust? Geology 35, 787–790.

Defant, M.J., Drummond, M.S., 1990. Derivation of some modern arc magmas by melting of young subducted lithosphere. Nature 347, 662–665.

Drummond, M.S., Defant, M.J., 1990. A model for Trondhjemite–Tonalite–Dacite genesis and crustal growth via slab melting: archean to modern comparisons. Journal of Geophysical Research: Solid Earth 95, 21503–21521.

Emparan, C., Pineda, G., 1999. Area Condoriaco-Rivadavia, Región de Coquimbo. Servicio Nacional de Geologia y Mineria, Mapas Geológicos, Santiago.

Ersoy, Y., Helvacı, C., 2010. FC–AFC–FCA and mixing modeler: a Microsoft® Excel© spreadsheet program for modeling geochemical differentiation of magma by crystal fractionation, crustal assimilation and mixing. Computers & Geosciences 36, 383–390.

Finney, S., 2007. The parautochthonous Gondwanan origin of the Cuyania (greater Precordillera) terrane of Argentina: a re-evaluation of evidence used to support an allochthonous Laurentian origin. Geologica Acta: An International Earth Science Journal 5, 127–158.

Fitton, J.G., Godard, M., 2004. Origin and evolution of magmas on the Ontong Java Plateau. Geological Society, London, Special Publications 229, 151–178.

Fitton, J.G., Saunders, A.D., Larsen, L.M., Hardarson, B.S., Norry, M.J., 1998. Volcanic rocks from the southeast Greenland margin at 63°N: composition, petrogenesis, and mantle sources. Proceedings of the Ocean Drilling Programme Scientific Results 152, 331–350.

Fromm, R., Zandt, G., Beck, S.L., 2004. Crustal thickness beneath the Andes and Sierras Pampeanas at 30°S inferred from Pn apparent phase velocities. Geophysical Research Letters 31, L06625.

Gans, C.R., Beck, S.L., Zandt, G., Gilbert, H., Alvarado, P., Anderson, M., Linkimer, L., 2011. Continental and oceanic crustal structure of the Pampean flat slab region, western Argentina, using receiver function analysis: new high-resolution results. Geophysical Journal International 186, 45–58.

Gilbert, H., Beck, S., Zandt, G., 2006. Lithospheric and upper mantle structure of central Chile and Argentina. Geophysical Journal International 165, 383–398.

Goss, A., Kay, S., Mpodozis, C., 2011. The geochemistry of a dying continental arc: the Incapillo Caldera and Dome Complex of the southernmost Central Andean Volcanic Zone (~28° S). Contributions to Mineralogy and Petrology 161, 101–128.

Goss, A.R., Kay, S.M., Mpodozis, C., 2013. Andean adakite-like high-Mg andesites on the northern margin of the Chilean–Pampean flat-slab (27–28.5° S) associated with frontal arc migration and fore-arc subduction erosion. Journal of Petrology 54, 2193–2234.

Gregory-Wodzicki, K.M., 2000. Uplift history of the Central and Northern Andes: a review. Geological Society of America Bulletin 112, 1091–1105.

Gutscher, M.-A., Maury, R., Eissen, J.-P., Bourdon, E., 2000a. Can slab melting be caused by flat subduction? Geology 28, 535–538.

Gutscher, M.A., Spakman, W., Bijwaard, H., Engdahl, E.R., 2000b. Geodynamics of flat subduction: seismicity and tomographic constraints from the Andean margin. Tectonics 19, 814–833.

Hildreth, W., Moorbath, S., 1988. Crustal contributions to arc magmatism in the Andes of Central Chile. Contributions to Mineralogy and Petrology 98, 455–489.

Irvine, T., Baragar, W., 1971. A guide to the chemical classification of the common volcanic rocks. Canadian Journal of Earth Sciences 8, 523–548.

Jacques, G., Hoernle, K., Gill, J., Hauff, F., Wehrmann, H., Garbe-Schönberg, D., van den Bogaard, P., Bindeman, I., Lara, L., 2013. Across-arc geochemical variations in the Southern Volcanic Zone, Chile (34.5–38.0° S): constraints on mantle wedge and slab input compositions. Geochimica et Cosmochimica Acta 123, 218–243.

James, D.E., 1982. A combined O, Sr, Nd, and Pb isotopic and trace element study of crustal contamination in central Andean lavas, I. Local geochemical variations. Earth and Planetary Science Letters 57, 47–62.

Jarvis, A., Reuter, H.I., Nelson, A., Guevara, E., 2008. Hole-filled SRTM for the Globe Version 4, Available from the CGIAR-CSI SRTM 90m Database.

JICA-MMAJ, 1999. In: SEGEMAR (Ed.), Informe de la exploración de mineral en la región Cordillera Oriental Andina, República Argentina, p. 164 Buenos Aires.

Jones, R.E., De Hoog, J.C.M., Kirstein, L.A., Kasemann, S.A., Hinton, R., Elliott, T., Litvak, V.D., 2014. Temporal variations in the influence of the subducting slab on Central Andean arc magmas: evidence from boron isotope systematics. Earth and Planetary Science Letters 408, 390–401.

Jones, R.E., Kirstein, L.A., Kasemann, S.A., Dhuime, B., Elliott, T., Litvak, V.D., Alonso, R., Hinton, R., 2015. Geodynamic controls on the contamination of Cenozoic arc magmas in the southern Central Andes: insights from the O and Hf isotopic composition of zircon. Geochimica et Cosmochimica Acta 164, 386–402.

Jordan, T.E., Isacks, B.L., Allmendinger, R.W., Brewer, J.A., Ramos, V.A., Ando, C.J., 1983. Andean tectonics related to geometry of subducted Nazca plate. Geological Society of America Bulletin 94, 341–361.

Kay, R.W., 1978. Aleutian magnesian andesites: melts from subducted Pacific ocean crust. Journal of Volcanology and Geothermal Research 4, 117–132.

Kay, S.M., Abbruzzi, J.M., 1996. Magmatic evidence for Neogene lithospheric evolution of the central Andean "flat slab" between 30°S and 32°S. Tectonophysics 259, 15–28.

Kay, S., Gordillo, C., 1994. Pocho volcanic rocks and the melting of depleted continental lithosphere above a shallowly dipping subduction zone in the central Andes. Contributions to Mineralogy and Petrology 117, 25–44.

Kay, S.M., Mpodozis, C., 2002. Magmatism as a probe to the Neogene shallowing of the Nazca plate beneath the modern Chilean flat slab. Journal of South American Earth Sciences 15, 39–57.

Kay, S.M., Orrell, S., 1996. Zircon and whole rock Nd–Pb isotopic evidence for a Grenville age and a Laurentian origin for the Basement of the Precordillera in Argentina. Journal of Geology 104, 637.

Kay, S.M., Maksaev, V., Moscoso, R., Mpodozis, C., Nasi, C., 1987. Probing the evolving Andean lithosphere; Mid–Late Tertiary magmatism in Chile (29°–30°30′S) over the modern zone of subhorizontal subduction. Journal of Geophysical Research 92, 6173–6189.

Kay, S.M., Ramos, V.A., Mpodozis, C., Sruoga, P., 1989. Late Paleozoic to Jurassic silicic magmatism at the Gondwana margin: analogy to the Middle Proterozoic in North America? Geology 17, 324–328.

Kay, S.M., Mpodozis, C., Ramos, V.A., Munizaga, F., 1991. Magma source variations for mid–late Tertiary magmatic rocks associated with a shallowing subduction zone and the thickening crust in the central Andes (28–33°S). Spec. Pap. Geological Society of America Bulletin 265, 113–137.

Kay, S.M., Orrell, S., Abbruzzi, J.M., 1996. Zircon and whole rock Nd–Pb isotopic evidence for a Grenville age and a Laurentian origin for the basement of the Precordillera in Argentina. The Journal of Geology 104, 637–648.

Kay, S.M., Godoy, E., Kurtz, A., 2005. Episodic arc migration, crustal thickening, subduction erosion, and magmatism in the south-central Andes. Geological Society of America Bulletin 117, 67–88.

Keller, M., 1999. Argentine precordillera: sedimentary and plate tectonic history of a Laurentian crustal fragment in South America. Geological Society of America Special Papers 341, 1–131.

Kelly, N., Hinton, R., Harley, S., Appleby, S., 2008. New SIMS U–Pb zircon ages from the Langavat Belt, South Harris, NW Scotland: implications for the Lewisian terrane model. Journal of the Geological Society 165, 967–981.

Kilian, R., Behrmann, J.H., 2003. Geochemical constraints on the sources of Southern Chile Trench sediments and their recycling in arc magmas of the Southern Andes. Journal of the Geological Society 160, 57–70.

Kirby, S., Engdahl, R.E., Denlinger, R., 1996. Intermediate-depth intraslab earthquakes and arc volcanism as physical expressions of crustal and uppermost mantle metamorphism in subducting slabs. Subduction top to bottom, pp. 195–214.

Kopp, H., Flueh, E.R., Papenberg, C., Klaeschen, D., 2004. Seismic investigations of the O'Higgins Seamount Group and Juan Fernández Ridge: aseismic ridge emplacement and lithosphere hydration. Tectonics 23.

Kurtz, A.C., Kay, S.M., Charrier, R., Farrar, E., 1997. Geochronology of Miocene plutons and exhumation history of the El Teniente region, Central Chile (34–35° 8). Andean Geology 24, 75–90.

Le Maitre, R.W., Bateman, P., Dudek, A., Keller, J., Lameyre, J., Le Bas, M., Sabine, P., Schmid, R., Sorensen, H., Streckeisen, A., 1989. A Classification of Igneous Rocks and Glossary of Terms: Recommendations of the International Union of Geological Sciences Subcommission on the Systematics of Igneous Rocks. Blackwell Oxford.

Leveratto, M., 1976. Edad de intrusivos cenozoicos en la Precordillera de San Juan y su implicancia estratigráfica. Revista de la Asociación Geológica Argentina 31, 53–58.

Limarino, C.O., Gutiérrez, P.R., Malizia, D., Barreda, V., Page, S., Ostera, H., Linares, E., 1999. Edad de las secuencias paleógenas y neógenas de las cordilleras de La Brea y Zancarrón, Valle del Cura, San Juan. Revista de la Asociación Geológica Argentina 54, 177–181.

Litvak, V.D., Page, S., 2002. Nueva evidencia cronológica en el Valle del Cura, provincia de San Juan, Argentina. Revista de la Asociación Geológica Argentina 57, 483–486.

Litvak, V.D., Poma, S., 2005. Estratigrafía y facies volcánicas y volcaniclásticas de la Formación Valle del Cura: magmatismo paleógeno en la Cordillera Frontal de San Juan. Revista de la Asociación Geológica Argentina 60, 402–416.

Litvak, V.D., Poma, S., 2010. Geochemistry of mafic Paleocene volcanic rocks in the Valle del Cura region: implications for the petrogenesis of primary mantle-derived melts over the Pampean flat-slab. Journal of South American Earth Sciences 29, 705–716.

Litvak, V.D., Kay, S.M., Mpodozis, M.,C., 2005. New K/Ar ages on Tertiary Volcanic Rocks in the Valle del Cura, Pampean flat slab segment, Argentina. Actas XVI Congreso Geológico Argentino 2, 159–164.

Litvak, V.D., Poma, S., Kay, S.M., 2007. Paleogene and Neogene magmatism in the Valle del Cura region: new perspective on the evolution of the Pampean flat slab, San Juan province, Argentina. Journal of South American Earth Sciences 24, 117–137.

Llambías, E.J., Sato, A.M., 1990. El Batolito de Colangüil (29–31° S) cordillera frontal de Argentina: estructura y marco tectonico. Andean Geology 17, 89–108.

Llambías, E.J., Sato, A.M., 1995. El batolito de Colangüil: transición entre orogénesis y anorogénesis. Revista de la Asociación Geológica Argentina 50, 111–131.

Llambias, E.J., Shaw, S., Sato, A.M., 1990. Lower Miocene plutons in the Eastern Cordillera frontal of San Juan (29° 75′ S, 69° 30′ W), 11° Congreso Geológico Argentino, San Juan, pp. 83–86.

Lonsdale, P., 2005. Creation of the Cocos and Nazca plates by fission of the Farallon plate. Tectonophysics 404, 237–264.

Lucassen, F., Harmon, R., Franz, G., Romer, R.L., Becchio, R., Siebel, W., 2002. Lead evolution of the Pre-Mesozoic crust in the Central Andes (18–27°): progressive homogenisation of Pb. Chemical Geology 186, 183–197.

Lucassen, F., Wiedicke, M., Franz, G., 2010. Complete recycling of a magmatic arc: evidence from chemical and isotopic composition of Quaternary trench sediments in Chile (36°–40°S). International Journal of Earth Sciences 99, 687–701.

Ludwig, K.R., 2008. User's Manual for Isoplot 3.7 – A Geochronological Toolkit for Microsoft Excel. Berkeley Geochronology Center Special Publication 4.

Macpherson, C.G., Dreher, S.T., Thirlwall, M.F., 2006. Adakites without slab melting: high pressure differentiation of island arc magma, Mindanao, the Philippines. Earth and Planetary Science Letters 243, 581–593.

Maksaev, V., Moscoso, R., Mpodozis, C., Nasi, C., 1984. Las unidades volcánicas y plutónicas del Cenozoico superior en la Alta Cordilera del Norte Chico (29°–31° S): Geología, Alteración hidrotermal y Mineralización. Revista Geológica de Chile 11, 12–51.

Martin, M.W., Clavero, R.,J., Mpodozis, M.,C., Cuitiño, L., 1995. Estudio Geológico de la Franja El Indio, Cordillera de Coquimbo. Servicio Nacional de Geología y Minería, Santiago.

Martin, M.W., Clavero, R.,J., Mpodozis, M.,C., 1997. Eocene to Late Miocene magmatic development of El Indio Belt, 30° S, North-central Chile, Congreso Congreso Geológico Chileno, 8 Actas 1, Antofagasta. pp. 149–153.

Martin, M.W., Clavero, R.,J., Mpodozis, M.,C., 1999. Late Paleozoic to Early Jurassic tectonic development of the high Andean Principal Cordillera, El Indio Region, Chile (29–30°S). Journal of South American Earth Sciences 12, 33–49.

McGlashan, N., Brown, L., Kay, S., 2008. Crustal thickness in the central Andes from teleseismically recorded depth phase precursors. Geophysical Journal International 175, 1013–1022.

Mpodozis, C., Cornejo, P.P., 1988. Hoja Pisco Elqui, Region de Coquimbo. In: Mpodozis, C., Davidson, J., Rivano, S. (Eds.), Carta Geologica de Chile, Servicio Nacional de Geología y Minería (SERNAGEOMIN), Santiago.

Mpodozis, C., Kay, S.M., 1990. Provincias magmáticas ácidas y evolución tectónica de Gondwana: Andes chilenos (28-31 S). Andean Geology 17, 153–180.

Mpodozis, C., Kay, S.M., 1992. Late Paleozoic to Triassic evolution of the Gondwana margin: evidence from Chilean Frontal Cordilleran batholiths (28 S to 31 S). Geological Society of America Bulletin 104, 999–1014.

Nasi, C., Mpodozis, M.,C., Cornejo, P., Moscoso, R., Maksaev, V., 1985. El Batolito Elqui-Limarí (Paleozoico Superior Triásico): características petrográficas, geoquímicas y significado tectónico. Revista Geológica de Chile 25, 26.

Nasi, C., Moscoso, R., Maksaev, V., 1990. Hoja Guanta, Regiones de Atacama y Coquimbo. In: Mpodozis, C., Davidson, J., Rivano, S. (Eds.), Carta Geologica de Chile, Servicio Nacional de Geología y Minería (SERNAGEOMIN), Santiago.

Nur, A., Ben-Avraham, Z., 1981. Volcanic gaps and the consumption of aseismic ridges in South America. Geological Society of America Memoirs 154, 729–740.

O'Driscoll, L.J., Richards, M.A., Humphreys, E.D., 2012. Nazca–South America interactions and the late Eocene–late Oligocene flat-slab episode in the central Andes. Tectonics 31.

Parada, M.A., 1990. Granitoid plutonism in central Chile and its geodynamic implications; a review. In: Kay, S.M., Rapela, C.W. (Eds.), Plutonism from Antarctica to Alaska. The Geological Society of America, Boulder, Colorado.

Parada, M.A., Rivano, S., Sepulveda, P., Herve, M., Herve, F., Puig, A., Munizaga, F., Brook, M., Pankhurst, R., Snelling, N., 1988. Mesozoic and Cenozoic plutonic development in the Andes of central Chile (30°30′–32°30′S). Journal of South American Earth Sciences 1, 249–260.

Parada, M.A., López-Escobar, L., Oliveros, V., Fuentes, F., Morata, D., Calderón, M., Aguirre, L., Féraud, G., Espinoza, F., Moreno, H., Figueroa, O., Bravo, J.M., Vásquez, R.T., Stern, C.R., 2007. Andean magmatism. In: Moreno, T., Gibbons, W. (Eds.), The Geology of Chile. The Geological Society, London, pp. 115–146.

Pardo Casas, F., Molnar, P., 1987. Relative motion of the Nazca (Farallón) and South America plates since Late Cretaceous time. Tectonics 6, 233–248.

Pearce, J.A., 2008. Geochemical fingerprinting of oceanic basalts with applications to ophiolite classification and the search for Archean oceanic crust. Lithos 100, 14–48.

Pilger, R.H., 1981. Plate reconstructions, aseismic ridges, and low angle subduction beneath the Andes. Geological Society of America Bulletin 92, 448–456.

Pilger, R.H., 1984. Cenozoic plate kinematics, subduction and magmatism: South American Andes. Journal of Geological Society London 141, 793–802.

Pineda, G., Calderón, M., 2008. Geología del área Monte Patria-El Maqui, Región de Coquimbo, Carta Geológica de Chile, Serie Geología Básica. Servicio Nacional de Geología y Minería, Santiago.

Pineda, G., Emparan, C., 2006. Geología del área Vicuña-Pichasca, Región de Coquimbo, Carta Geológica de Chile, Serie Geología Básica. Servicio Nacional de Geología y Minería, Santiago.

Plank, T., Langmuir, C.H., 1998. The chemical composition of subducting sediment and its consequences for the crust and mantle. Chemical Geology 145, 325–394.

Poma, S., Limarino, C., Litvak, V., 2005. Formación Las Trancas: expresión del arco magmático terciario en el faldeo occidental de la Precordilera de San Juan. Actas, Congreso Geológico Argentino, 16th, La Plata. Asociación Geológica Argentina, Buenos Aires, pp. 331–334.

Ramos, V.A., Kay, S.M., Page, R., Munizaga, F., 1989. La Ignimbrita Vacas Heladas y el cese del volcanismo en el valle del Cura, provincia de San Juan. Revista de la Asociación Geológica Argentina 44, 336–352.

Ramos, V.A., Cristallini, E., Pérez, D.J., 2002. The Pampean flat-slab of the Central Andes. Journal of South American Earth Sciences 15, 59–78.

Ramos, V.A., Zapata, T., Cristallini, E., Introcaso, A., 2004. The Andean thrust system—latitudinal variations in structural styles and orogenic shortening. Thrust Tectonics and Hydrocarbon Systems 82, 30–50.

Rapela, C., Pankhurst, R., Casquet, C., Baldo, E., Saavedra, J., Galindo, C., 1998. Early evolution of the Proto-Andean margin of South America. Geology 26, 707–710.

Rapela, C.W., Pankhurst, R.J., Casquet, C., Baldo, E., Galindo, C., Fanning, C.M., Dahlquist, J.M., 2010. The Western Sierras Pampeanas: Protracted Grenville-age history (1330–1030 Ma) of intra-oceanic arcs, subduction–accretion at continental-edge and AMCG intraplate magmatism. Journal of South American Earth Sciences 29, 105–127.

Reich, M., Parada, M.A., Palacios, C., Dietrich, A., Schultz, F., Lehmann, B., 2003. Adakite-like signature of Late Miocene intrusions at the Los Pelambres giant porphyry copper deposit in the Andes of central Chile: metallogenic implications. Mineralium Deposita 38, 876–885.

Richards, J.P., Kerrich, R., 2007. Special paper: adakite-like rocks: their diverse origins and questionable role in metallogenesis. Economic Geology 102, 537–576.

Rodríguez, C., Sellés, D., Dungan, M., Langmuir, C., Leeman, W., 2007. Adakitic dacites formed by intracrustal crystal fractionation of water-rich parent magmas at Nevado de Longaví Volcano (36·2°S; Andean Southern Volcanic Zone, Central Chile). Journal of Petrology 48, 2033–2061.

Rooney, T., Franceschi, P., Hall, C., 2011. Water-saturated magmas in the Panama Canal region: a precursor to adakite-like magma generation? Contributions to Mineralogy and Petrology 161, 373–388.

Sato, A.M., Llambías, E.J., Basei, M.A.S., Castro, C.E., 2015. Three stages in the Late Paleozoic to Triassic magmatism of southwestern Gondwana, and the relationships with the volcanogenic events in coeval basins. Journal of South American Earth Sciences 63, 48–69.

Sigmarsson, O., Condomines, M., Morris, J.D., Harmon, R.S., 1990. Uranium and 10Be enrichments by fluids in Andean arc magmas. Nature 346, 163–165.

Silver, P.G., Russo, R.M., Lithgow-Bertelloni, C., 1998. Coupling of South American and African plate motion and plate deformation. Science 279, 60–63.

Somoza, R., 1998. Updated azca (Farallon)–South America relative motions during the last 40 My: implications for mountain building in the central Andean region. Journal of South American Earth Sciences 11, 211–215.
Somoza, R., Ghidella, M.E., 2012. Late Cretaceous to recent plate motions in western South America revisited. Earth and Planetary Science Letters 331–332, 152–163.
Stern, C.R., 1991. Role of subduction erosion in the generation of Andean magmas. Geology 19, 78–81.
Stern, C.R., 2004. Active Andean volcanism: its geologic and tectonic setting. Revista Geológica de Chile 31, 161–206.
Stern, C.R., Kilian, R., 1996. Role of the subducted slab, mantle wedge and continental crust in the generation of adakites from the Andean Austral Volcanic Zone. Contributions to Mineralogy and Petrology 123, 263–281.
Stern, C.R., Skewes, M.A., 1995. Miocene to present magmatic evolution at the northern end of the Andean Southern Volcanic Zone, Central Chile. Andean Geology 22, 261–272.
Sun, S.S., McDonough, W.F., 1989. Chemical and isotopic systematics of oceanic basalts: implications for mantle compositions and processes. Geological Society, London, Special Publications 42, 313–345.
Syracuse, E.M., van Keken, P.E., Abers, G.A., 2010. The global range of subduction zone thermal models. Physics of the Earth and Planetary Interiors 183, 73–90.
Taylor, S.R., McLennan, S.M., 1995. The geochemical evolution of the continental crust. Reviews of Geophysics 33, 241–265.
Thomas, W.A., Astini, R.A., 2003. Ordovician accretion of the Argentine Precordillera terrane to Gondwana: a review. Journal of South American Earth Sciences 16, 67–79.
Thomas, W.A., Astini, R.A., Mueller, P.A., Gehrels, G.E., Wooden, J.L., 2004. Transfer of the Argentine Precordillera terrane from Laurentia: constraints from detrital-zircon geochronology. Geology 32, 965–968.
Vandervoort, D.S., Jordan, T.E., Zeitler, P.K., Alonso, R.N., 1995. Chronology of internal drainage development and uplift, southern Puna plateau, Argentine central Andes. Geology 23, 145–148.
Völker, D., Geersen, J., Contreras-Reyes, E., Reichert, C., 2013. Sedimentary fill of the Chile Trench (32–46°S): volumetric distribution and causal factors. Journal of the Geological Society 170, 723–736.
von Huene, R., Corvalán, J., Flueh, E., Hinz, K., Korstgard, J., Ranero, C., Weinrebe, W., 1997. Tectonic control of the subducting Juan Fernández Ridge on the Andean margin near Valparaiso, Chile. Tectonics 16, 474–488.
Wetten, A.F., 2005. Andesita Cerro Bola: Nueva unidad vinculada al magmatismo mioceno de la Cordillera de Olivares, San Juan, Argentina (30° 35′ S; 69° 30′ O). Revista de la Asociación Geológica Argentina 60, 003–008.
Wilson, B.M., 1989. Igneous Petrogenesis A Global Tectonic Approach. Springer.
Winocur, D., Litvak, V., Ramos, V., 2015. Magmatic and tectonic evolution of the Oligocene Valle del Cura basin, main Andes of Argentina and Chile: evidence for generalized extension. Geological Society, London, Special Publications 399, 109–130.
Wörner, G., Moorbath, S., Harmon, R.S., 1992. Andean Cenozoic volcanic centers reflect basement isotopic domains. Geology 20, 1103–1106.
Yañez, G.A., Ranero, C.R., von Huene, R., Díaz, J., 2001. Magnetic anomaly interpretation across the southern central Andes (32°–34°S): the role of the Juan Fernández Ridge in the late Tertiary evolution of the margin. Journal of Geophysical Research 106, 6325–6345.
Yañez, G.A., Cembrano, J., Pardo, M., Ranero, C.R., Selles, D., 2002. The Challenger–Juan Fernández–Maipo major tectonic transition of the Nazca–Andean subduction system at 33–34°S: geodynamic evidence and implications. Journal of South American Earth Sciences 15, 28–38.

CARACTERIZACIÓN PETROLÓGICA Y NUEVAS EDADES DE LOS BASALTOS DE CHUCULAQUI, PUNA AUSTRAL, PROVINCIA DE SALTA

Emma Beatriz MAISONNAVE[1] y Stella POMA[1,2]

[1] Instituto de Geociencias Básicas, Aplicadas y Ambientales de Buenos Aires (IGEBA), Departamento de Ciencias Geológicas, Facultad de Ciencias Exactas y Naturales, Universidad de Buenos Aires. E-mail: beatriz@gl.fcen.uba.ar
[2] CONICET.

RESUMEN

Se estudió un campo de lavas basálticas y basandesíticas que se exponen en Puna Austral, en cercanías de la estación ferroviaria Chuculaqui, ubicada al oeste del salar de Arizaro en la sierra de Caipe, provincia de Salta. Como resultado se presentan nuevos datos químicos y edades de estas volcanitas. De acuerdo con las relaciones de campo y las características petrográficas y geoquímicas, se reconocen dos unidades lávicas. La primera, de edad pliocena, está formada por basaltos porfíricos con fenocristales de olivina y plagioclasa. La segunda unidad, de edad pleistocena, está constituida por basandesitas porfíricas con fenocristales de plagioclasa, piroxeno y anfíbol. Con esta información se caracterizaron petrológicamente estos afloramientos y se modificó su asignación estratigráfica, ampliando el registro volcánico del Plioceno en esa región.

Palabras clave: *Volcanismo, Plioceno, Pleistoceno, Puna*

ABSTRACT

Petrological Characterization and new ages of Estación Chuculaqui Basalts, Southern Puna, Province of Salta

A basaltic and basandesite field is located west of Salar de Arizaro on Caipe range, near the old railroad Chuculaqui Station, in Southern Puna, Salta province. New ages and geochemical data set of these volcanic rocks are presented. Based on their petrographic, geochemical characteristics and field relationships, two lava flow units have been recognized. The first one, of Pliocene age, is formed by porphyritic basalts with olivine and plagioclase phenocrysts. The second one, of Pleistocene age, is a porphyritic basandesite with plagioclase, pyroxene and amphibole phenocrysts. This information allows the petrologic characterization and new stratigraphic assignation of these rocks, extending the volcanic record of Pliocene age in this region.

Keywords: *Volcanism, Pliocene, Pleistocene, Puna*

INTRODUCCIÓN

El volcanismo neógeno y cuaternario desarrollado en la Puna se vincula con la actividad del margen continental activo y los procesos que provocaron acortamiento horizontal con engrosamiento, bajo condiciones dominantemente compresivas. En la Puna salteña durante los últimos 7 Ma ocurrieron episodios distensivos a los que se asocia la efusión de lavas fisurales de composiciones básicas a intermedias, de gran dispersión areal y escaso volumen.

En la sierra de Caipe, ubicada al oeste del salar de Arizaro en la Puna salteña, al noreste de la estación Chuculaqui del ramal C^{14} del ferrocarril Belgrano, se exponen afloramientos predominantemente basálticos, que fueron incluidos por Méndez *et al.* (1979) entre sus fenobasaltos y posteriormente denominados como Basaltos de Chuculaqui en la Hoja Geológica Socompa (Zappettini y Blasco 2001).

Por el grado de preservación de la morfología de las coladas y las relaciones estratigráficas con las volcanitas de Arizaro, Zappettini y Blasco (2001) los asignaron al Pleistoceno.

En esta contribución se completa la información aportada en publicaciones anteriores (Maisonnave y Poma 2010) presentando datos químicos, microanálisis cuantitativos de las fases minerales predominantes y edades obtenidas mediante dataciones radimétricas. Esta nueva información permite caracterizar petrológicamente a las volcanitas estudiadas y proponer una nueva ubicación estratigráfica así como interpretar su significado en la evolución geológica del sector estudiado.

METODOLOGÍA

Un conjunto de muestras frescas y representativas de las unidades estudiadas fueron enviadas para su análisis a Activation Laboratories Ltd. de Canadá, donde mediante activación neutrónica y espectrometría de plasma por emisión, se determinaron tanto los elementos mayoritarios como los minoritarios y traza.

Para los microanálisis cuantitativos de

detalle en cristales de las fases minerales dominantes se utilizó un equipo CAMEBAX SX-50 con 4 espectrómetros, de la Universidad de Barcelona, España. Las determinaciones se efectuaron con un potencial de aceleración de 20 kV, empleando para las fases minerales una corriente de 15 nA.

Una de las determinaciones de edad se efectuó mediante el método $^{40}Ar/^{39}Ar$ en vidrio en el Laboratorio de Geocronología del Servicio Geológico de Canadá, y la restante determinación se realizó por el método K/Ar en roca total en el Laboratorio de Geocronología del Servicio Nacional de Geología y Minería de Chile.

AFLORAMIENTOS ESTUDIADOS

En las cercanías de la estación ferroviaria Chuculaqui (24°45'00"S y 68°03'45"O) se extiende un afloramiento lávico melanocrático de unos 6 m de potencia. Los espesores fueron medidos en los cortes laterales y el afloramiento, que cubre una superficie de unos 13 km² (Fig. 1), se apoya sobre una secuencia volcánica mesosilícea a ácida de color gris claro verdoso que integra el Complejo volcanosedimentario Quebrada del Agua, asignada al Oligoceno – Mioceno inferior (Zappettini y Blasco 2001).

Las volcanitas estudiadas forman dos unidades lávicas independientes, de espesores similares (hasta 5-6 metros en su fase distal), que constituyen derrames fisurales extruídos a partir de una fractura, expresión estructural de un lineamiento mayor de rumbo aproximadamente N-S reconocido por Zappettini y Blasco (2001). Estos dos flujos lávicos se extienden en direcciones opuestas, la colada más antigua se derrama hacia el oeste y la restante hacia el este. Las rocas que forman las coladas son de color gris oscuro a negro, presentan un relieve suave y se diferencian entre sí por sus características mineralógicas y texturales. La colada más antigua es de composición basáltica, menos extensa y se encuentra emplazada sobre una superficie de relieve relativamente plano, mientras que el flujo lávico más joven conforma una colada más extendida y de composición basandesítica que cubre un sector de topografía accidentada en la cumbre de la sierra de Caipe.

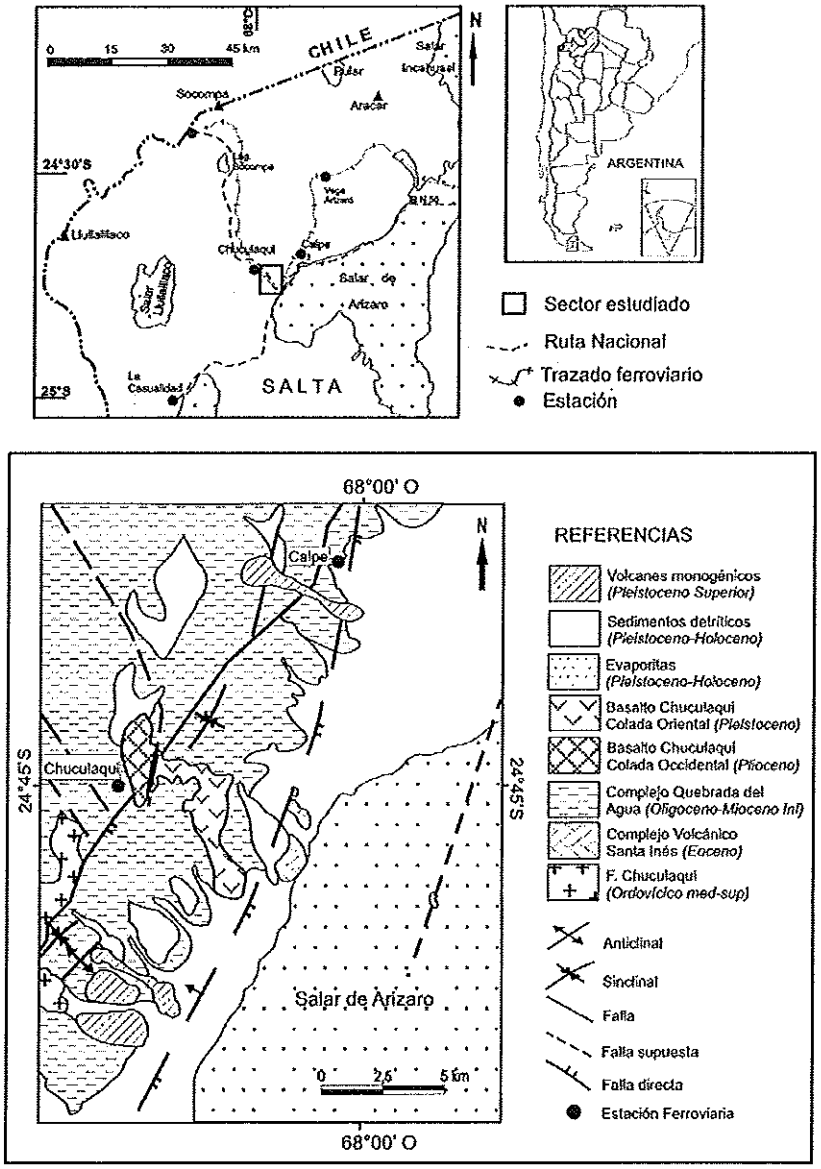

Figura 1: Croquis de ubicación y bosquejo geológico del área estudiada. Modificado de Zappettini y Blasco (2001).

Las rocas de la colada occidental, la más antigua, presentan estructura marcadamente vesicular y textura porfírica dada por abundantes fenocristales de olivina, mientras que las rocas de la colada oriental son escasamente vesiculares y la textura porfírica está caracterizada por la presencia de fenocristales de piroxeno y anfíbol (Fig. 2). En ambas coladas se preservan amígdalas irregulares de hasta 1 cm de longitud máxima, con relleno de material secundario de color blanco. El material piroclástico asociado es escaso.

Petrografía

La colada occidental está formada por lava en bloques y abarca unos 3 km², con un espesor de 4 a 5 m. Es de diseño irre-

gular y está constituida por fenobasaltos de color gris oscuro a negro, que presentan una conspícua estructura vesicular caracterizada por abundantes cavidades subredondeadas, de 1 a 15 mm de longitud máxima, que le confieren a la roca un aspecto pumíceo a escoriáceo. La textura porfírica está determinada por fenocristales de olivina (10%) y en cantidad subordinada cristales de plagioclasa (5%) distribuidos en una pasta afanítica. Se observan algunas amígdalas de hasta 1 cm de longitud, con relleno de color blanquecino, probablemente conformado por sílice de alta temperatura y zeolitas. En sección delgada se observa un gran número de vesículas muy pequeñas de diseño irregular y que ocupan, aproximadamente, el 20% del volumen de la roca. Los fenocristales (15%) están mayoritariamente constituidos por olivina fresca de hábito euhedral a subhedral y plagioclasa en menor proporción. Ésta conforma fenocristales y microfenocristales tabulares subhedrales, en general frescos y con maclado polisintético irregular, son escasos los individuos con zonalidad. Se identificaron escasos microfenocristales de clinopiroxeno subhedral.

Los fenocristales se encuentran inmersos en una pasta hialopilítica a intersertal, integrada, por orden de abundancia, por microlitos dispuestos al azar de plagioclasa fresca, abundantes gránulos subhedrales de clinopiroxeno, frecuentemente maclados, cristales de olivina y cristales subhedrales de minerales opacos. El conjunto está amalgamado en una mesostasis de vidrio castaño oscuro. Es común observar en la pasta cristales de diseño irregular de clinopiroxeno agrupados en glomérulos.

El segundo flujo lávico es más extendido, abarcando una superficie de unos 10 km^2. Se derrama hacia el oriente y presenta una planta de diseño irregular con unos 6 m de espesor reconocido. Está conformado por rocas de color gris oscuro a negro en las que se reconoce un arreglo mineral más evolucionado, respecto de la colada occidental, y escasa proporción de vesículas. La textura es porfírica y está caracterizada por fenocristales de plagioclasa, piroxeno y más escasos de anfíbol, con tamaños entre 1 y 3 mm. Macroscópicamente se reconocen agregados de cristales de piroxeno, de formas irregulares y hasta 1 cm de largo.

En sección delgada se observan escasas vesículas irregulares y la textura porfírica está determinada, en orden de abundancia, por fenocristales de plagioclasa (50%), clinopiroxeno (30%) y ortopiroxeno (15%) y escasos fenocristales de anfíbol (5%). La plagioclasa se presenta en tablillas frescas, frecuentemente con macla polisintética y más raramente con zonalidad, sus núcleos tienen composición bitownítica (An_{76-80}) y los bordes corresponden a labradorita (An_{72-65}). El clinopiroxeno es augita (Wo_{36-45} - En_{45-54}), se observa en gránulos de pequeño tamaño, a menudo zonales, mientras que los individuos de ortopiroxeno, cuya composición corresponde a enstatita incolora y no pleocroica (En_{72-81} - Wo_{3-5}), desarrollan prismas largos subhedrales. El mineral máfico de mayor desarrollo es el anfíbol, que forma cristales elongados de hasta 3 mm, con un conspicuo borde de resorción formado por una orla de minerales opacos. Los fenocristales se encuentran distribuidos en una mesostasis hialopilítica formada por microlitos de plagioclasa de composición más sódica distribuidos al azar, clinopiroxeno y anfíbol, en una base de vidrio castaño.

Una característica remarcable que exhiben estas volcanitas es la presencia de texturas de reacción. Estas texturas se interpretan como consecuencia de la incorporación de gránulos de cuarzo en la lava basáltica. Se observan xenocristales de cuarzo con diferentes grados de preservación, desde individuos de varios milímetros rodeados por una delgada película vítrea con crecimiento epitáxico de cristales aciculares de clinopiroxeno, hasta sectores en los que el cuarzo ha sido completamente consumido y se reconoce su existencia previa por relaciones texturales y el desarrollo particular de los cristales de piroxeno (Fig. 2f). Estas rocas presentan escasas vesículas, parcialmente rellenas por un material que por sus propiedades ópticas se identificó como cristobalita.

CARACTERÍSTICAS QUÍMICAS

Las rocas analizadas contienen en base anhidra entre 51 y 55% en peso de SiO_2 y entre 3,9 y 4,9% de álcalis. El contenido de Al_2O_3 oscila entre 15,7 y 17%. Los datos obtenidos mediante análisis químicos se presentan en el cuadro 1. En el diagrama TAS (Total Alkali vs Silica, Le Maitre 1989) las muestras de la colada occidental de las volcanitas de Estación Chuculaqui se clasifican químicamente como basaltos, mientras que las muestras representativas de la colada oriental se clasifican como basandesitas, todas ellas con tendencia calcoalcalina normal (Fig. 3).

Al graficar los contenidos de álcalis, FeO* y MgO en un diagrama AFM (Irvine y Baragar 1971) se observa que las rocas muestran una tendencia evolutiva sin enriquecimiento en hierro y con enriquecimiento en álcalis, como es esperable en rocas de la serie calcoalcalina (Fig. 4).

El diagrama para las concentraciones de los elementos de las tierras raras (Fig. 5), normalizados a condrito según los valores propuestos por Sun (1982), muestra un diseño similar para ambos grupos de rocas, aunque las volcanitas de la colada más joven presentan una pendiente más empinada con valores para la relación La/Yb entre 13 y 17,8 [(La/Yb) N=8,7 a 11,9] mientras que las volcanitas correspondientes a la colada basal, tienen cocientes La/Yb cercanos a 5 [(La/Yb) N=3,3 a 3,8]. Se observa una leve depresión en las tierras raras intermedias y una pequeña anomalía de Eu, lo que podría sugerir anfíbol y plagioclasa retenidos en la fuente. Estas características permiten inferir que los fundidos se habrían generado a presiones relativamente bajas, las que en un corto período de tiempo habrían evolucionado hacia condiciones de fusión a mayor presión, durante la generación de los fundidos que dieron origen a los flujos lávicos más jóvenes.

En un diagrama multielemental normalizado (valores de MORB de acuerdo con Pearce 1983), las muestras representantivas de ambas unidades presentan diseños en los que se reconocen características inherentes a los fundidos de arco (por ej.

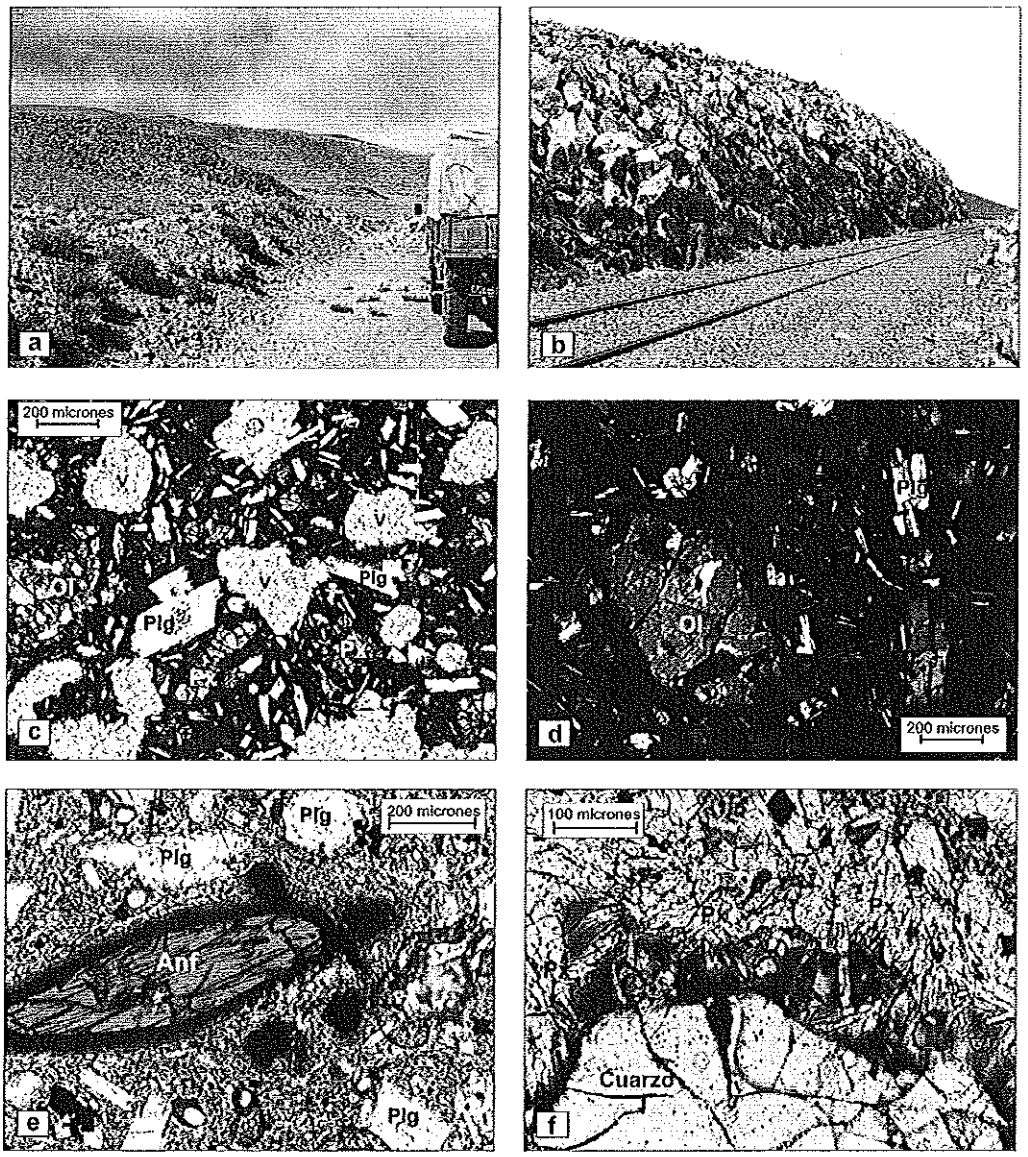

Figura 2: a-b) Aspecto del afloramiento, a) colada occidental, b) colada oriental, c-d) Fotomicrografías de la colada occidental; c) Textura porfírica con fenocristales de olivina (Ol), microfenocristales de plagioclasa (Plg) y piroxeno (Px), y abundantes vesículas (V); d) Detalle de fenocristal de olivina (Ol); e-f) Fotomicrografías de la colada oriental: (e) textura y detalle de fenocristal de anfíbol (Anf), (f) Detalle de xenocristal de cuarzo con crecimiento epitáxico de cristales aciculares de piroxeno (Px). Fotomicrografías sin analizador interpuesto, excepto c).

anomalía negativa de Nb), sin embargo en las muestras pertenecientes a la colada más joven, si bien perduran las características de arco, se hace evidente una impronta de intraplaca (Fig. 6).

EDAD

Dadas las diferencias composicionales, morfológicas y petrográficas observadas en el flujo lávico oriental con respecto a la colada occidental, se consideró necesario establecer con precisión la edad de esta manifestación eruptiva por lo que se efectuaron estudios geocronólogicos en muestras representativas de ambas coladas. En el marco del proyecto MAP (Multinational Andean Project) del que participó el Servicio Geológico Minero Argentino, se efectuó una datación en una volcanita fresca de la colada occidental obteniéndose una edad $^{40}Ar/^{39}Ar$ (en vidrio) de 3,4 ± 0,1 Ma, lo que permite asignarla al Plioceno (Fig. 7).

Por otra parte, se analizó una muestra representativa de la colada oriental utilizando el método K/Ar en roca total en el laboratorio de Geocronología dependiente del Servicio Nacional de Geología y Minería de Chile, obteniéndose una edad de 2,1 ± 0,3 Ma, por lo que este derrame lávico se asigna al Pleistoceno (Cuadro 2).

Las diferencias observadas entre estas dos unidades se explican entonces, al considerar que existió un lapso entre las emisiones lávicas que las originaron, ya que una es de edad pliocena y la otra pleistocena.

DISCUSIÓN Y RESULTADOS

Estos afloramientos fueron incluidos en los denominados Basaltos de Chuculaquí y Samenta y asignados al Pleistoceno en la Hoja Geológica Socompa (Zappettini

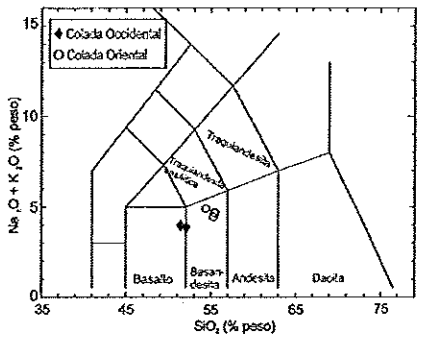

Figura 3: Diagrama TAS (Total Alcalis versus Silica) para la clasificación química de rocas volcánicas (Le Maitre 1989) para las volcanitas estudiadas.

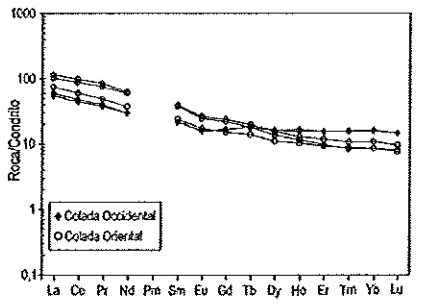

Figura 4: Diagrama AFM (Irvine y Baragar 1971) para las rocas estudiadas.

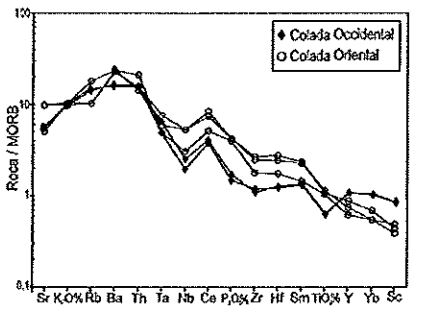

Figura 5: Diagrama de elementos de las Tierras Raras normalizados a condrito de acuerdo con los valores propuestos por Sun (1982).

y Blasco 2001). En el marco de investigaciones posteriores, Maisonnave y Poma (2010) con base en el análisis textural, la paragénesis mineral y las relaciones de campo de estos afloramientos, establecieron una edad pliocena para el flujo lávico occidental y otra pleistocena para la colada que se derrama hacia el oriente. Estas edades se confirmaron mediante estu-

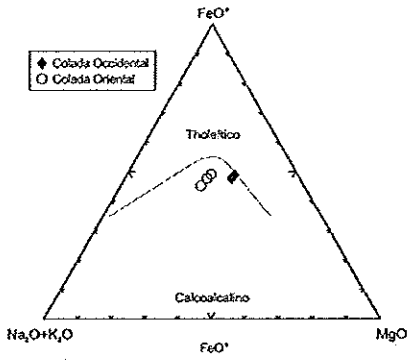

Figura 6: Diagrama multielemental para los elementos traza, normalizados respecto del MORB definido por Pearce (1983).

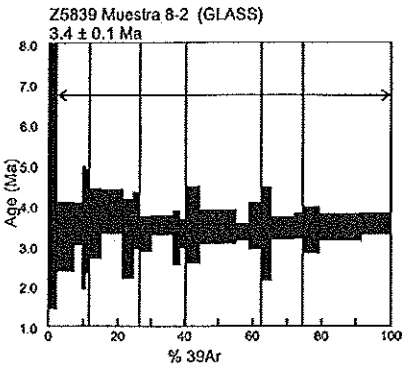

Figura 7: Datación $^{40}Ar/^{39}Ar$ en vidrio de la colada oriental (muestra BM8-2). Edad obtenida: 3,4 ± 0,1 Ma. Alícuotas con edades reproducibles en cada etapa, sin evidencias de disrupción.

dios geocronológicos cuyos resultados se presentan en esta contribución.

Los afloramientos estudiados representan dos eventos independientes. Las diferencias texturales, composicionales y en las paragénesis minerales observadas, sugieren que los fundidos que originaron las rocas de la colada pliocena son menos evolucionados y habrían tenido un tiempo menor de residencia en el reservorio magmático, respecto a los fundidos que generaron las volcanitas del derrame más joven, de edad pleistocena.

La caracterización petrográfica y química de estas rocas indica una rápida evolución de los fundidos hacia productos de fusión a mayor presión, lo que podrían interpretarse como indicativo del aumento en el espesor cortical durante el período de generación de estos magmas. De acuerdo a

CUADRO 1: Análisis químicos de las coladas estudiadas. Concentraciones de óxidos expresadas en porcentaje en peso (p.p.%), concentraciones de elementos de las Tierras Raras y trazas expresados en ppm.

Colada:	Occidental		Oriental		
Muestra	BM 8-1	BM 8-2	BM 8-3	BM 8-5	BM 14-3
SiO_2	51,58	50,98	55,19	55,32	52,86
TiO_2	0,97	0,942	1,60	1,646	1,767
Al_2O_3	17,17	16,73	16,77	15,71	15,45
Fe_2O_3	10,41	9,91	8,62	9,55	9,22
MnO	0,18	0,181	0,12	0,135	0,118
MgO	6,14	5,98	4,13	4,43	4,29
CaO	9,77	9,28	7,98	8,28	8,19
Na_2O	2,45	2,31	3,06	2,85	3,26
K_2O	1,55	1,48	1,60	1,61	1,51
P_2O_5	0,21	0,18	0,49	0,52	0,52
LOI	0,42	0,39	0,72	0,68	1,14
TOTAL	100,84	98,36	100,27	100,7	98,33
La	19,8	18	24,7	37,6	33,8
Ce	41,8	38,5	52,5	85,7	76,1
Pr	5,25	4,9	6,4	11,1	9,81
Nd	18,6	19	23,7	39,8	38,1
Sm	4,5	4,4	4,9	8	7,7
Eu	1,2	1,23	1,35	2,05	1,9
Gd	4,6	4,7	4,2	6,6	6,1
Tb	0,9	0,9	0,7	1	0,9
Dy	5,6	5,6	3,8	5,4	4,7
Ho	1,2	1,3	0,8	1	0,9
Er	3,5	3,5	2,1	2,7	2,2
Tm	0,55	0,56	0,31	0,38	0,3
Yb	3,5	3,6	1,9	2,4	1,9
Lu	0,5	0,5	0,28	0,33	0,26
Y	33,0	33,0	19,0	27,0	23,0
Sr	665,0	703,0	621,0	1212,0	1231,0
Rb	31,0	29,0	37,0	21,0	21,0
Ba	327,0	344,0	482,0	464,0	490,0
Cs	0,7	0,9	1,5		
U	1,0	1,1	1,3	0,8	0,8
Th	3,1	3,3	4,3	3,2	2,9
Hf	2,9	3,0	4,3	6,8	6,0
Ta	1,7	0,9	0,9	1,4	1,1
Sc	35,5	35,0	20,0	18,0	16,0
Cr	137,0	130,0	30,0	40,0	50,0
Ni	21,0		20,0		
Co	33,7	26,0	25,0	24,0	21,0
Nb	9,0	7,0	11,0	19,0	19,0
Zr	119,0	109,0	165,0	248,0	229,0
Cu	37,0	40,0	70,0	20,0	30,0
V	274,0	279,0	201,0	233,0	231,0

los rasgos texturales descriptos, se interpreta que los fundidos magmáticos involucrados habrían ascendido y enfriado rápidamente, incorporando escaso material de roca de caja, y alcanzado la superficie a través de estructuras de falla de dirección ENE-OSO generadas o reactivadas durante episodios distensivos.

Asimismo, la asignación geocronológica de estos eventos, permite ampliar el registro de la actividad volcánica en la región estudiada, que habría sido prácticamente contínua a lo largo del Plioceno y Pleistoceno, aunque volumétricamente menos importante que la intensa actividad magmática que caracterizó al Mioceno.

AGRADECIMIENTOS

Este trabajo fue parcialmente financiado por los proyectos UBACyT /628BA y PIP 2011-2013 GI /453. Las autoras expresan su agradecimiento al Dr. Eduardo Zappettini por posibilitar una datación a través del Proyecto MAP-SEGEMAR, y a las Dras. Brígida Castro de Machuca y Silvia L. Lagorio por las valiosas observaciones y sugerencias que permitieron mejorar el manuscrito original.

CUADRO 2: Datación K/Ar en roca total de la colada occidental (muestra BM8-5). Edad obtenida: 2,1 ± 0,3 Ma.

Muestra	Material	%K	Ar rad. nl/g	%Ar atm.	Edad Ma	Error 2σ
BM 8-5	Roca Total	1,455	0,137	93	2,4	±0,7
BM 8-5	Roca Total	1,455	0,121	85	2,1	±0,3
	Media ponderada de estos dos análisis:				2,1	±0,3

TRABAJOS CITADOS EN EL TEXTO

Irvine, T.N. y Baragar, W.R.A. 1971. A guide to the chemical classification of the common volcanics rocks. Canadian Journal of Earth Science 8: 523-548.

Le Maitre, R.W. 1989: A Classification of Igneous Rocks and Glossary of Terms. Blackwell, 193 p., Oxford.

Maisonnave, E.B y Poma, S. 2010. Basaltos de Chuculaqui, Puna salteña: caracterización petrográfica y química. 10° Congreso de Mineralogía y Metalogenia. Avances en Mineralogía, Metalogenia y Petrología: 303- 306, Río Cuarto.

Mendez, V.,Turner, J.C.M., Navarini, A., Amengual, R. y Viera, V.O. 1979. Geología de la región noroeste, provincias de Salta y Jujuy, República Argentina. DGFM, 118 p., Buenos Aires.

Pearce, J.A. 1983. Role of the sub-continental lithosphere in magma genesis at active continental margins. En: C.J.Hawkesworth y M.J.Norry (eds.), Continental Basalts and Mantle Xenoliths: 230-249.

Sun, S.S. 1982: Chemical composition and origin of the earth's primitive mantle. Geochimica et Cosmochimica Acta 46: 179-192.

Zappettini, E.O. y Blasco, G. 2001. Hoja Geológica 2569-II, Socompa, provincia de Salta. Instituto de Geología y Recursos Minerales, Servicio Geológico Minero Argentino, Boletín 260: 62 p., Buenos Aires.

Recibido: 2 de diciembre, 2015
Aceptado: 8 de septiembre, 2016

En Prensa

The making of the Chilean-Argentinean Andes

The making of the Chilean-Argentinean Andes

Editors. Folguera, A., Contreras Reyes, E., Heredia, N., Encinas, A., Iannelli, S., Oliveros, V., Dávila, F., Collo, G., Giambiagi, L., Maksymowicz, A., Iglesia Llanos, P., Turienzo, M., Naipauer, M., Orts, D., M., Litvak, V., Alvarez, O., Arriagada, C.

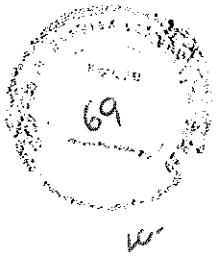

The making of the Chilean-Argentinean Andes

Book structure

Part 3. The Early Andean arc in the Chilean-Argentinean margin

Part 4. The Early Andean phases in the Chilean-Argentinean margin

Part 5. The late Andean stages in the Chilean-Argentinean margin

Preface

This book analyzes the tectonic evolution of the Argentinean and Chilean Andes through four sections, the first dealing with the structure of the fore-arc from bathymetric, gravimetric and seismic data; a second section that discusses the Paleozoic evolution of this sector, first showing the paleomagnetic behavior of the continent during this period and then discussing the different hypothesis associated with the accretion of continental slivers and consequent closure of ocean basins, producing deformation and metamorphism, reconstructing the geometry of the Early Paleozoic orogens and arcs across South American western sector; the third section analyzes the proto-Andean arc evolution, showing the paleomagnetic path of the margin, clues about its early arc activity, its relation to LIP activity associated with Pangea supercontinent desintegration and subduction zone; a fourth section discusses early development of the Andes that started as a non-organized collage of within-plate deformation sectors that lately established next to the subduction zone when the south Atlantic ocean started to expand; and finally a fifth section that discusses different aspects of the Cenozoic evolution of the Andes and its contemporaneous volcanic arc, such as development of shallow subduction settings through time, the role of dynamic subsidence, opening and closure of intra- and back-arc basins, etc.

In detail the first section is composed of three chapters. The first by Contreras Reyes et al. analyzes from wide-angle seismic data the structure of the submerged fore-arc as a result of the balance between sediment accretion and sediment subduction and crustal erosion. Then different segments are subdivided that are characterized by dominant frontal erosion or accretion and are defined by climate conditions, sediment dispersal pattern along the trench and subduction of bathymetric highs. The second chapter by Maksymowicz and Tassara analyzes the geometry of the submerged frontal prism as a function of basal and poral pressure conditions. Those systems that are subjected to frontal crustal erosion become oversteepened since these are affected by normal faulting that trigger internal saturation with sea water. Additionally, this chapter highlights the role of these morphological variations on seismic segmentation along the subduction zone. The third chapter in this first section belongs to Alvarez et al. and analyzes vertical gradients in gravity anomalies and their relation to co- and post-seismic rupture zones of giant earthquakes along the subduction zone and their complex internal structure. Additionally satellite measurements can show changes in the gravity field that could be used to predict rupture propagation along the subduction zone. Then variable fore-arc structure revealed by gravity data shows to have an important influence in the way that ruptures propagate and therefore in seismic segmentation and their potential.

The second section starts with Rapalini et al. chapter that deals with paleomagnetic reconstructions that describe South American path as part of Gondwana during the Paleozoic. The second chapter by Heredia et al. discusses the complex collage of continental slivers that have formed the western Gondwana border that is being reconstructed on the basis of the recognition of different deformational vergences, superimposed metamorphic and deformational events and recognition of internal and external parts of collisional orogens. The third chapter by Ramos is a reconstruction of the Early Paleozoic arc and consequently the western border of Gondwana, allowing identifying subsequent crustal accretions though differential exhumation levels preserved along the margin.

The third section starts with the Oliveros et al. chapter that analyzes magmatism in northern Chile showing that arc activity had already established since the Triassic, a period that had been considered devoid of subduction processes in western Gondwana. A short magmatic lull appeared at the time when the arc established nearer the subduction zone, at the time when the crust became less assimilated by mantle derived products. Naipauer et al. discuss this same magmatic stage in Northern Patagonia discussing its relation to the proto-Pacific border and LIP activity in the Karoo-Ferrar anomaly, concluding that at these latitudes plume activity influenced considerably composition of near-trench magmatism.

The fourth section starts with the Iglesia Llanos chapter that illustrates from paleomagnetic data the path of southern Gondwana and particularly South America in Jurassic times when experiments important latitudinal variations, first displacing to the north, and then returning to southern latitudes. These shift changes together with the opening of the Weddell sea at southern Gondwana are the clue to explain in a second chapter by Navarrete et al. within-plate deformations in Patagonia. This chapter also describes early deformations through the western border of Patagonia at the time of South Atlantic opening. These proto-Andean deformations are also recorded in northern Chile, lately reactivated during the development of the Neogene Chilean-Pampean flat subduction zone, as it is described in a third chapter made by Martínez et al. Gianni et al. in the fourth chapter identify synorogenic sedimentation in Northern Patagonia and southern Central Andes showing a diachronism in the uplift of the Cretaceous proto-Andes as a function of subduction of active ocean ridges as recent plate models indicate. The next chapter by Arriagada analyzes first order inflections of the South American subduction border using paleomagnetic data, determining their origin as oroclines formed diachronosly and linked to basement heterogeneities associated with crustal amalgamation in Proterozoic to Paleozoic times. Finally in this section, the chapter of Iannelli et al. calculates ancient crustal

thicknesses and degree of influence of the subduction slab on arc-related rocks of Paleogene age, determining that the Andean roots produced during the proto-Andean evolution times were practically lost during Eocene to Oligocene extensional stages along the Southern Andes. This crustal stretching could have developed in relation to the combination of an opening of a slab window during mid ocean ridge subduction and trench roll back.

The fifth section starts with the Dávila et al. chapter that quantifies subsidence and uplift influenced by the mantle dynamics, superimposed to tectonic topography. This chapter predicts within-plate subsidence next to flat subduction settings and discusses subsidence components in ancient rift systems that cannot be fully explained by thermal decay, such as the Triassic rift systems in central Argentina. Additionally this chapter analyzes mantle upwelling component associated with Neopaleozoic regional uplift and glacial activity in southern Gondwana. The second chapter by Lossada et al. is a review centered on the Frontal Cordillera uplift constituting the major mountain system developed in central Argentina whose origin was thought to be associated with the development of Chilean-Pampean flat subduction zone. Thermochronological data show that exhumation of this system is previous to the development of the flat subduction and is most likely influenced by pre-existing heterogeneities linked to the Gondwana break-up. A third chapter by Turienzo et al. analyzes mechanics of deformation of fold and thrust belt at the Southern Central Andes suggesting that shortenings have been somehow underestimated and that the structure could be considerably more complex than previously assumed. The fourth chapter by Encinas et al. discusses subsidence mechanisms associated with the late Oligocene to early Miocene transgressions in Patagonia as part of the rifting activity that started in Eocene times and continued in the early Neogene, as broad sag basins that flooded most of the ancient-collapsed Andes. The fifth chapter by Folguera et al. analyzes Cenozoic deformations of the North Patagonian Andes from the study of synorogenic sedimentation. This concludes that an intra-arc basin closure and a shallowing of the subducted slab could have contributed together to the Neogene uplift of western Patagonia. In a sixth chapter, Litvak et al. study arc-related composition of magmatism associated with the development of the Chilean-Pampean flat subduction zone and Payenia shallow subduction setting to the south, concluding that most likely these behaved as one single system in the 15-4 Ma period. Finally, the seventh chapter by Collo et al. constitutes a compilation of heat flow from wells that illustrate how the Chilean-Pampean flat subduction zone has refrigerated the lithosphere, expelling the mantle asthenosphere off the shallow configuration.

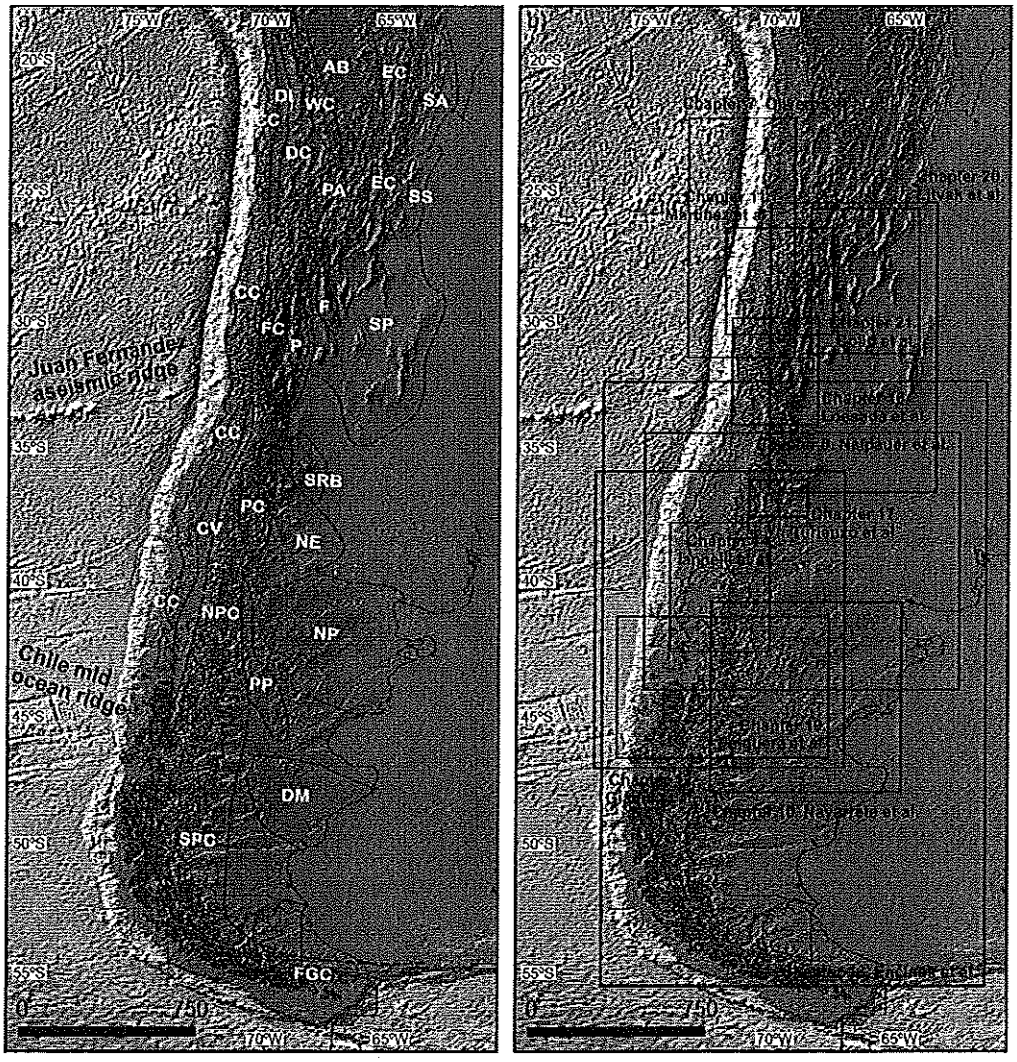

Fig. 1 To the left: Main morphostructural provinces in which the Southern Andes are divided. CC: Cordillera de la Costa, DI: Depresión Intermedia, DC: Cordillera de Domeyko, WC: Cordillera Occidental; PA: Puna; AB: Altiplano Boliviano; EC: Cordillera Oriental; SA: Sierras Subandinas; SS: Sistema de Santa Bárbara; FC: Cordillera Frontal; P: Precordillera; F: Sistema de Famatina; SP: Sierras Pampeanas; CV: Valle Central; PC: Cordillera Principal; NE: Engolfamiento Neuquino; SRB: Bloque de San Rafael; NPC: Cordillera Norpatagónica; PP: Precordillera Patagónica; NP: Macizo Norpatagónico; SPC: Cordillera Surpatagónica; DM: Macizo del Deseado; FGC: Cordillera Fueguina. To the right: Book structure (empty rectangles indicate areas analyzed in each chapter.

Acknowledgements
The authors acknowledge Jorge Rabassa for the opportunity to show their research through this book

Contributors

Juan Juis Alonso Departamento de Geología. Universidad de Oviedo. C/Jesús Árias de Velasco s/n, E33005

César Arriagada Departamento de Geología, Facultad de Ciencias Físicas y Matemáticas, Universidad de Chile, Plaza Ercilla 803, Santiago, Chile

Pilar Ávila CICTERRA - CONICET / Universidad Nacional de Córdoba

Orlando Álvarez Instituto Geofísico y Sismológico Ing. Volponi, Universidad Nacional de San Juan, Ruta 12-Km17, San Juan, Argentina. CONICET, Consejo Nacional de Investigaciones Científicas y Técnicas, Argentina

César Arriagada Departamento de Geología. Universidad de Chile. Plaza Ercilla 803, Santiago, Chile.

Pablo Bernabé Departamento de Ciencias de la Tierra, Universidad de Concepción, Casilla 160-C, Concepción, Chile

Sebastián Bascuñan Departamento de Geología. Universidad de Chile. Plaza Ercilla 803, Santiago, Chile.

Luis Buatois Department of Geological Sciences, University of Saskatchewan, 114 Science Place, Saskatoon, SK S7N 5E2, Canada.

Francisco Bastias Departamento de Ciencias de la Tierra, Universidad de Concepción, Casilla 160-C, Concepción, Chile.

Florencia Bechis Instituto de Investigaciones en Diversidad Cultural y Procesos de Cambio (IIDyPCa), CONICET - Universidad Nacional de Río Negro, Mitre 630, CP 8400, San Carlos de Bariloche, Argentina

Carla Braitenberg Dipartimento di Matematica e Geoscienze, Universita di Trieste, Via Weiss 1, 34100 Trieste, Italy

Luis Buatois Department of Geological Sciences, University of Saskatchewan, 114 Science Place, Saskatoon, SK S7N 5E2, Canada.

Pere Busquets Facultad de Geología. Universidad de Barcelona. C/Martí i Franqués s/n, E08028,Barcelona, España

Ricardo Calegari YPF S.A. Exploración. Macacha Güemes 515, 1106, Buenos Aires, Argentina

Horacio Canelo CICTERRA - CONICET / Universidad Nacional de Córdoba

Raúl Cardó Universidad de San Juan y Servicio Geológico Minero Argentino, Sargento Cabral, 685 Oeste. 5400 San Juan, Argentina

Reynaldo Charrier Departamento de Geología. Universidad de Chile. Plaza Ercilla 803, Santiago, Chile. Universidad Andrés Bello, Sazié 2115, Santiago, Chile.

Pilar Clariana Instituto Geológico y Minero de España. C/Ríos Rosas 23, E28003 Madrid, España.

Gilda Collo CICTERRA - CONICET / Universidad Nacional de Córdoba

Eduardo Contreras-Reyes Departamento de Geofísica, Facultad de Ciencias Físicas y Matemáticas, Universidad de Chile

Ferrán Colombo Facultad de Geología. Universidad de Barcelona. C/Martí i Franqués s/n, E08028,Barcelona, España.

Christian Creixell Servicio Nacional de Geología y Minería, Av. Santa María 0140, Providencia, Santiago, Chile.

Andrés Cuesta Departamento de Geología. Universidad de Oviedo. C/Jesús Árias de Velasco s/n, E33005

José Cuitiño Instituto Patagónico de Geología y Paleontología, CCT CENPAT-CONICET. Boulevard Brown 2915 (U9120ACD), Puerto Madryn, Chubut, Argentina

Federico M. Dávila CICTERRA - CONICET / Universidad Nacional de Córdoba

Luis Dimieri INGEOSUR. CONICET. Departamento de Geología, Universidad Nacional del Sur, San Juan 670, Bahía Blanca (8000)

Andrés Echaurren Instituto de Estudios Andinos Don Pablo Groeber, UBA - CONICET. Departamento de Ciencias Geológicas, FCEN, Universidad de Buenos Aires

Alfonso Encinas Departamento de Ciencias de la Tierra, Universidad de Concepción, Casilla 160-C, Concepción, Chile

Miguel Ezpeleta CICTERRA - CONICET / Universidad Nacional de Córdoba

Mauricio Espinoza Departamento de Ciencias de la Tierra, Universidad de Concepción, Casilla 160-C, Concepción, Chile

Pedro Farias Departamento de Geología. Universidad de Oviedo. C/Jesús Árias de Velasco s/n, E33005

Lucas Fennell IDEAN. Instituto de Estudios Andinos. Universidad de Buenos Aires-Conicet, Argentina

Lucía Fernández Paz Idean. Instituto de Estudios Andinos. Universidad de Buenos Aires-Conicet, Argentina

Kenneth L. Finger University of California Museum of Paleontology, Valley Life Sciences Building 1101, Berkeley, California 94720, USA

Andrés Folguera Idean. Instituto de Estudios Andinos. Universidad de Buenos Aires. CONICET, Consejo Nacional de Investigaciones Científicas y Técnicas, Argentina

Pablo R. Franceschinis Laboratorio de Paleomagnetismo Daniel A.Valencio, Instituto de Geociencias Básicas, Aplicadas y Ambientales de Buenos Aires, Departamento de Cs. Geologicas, Fac. Cs. Exactas y Naturales, Universidad de Buenos Aires, CONICET

Jorge Gallastegui Departamento de Geología. Universidad de Oviedo. C/Jesús Árias de Velasco s/n, E33005

Gloria Gallastegui Instituto Geológico y Minero de España. C/Ríos Rosas 23, E28003 Madrid, España

Ezequiel García Morabito Instituto de Estudios Andinos "Don Pablo Groeber" (UBA – CONICET, Argentina). Swiss Federal Institute of Technology (ETH Zurich)

Silvana E. Geuna Laboratorio de Paleomagnetismo Daniel A.Valencio, Instituto de Geociencias Básicas, Aplicadas y Ambientales de Buenos Aires, Departamento de Cs. Geologicas, Fac. Cs. Exactas y Naturales, Universidad de Buenos Aires, CONICET

Laura Giambiagi Unidad de Tectónica. IANIGLA-CONICET. Avda. Ruiz Leal s/n, 5500 Mendoza, Argentina
Guido Gianni IGSV. Instituto Geofísico Sismológico Ing. Volponi. Universidad de Nacional San Juan. Conicet

Mario Gimenez CONICET. Instituto Geofísico-Sismológico Volponi. UNSJ, San Juan, Argentina

Javiera González Departamento de Ciencias de la Tierra, Universidad de Concepción, Casilla 160-C, Concepción, Chile

Luis González-Menéndez Instituto Geológico y Minero de España. C/Ríos Rosas 23, E28003 Madrid, España

Joaquín García-Sansegundo Departamento de Geología. Universidad de Oviedo. C/Jesús Árias de Velasco s/n, E33005

Raúl Giacosa Universidad de Río Negro y Servicio Geológico y Minero Argentino. Parque Industrial, 8332 General Roca, Río Negro, Argentina.

Laura Giambiagi Centro Regional de Investigaciones Científicas y Tecnológicas, IANIGLA, CCT Mendoza, Mendoza, Argentina

Mario Ernesto Gimenez Instituto Geofísico y Sismológico Ing. Volponi, Universidad Nacional de San Juan, Ruta 12-Km17, San Juan, Argentina. CONICET, Consejo Nacional de Investigaciones Científicas y Técnicas, Argentina

Nemesio Heredia Instituto Geológico y Minero de España. C/Ríos Rosas 23, E28003 Madrid, España

Greg Hoke Department of Earth Sciences, Syracuse University, Syracuse NY 12344, USA

Fernando Hongn IBIGEO (CONICET-UNSA). 9 de julio 14, (4405) Rosario de Lerma-Salta-Argentina.

Sofía Iannelli Idean. Instituto de Estudios Andinos. Universidad de Buenos Aires-Conicet, Argentina

María Paula Iglesia Llanos Laboratorio de Paleomagnetismo Daniel A.Valencio, Instituto de Geociencias Básicas, Aplicadas y Ambientales de Buenos Aires, Departamento de Cs. Geologicas, Fac. Cs. Exactas y Naturales, Universidad de Buenos Aires, CONICET

Rosemary E. Jones Department of Earth Sciences, University of Oxford, South Parks Road, Oxford, OX1 3AN, United Kingdom

Linda A. Kirstein School of GeoSciences, University of Edinburgh, The King's Buildings, James Hutton Road, Edinburgh EH9 3FE, United Kingdom

Fernando Lebinson INGEOSUR. CONICET. Departamento de Geología, Universidad Nacional del Sur, San Juan 670, Bahía Blanca (8000)

Oscar Limarino Facultad de Geología. Universidad de Buenos Aires. C/ Intendente Güiraldes 2160, Ciudad Universitaria, Pabellón II, C1428EGA Buenos Aires, Argentina.

Federico LinceKlinger Instituto Geofísico y Sismológico Ing. Volponi, Universidad Nacional de San Juan, Ruta 12-Km17, San Juan, Argentina. CONICET, Consejo Nacional de Investigaciones Científicas y Técnicas, Argentina

Carolina Lithgow-Bertelloni University College London

Vanesa D. Litvak Idean. Instituto de Estudios Andinos. Universidad de Buenos Aires-Conicet, Argentina

Lizet De Girolamo Del Mauro Departamento de Ciencias de la Tierra, Universidad de Concepción, Casilla 160-C, Concepción, Chile

Ana Lossada Centro Regional de Investigaciones Científicas y Tecnológicas, IANIGLA, CCT Mendoza, Mendoza, Argentina

Juan Lovecchio YPF S.A. Exploración. Macacha Güemes 515, 1106, Buenos Aires, Argentina

Andrei Maksymowicz Departamento de Geofísica, Facultad de Ciencias Físicas y Matemáticas, Universidad de Chile

Marcelo Manassero Centro de Investigaciones Geológicas (UNLP – CONICET, Argentina)

Fidel Martín-González Área de Geología ESCET. Universidad Rey Juan Carlos. C/Tulipán s/n, 28933 Mostoles, Madrid, España.

Federico Martina CICTERRA - CONICET / Universidad Nacional de Córdoba

Fernando Martínez Facultad de Ingeniería y Ciencias Geológicas, Departamento de Geología, Universidad Católica del Norte, Angamos 0610, Antofagasta, Chile

Patricia Martínez Instituto Geofisico Sismológico Ing. Volponi. Universidad de San Juan. Conicet.

Manuela Mazzitelli Centro Regional de Investigaciones Científicas y Tecnológicas, IANIGLA, CCT Mendoza, Mendoza, Argentina

José Mescua Centro Regional de Investigaciones Científicas y Tecnológicas, IANIGLA, CCT Mendoza, Mendoza, Argentina

Maximiliano Naipauer Instituto de Estudios Andinos "Don Pablo Groeber" (UBA – CONICET, Argentina)

César R. Navarrete Universidad Nacional de la Patagonia San Juan Bosco. Dpto. de Geología. Comodoro Rivadavia. Chubut. Argentina

Sven N. Nielsen Instituto de Ciencias de la Tierra, Universidad Austral de Chile, Capus Isla Teja s/n, Valdivia, Chile.

Julieta Nóbile CICTERRA - CONICET / Universidad Nacional de Córdoba

Verónica Oliveros Departamento de Ciencias de la Tierra, Universidad de Concepción, Casilla 160-C, Concepción, Chile.

Darío Orts Instituto de Investigación en Paleobiología y Geología, Universidad Nacional de Río Negro – CONICET, Av. J.A. Roca 1242. CP 8332, General Roca, Argentina

David Pedreira Departamento de Geología. Universidad de Oviedo. C/Jesús Árias de Velasco s/n, E33005

Felipe Pérez Departamento de Ciencias de la Tierra, Universidad de Concepción, Casilla 160-C, Concepción, Chile

Stella Poma IGEBA. Instituto de Geociencias Básicas y Aplicadas de Buenos Aires, Universidad de Buenos Aires- Conicet, Argentina

Paulo Quezada Universidad Andres Bello, Departamento de Geología.

Luis Quintana Departamento de Geología. Universidad de Oviedo. C/Jesús Árias de Velasco s/n, E33005

Miguel Ramos Idean. Instituto de Estudios Andinos. Universidad de Buenos Aires-Conicet, Argentina

Victor A. Ramos Idean. Instituto de Estudios Andinos. Universidad de Buenos Aires. CONICET, Consejo Nacional de Investigaciones Científicas y Técnicas, Argentina.

Augusto E. Rapalini Laboratorio de Palcomagnetismo Daniel A.Valencio, Instituto de Geociencias Básicas, Aplicadas y Ambientales de Buenos Aires, Departamento de Cs. Geologicas, Fac. Cs. Exactas y Naturales, Universidad de Buenos Aires, CONICET

Ricardo Riffo Departamento de Ciencias de la Tierra, Universidad de Concepción, Casilla 160-C, Concepción, Chile

Luis Roberto Rodríguez-Fernández Instituto Geológico y Minero de España. C/Ríos Rosas 23, E28003 Madrid, España.

Pablo Rossel Universidad Andrés Bello, Facultad de Ingeniería, Geología, Autopista Talcahuano, 7100, Concepción, Chile.

Alvaro Rubio-Ordóñez Departamento de Geología. Universidad de Oviedo. C/Jesús Árias de Velasco s/n, E33005
Francisco Ruiz Instituto Geofísico Sismológico Ing. Volponi. Universidad de San Juan.

Francisco Sánchez CICTERRA - CONICET / Universidad Nacional de Córdoba

Natalia Sánchez INGEOSUR. CONICET. Departamento de Geología, Universidad Nacional del Sur, San Juan 670, Bahía Blanca (8000)

Francisco Sánchez-Nassif CICTERRA, CONICET-Universidad Nacional de Córdoba, Córdoba, Argentina.

Raúl Seggiaro Universidad de Salta y Servicio Geológico y Minero Argentino. Avda. Bernardo Houssay 1099, Barrio Castañeras, 4400 Salta, Argentina
Daniel Sellés Aurum Consultores, Santiago, Chile

Fernando Sepúlveda Departamento de Ciencias de la Tierra, Universidad de Concepción, Casilla 160-C, Concepción, Chile.

Samanta Serra-Varela Instituto de Investigación en Paleobiología y Geología

Schiuma, M. YPF S.A. Exploración. Macacha Güemes 515, 1106, Buenos Aires, Argentina

Santiago Soler Instituto Geofísico-Sismológico Volponi. UNSJ, San Juan, Argentina

Cecilia M. Spagnuolo CONICET- Facultad de Ciencias Naturales e Instituto Miguel Lillo, Universidad Nacional de Tucumán, Miguel Lillo 205, T4000JFE, San Miguel de Tucumán, Argentina

Mauro Spagnuolo Idean. Instituto de Estudios Andinos. Universidad de Buenos Aires-Conicet, Argentina

Luis Spalletti Centro de Investigaciones Geológicas. Universidad de La Plata. Diagonal 113 n° 275, B1904DPK La Plata, Argentina

Julieta Suriano IGeBA - FCEyN, UBA-CONICET

Francisca Tapia Departamento de Ciencias de la Tierra, Universidad de Concepción, Casilla 160-C, Concepción, Chile

Andres Tassara Departamento de Ciencias de la Tierra, Universidad de Concepción, Casilla 160-C, Concepción, Chile

José María Tubía Departamento de Geodinámica, Universidad del País Vasco (UPV/EHU), Vizcaya, España

Jonathan Tobal IDEAN. Instituto de Estudios Andinos. Universidad de Buenos Aires-Conicet, Argentina

Martín Turienzo INGEOSUR. CONICET. Departamento de Geología, Universidad Nacional del Sur, San Juan 670, Bahía Blanca (8000)

Victor Valencia School of the Environment, Washington State University, Pullman, Washington 99164, USA

Paulina Vásquez Servicio Nacional de Geología y Minería, Av. Santa María 0140, Providencia, Santiago, Chile.

Patricio Zambrano Universidad Andres Bello, Facultad de Ingeniería, Geología, Autopista Talcahuano, 7100, Concepción, Chile

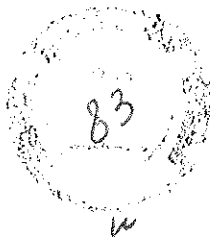

For our partners of marvelous voyages through the Andes

Chapter 20
The Late Paleogene to Neogene volcanic arc in the Southern Central Andes (28°-37°S)

Vanesa D. Litvak, Stella Poma, Rosemary E. Jones, Lucía Fernández Paz, Sofía Iannelli, Mauro Spagnuolo, Linda A. Kirstein, Andrés Folguera and Víctor A. Ramos

Abstract Evolution of arc magmatism along the Southern Central Andes (~28°-37°S) is strongly controlled by changes in the geometry of the downgoing slab (e.g., slab dip angle). This is particularly evident in the present-day Chilean-Pampean flat-slab and the late Miocene Payenia shallow subduction segments. Typical Andean type volcanism was established during the late Oligocene to late Miocene in the high Andes (29°30"-30°30"S), with arc-related calc-alkaline volcanism having geochemical signatures that reflect changes in the residual mineral assemblages related to increased crustal thickness (>50 km). The increase in crustal thickness resulted from increased compression along the Southern Central Andean margin due to the subduction of the Juan Fernandez Ridge, and consequent shallowing of the downgoing slab in the late Miocene. Associated with the decrease in the slab-dip angle, the volcanic front migrated to the east. Further south, magmas developed across the present-day Payenia back-arc region (35°-37°S) show an increase in slab-derived components in the middle Miocene to early Pliocene times, which also suggests a progressive shallowing of the subducting slab at these latitudes. However, trace elements ratios indicate a low to intermediate pressure residual mineral assemblage and no significant increase in crustal thickness is apparent, unlike further north in the Chilean-Pampean flat-slab segment. Although flat slab geometry still prevails in this latter segment, re-steepening of the slab during early Pliocene times (~5-3 Ma) promoted an increase of arc and back-arc magmatism at these more southerly latitudes of the Southern Central Andes. A dynamic link between slab geometry, geochemistry and volcanic activity is therefore observed in the Southern Central Andes.

Keywords Payenia shallow subduction, Pampean flat-slab, crustal thickness, geochemistry, arc magmatism

1 Introduction

Topographic variability along the length of the Andean mountain chain can be linked to the changes in the geodynamic driving forces, which correlate with the development of arc magmatism. The geometry of the subducting slab (e.g., slab dip angle) through time is one of the major factors controlling the development, intensity, migration and/or expansion of volcanic arcs (Kay et al. 1991, 1999; Ramos and Folguera 2005; Litvak et al. 2007).

The geodynamic setting of the Southern Central Andean margin (~28°-37°S) has changed significantly through the Cenozoic. In the late Oligocene (~25 Ma) the Farallón plate broke up into the Nazca and Cocos plates (see Chapter 14), which resulted in a change from oblique to orthogonal convergence (e.g. Pardo-Casas and Molnar 1987; Barckhausen et al. 2008). Typical Andean type arc-volcanism was initiated with a ~30° subduction angle. However, in the Southern Central Andes the intersection of the Juan Fernandez ridge with the continental margin in the early Miocene resulted in the shallowing of the angle at which the Nazca plate subducts beneath the South American plate. There are two regions affected by Cenozoic shallow and/or flat subduction in the Southern Central Andes: the present-day Chilean-Pampean flat-slab segment and the late Miocene Payenia shallow subduction segment (Kay et al. 1991, 1999; Kay and Mpodozis 2002; Kay et al. 2006a, b; Litvak et al. 2007, 2015; Jones et al. 2016; Fig. 1). Andean type subduction and arc volcanism was developed along both of these segments in the late Oligocene. By Miocene times a shallow and hence, a more compressive subduction regime commenced, leading to the expansion of the arc activity towards the retro-arc and an increase of deformation into the Argentinean foreland. The main difference in the evolution of the volcanic arc within these segments is that the crust increased in thickness from ~30 km to >50 km in the Chilean-Pampean flat-slab segment during the latter part of the Cenozoic (Allmendinger et al. 1990; Fromm et al. 2004; McGlashan et al. 2008; Chulick et al. 2013). Moreover, while the flat-slab geometry is still ongoing in the Chilean-Pampean flat-slab segment, the shallow subduction regime in the Payenia segment prevailed only until the beginning of the Pliocene (~5-3 Ma), when the subducting slab returned to a normal-angle (Kay et al. 2006; Ramos et al. 2014; Litvak et al. 2015). Given the spatial configuration and the timing at which the angle of subduction changed of both Chilean-Pampean and Payenia segments, the collision of the Juan Fernandez ridge is likely to explain the continuity and progressive shallowing throughout both segments during the Miocene. The variable influence of the ridge collision from N to S along the Andean margin could eventually result in a change in the dip of the subducted slab away the Juan Fernández ridge (around 33°S).

This review chapter focuses on the lithological and geochemical features of arc volcanism from the late Oligocene to early Pliocene in the Chilean-Pampean flat-slab segment and the Payenia shallow subduction zone, in order to determine the influence of changes in

subduction parameters through time on arc magmatism. Variations in geochemical signatures provide information about the conditions beneath active volcanic arcs and thus, are good indicators of the changes in the geodynamic setting of the Southern Central Andean margin.

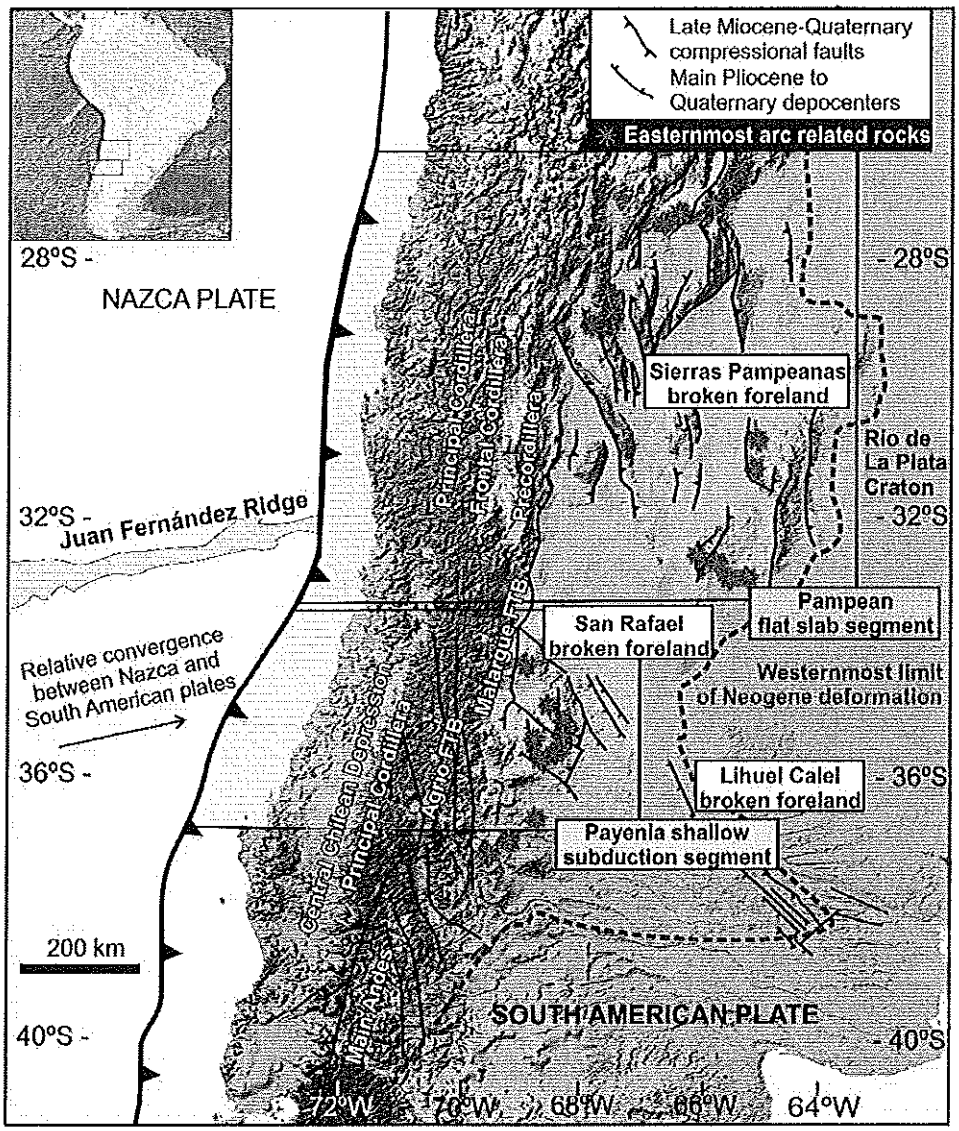

Fig. 1 Location and main morphotectonic features of the present-day Chilean-Pampean flat-slab segment and the partially contemporaneous late Miocene Payenia shallow subduction zone. The compressive regimes associated with both flat and shallow segments are responsible for the uplifting of the Sierras Pampeanas and San Rafael Block, respectively, in the foreland area. Location of arc-related centers after Ramos et al. (2002) (modified from Litvak et al. 2015).

The first and main scientific contributions to understanding the geochemical and tectonic evolution of Chilean-Pampean flat-slab arc rocks were made by Kay et al. (1987, 1988, 1991, 1999) and Ramos et al. (1987, 1989), while data on age and petrological features were later reported by Bissig et al. (2001, 2003), Litvak et al. (2007), Litvak and Poma (2010, 2014)

and Jones et al. (2014, 2015, 2016). The Payenia shallow subduction regime was first proposed by Kay et al. (2006a, b), primarily based on studies on the Chachahuén Volcanic Complex, and was later discussed by Spagnuolo et al. (2012), Dyhr et al. (2013a, b) Ramos et al. (2014) and Litvak et al. (2015).

2 Tectonic and regional setting of the Chilean-Pampean flat-slab and Payenia shallow subduction segments

The Chilean-Pampean flat-slab segment, located between ~28–32°S in the Southern Central Andes is comprised of, in a W-E direction, the Coastal and Principal Cordilleras in Chile and the Frontal Cordillera, Precordillera and Sierras Pampeanas of Argentina (Fig. 1) (see Chapters 11 and 16). While the Payenia shallow subduction zone, between ~34–37°S, includes part of the Central Depression in Chile and the Cordillera Principal of Chile and Argentina, together with a lower mountain system to the east known as the San Rafael Block (Fig. 1). The San Rafael Block lies in a similar longitudinal position to the Precordillera in the present-day Pampean flat-slab segment (Fig. 1). However, its morphology, which corresponds to a dismembered peneplain that emerges in the foreland region, and the mechanics of its exhumation, makes the San Rafael Block similar to the Sierras Pampeanas, which is part of a broken foreland, located to the north of the San Rafael Block and to the east of the Precordillera. Formation of the Sierras Pampeanas and the San Rafael Block have been linked to compressive regimes, resulting from the shallowing of the subducting Nazca plate in Miocene times and the reactivation of high-angle basement faults during Miocene to Quaternary times.

Since the Triassic the Andean margin has been magmatically active at various intervals, producing a series of volcanic arcs in a setting which developed from being more extensional in the initial stages to increasingly compressive after the Late Cretaceous and then from the late Oligocene (e.g., Ramos et al., 2002; Charrier et al., 2007) (see Chapters 7, 8, 10, 11, 12 and 14). The breakup of the Farallón plate (~25 Ma) into the Nazca and Cocos caused an increase in convergence rates from ~8 cm/yr to ~15 cm/yr and a change from oblique to orthogonal convergence (Pardo Casas and Molnar 1987; Somoza 1998; Somoza and Ghidella 2012). In the Chilean-Pampean flat-slab segment, Andean type-volcanism was developed under this new plate configuration. One of the key areas for understanding the evolution of the arc is the El Indio-Valle del Cura belt (~29-30°S; Fig. 2), where late Oligocene-early Miocene main volcanic arc was formed of dacitic to andesitic pyroclastic and lava flows located in the present-day Chile, with associated volcanoclastic deposits primarily located in retro-arc extensional basins (Figs. 1 and 2) (Maksaev et al. 1984; Kay et al. 1991; Litvak et al. 2007; Winocur et al. 2015).

The Juan Fernandez ridge began intersecting the Andean margin by the Early Miocene (~20-18 Ma at ~30°S) (see Chapters 1 and 3), which led to the shallowing of the angle of subduction (Pilger 1981, 1984; Gutscher et al. 2000b; Kay and Mpodozis 2002; Yañez et al. 2002, 2001; Jones et al. 2014). As a result, the volcanic arc front migrated into the present-day Argentinean Frontal Cordillera, while arc-magmatism broadened and expanded to the east, as far as ~700 km away from the present trench (Kay and Gordillo 1994; Poma et al. 2005, 2014). The shallow subduction geometry caused a reduction in the magma volume erupted within the main arc, with cessation of arc magmatism by late Miocene (~6 Ma) times in the Chilean-Pampean flat-slab region (Ramos et al. 1989; Kay et al. 1991; Bissig et al. 2001; Litvak et al. 2007).

The Payenia shallow subduction segment is located immediately to the south of the Chilean-Pampean flat-slab (Fig. 1). This segment is characterized by widespread volcanic sequences that cover most of the retro-arc region, over 550 km east of the trench in the Cenozoic (Bermúdez 1991; Bermúdez et al. 1993; Nullo et al. 2002; Kay et al. 2006a, b; Spagnuolo et al. 2012; Dyhr et al. 2013a, b). As summarized by Dyhr et al. (2013a), the evolution of the mid to late Cenozoic volcanism in the retro-arc of the Payenia region, can be subdivided into three main episodes. These are differentiated on the basis of their age, composition and tectonic setting: i) an early Miocene episode of alkaline volcanism (Kay and Copeland 2006; Kay et al. 2006b; Dyhr et al. 2013b); ii) A middle Miocene to early Pliocene 'arc-like' episode (Nullo et al. 2002; Kay et al. 2006a, b; Spagnuolo et al. 2012; Dyhr et al. 2013a; Litvak et al. 2015); and iii) An episode of late Pliocene-Recent volcanism, with alkali basalts displaying typical back-arc compositions and variable slab input (Bermúdez et al. 1993; Bertotto et al. 2009; Gudnason et al. 2012; Søager et al. 2013; Hernando et al. 2014). The second volcanic episode is key to understanding the development of the Payenia shallow subduction regime which is thought to have occurred between 18 and 3.5 Ma, with the plate at its shallowest angle between ~7.3 and 3.5 Ma when the easternmost arc-related sequences erupted over the present-day Payenia retro-arc zone (Kay et al. 2006a, b; Litvak et al. 2015).

The Andes between 34° and 38°S are formed of two east verging mountain systems: firstly, the Malargüe fold and thrust belt and its continuation to the south into the Agrio fold and thrust belt (see Chapters 16 and 17), and secondly, the San Rafael Block (Fig. 1). Arc-related volcanism was particularly developed at these latitudes within retro-arc and intra-arc basins, such as the Abanico and Cura Mallin basins, that were developed during the Late Oligocene to Early Miocene (see Chapter 14), as the westernmost sections of the Malargüe and Agrio fold and thrust belts experienced an episode of extension. These basins contain volcanic and volcaniclastic sequences of over 3,000 m in thickness, derived from activity in the main volcanic-arc (e.g. Suárez and Emparán 1995; Charrier et al. 2002; Radic et al. 2002; Burns et al. 2006; Flynn et al. 2008; Kay et al. 2006a, b; Muñoz et al. 2006). Extension in late Oligocene-

early Miocene times was likely related to roll back of the subducting Nazca plate caused by the deceleration of the South American plate (see Chapter 18). Within this setting, retro-arc alkaline, volcanic successions of late Oligocene-early Miocene age accumulated to the east, in the region of the southern section of the present-day Payenia retro-arc (Ramos and Barbieri 1989; Kay et al. 2006a, b; Dyhr et al. 2013b).

The middle Miocene to early Pliocene calc-alkaline volcanic sequences covered the distal foreland deposits within the present-day Payenia retro-arc (Fig. 3) (Kay et al. 2006a, b; Ramos et al. 2014; Litvak et al. 2015). Steepening of the subducting Nazca plate (~5-3 Ma) in these region resulted in an extensional regime across the foreland, and the emplacement of Quaternary, mafic volcanic sequences that comprise one of the major volcanic provinces in the Andean back-arc (Groeber 1946; Muñoz Bravo et al. 1989; Bermúdez et al. 1993; Ramos and Folguera 2005b, 2011; Folguera et al. 2009; Llambías et al. 2010; Gudnason et al. 2012; Søager et al. 2013; Hernando et al. 2014)

3 Age, distribution and lithological features of Cenozoic arc-related volcanism in Southern Central Andes

3.1 *The Chilean-Pampean flat-slab segment: Valle del Cura and Iglesia basins*

Arc-related volcanic units are distributed between ~29°30′-30°15′S in the Valle del Cura basin, which forms part of the Cordillera Frontal in the high Andes of Argentina, and in the Valle de Iglesia basin, which lies in the most westerly part of the Precordillera (Fig. 1). These two basins are divided by the Colangüil Cordillera (as part of the Cordillera Frontal), which is mostly comprised of Late Paleozoic and Permo-Triassic basement (Fig. 2).

The Valle del Cura basin constitutes a mineralized hydrothermal system that, together with the El Indio belt in Chile, forms a north-south-trending block limited by high-angle reverse faults associated with both Au-Ag-Cu-rich epithermal and porphyry type mineral deposits (e. g. Martin et al. 1995; Bissig et al. 2001, 2015; Litvak et al. 2007). Arc-related early Cenozoic volcanic rocks in the high Andes are mainly restricted to the Chilean Principal Cordillera with epizonal granodioritic plutons and extrusive basaltic to rhyolitic lavas and tuffs of Paleocene to Eocene age (Cogotí Supergroup and Los Equinos Formation, respectively, Parada et al. 1988, Pineda and Emparan 2006; Charrier et al. 2007; Jones et al. 2016). Paleocene volcanism was also developed to the east, in present-day Argentina, as volumetrically restricted, back-arc alkaline mafic volcanism (Río Frío Basalts), for which a K-Ar whole rock age of 55.9 ± 1.9 Ma has been obtained (Litvak and Page 2002; Litvak and Poma 2010) (Fig. 2). Overall, arc-activity was reduced between ~39 and 26 Ma in the Southern Central Andes; however, some minor arc magmatism occurred, as represented by small dioritic and granodioritic subvolcanic bodies with

reported K-Ar ages of 31.1±1.2 and 39.5±1.3 and Ar-Ar of 30.0±1.9 and 35.9±1.2 Ma (Bocatoma Unit; Nasi et al. 1990; Martin et al. 1995; Bissig et al. 2001).

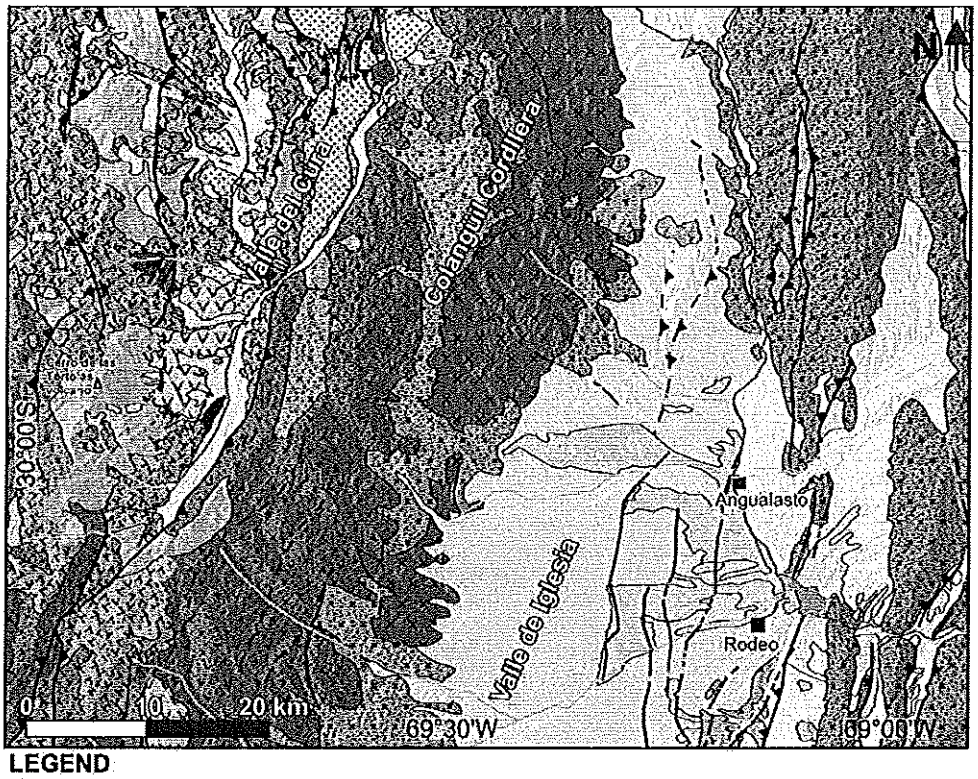

LEGEND

- Ephimeral stream
- Permanet stream
- Lake
- Localities
- International border
- Lineament
- Reverse fault
- Normal Fault
- Anticline-Sincline

Precordillera

- Quaternary
- Miocene volcanic and volcaniclastic rocks (Tertiary and Miocene Intrusives, Lomas del Campanario y Las Trancas Fms.)
- Miocene to Pliocene sedimentary and volcaniclastic rocks
- Early-Middle Paleozoic sedimentary basement

Cordillera

- Quaternary
- Miocene to Pliocene sedimentary rocks
- Pliocene basalts
- Late Miocene: Vacas Heladas Ignimbrites
- Middle to Late Miocene: Cerro de las Tórtolas and Tambo Fms. and Infiernillo Unit
- Late Oligocene-Early Miocene: Doña Ana Group
- Late Oligocene-Early Miocene: Las Máquinas Basalts
- Late Paleocene: Río Frío Basalts
- Mesozoic basement
- Permotriassic volcanism basement
- Permotriassic granitites basement
- Late Paleozoic sedimentary basement

Fig. 2 Geological setting and distribution of arc-like sequences between 29°-30°S across the Frontal Cordillera and Precordillera, from the Valle del Cura to the Iglesia basin, over the present-day Chilean-Pampean flat-slab segment (based on Litvak et al. 2007; Alonso et al. 2011; Litvak and Poma 2014).

Extensive arc magmatism was developed in the Southern Central Andes in the Late Oligocene (~25 Ma) as a consequence of the tectonic reconfiguration of the South American margin. This volcanism comprises the Doña Ana Group sequences, which crop out in both the Chilean and Argentinean side of the margin representing arc and retro-arc volcanic activity respectively (Fig. 2). The older member of the Doña Ana Group, the Tilito Formation, includes rhyolitic and dacitic lavas and ignimbrites associated with minor basalts and andesites with reported ages from 27 to 23 Ma, based K-Ar, Ar-Ar, and U-Pb age dating; the younger member, the Escabroso Formation, is mainly composed of basaltic to andesitic lavas interbedded with volcanic agglomerates and breccias with reported ages between 21 and 18 Ma (Maksaev et al. 1984; Nasi et al. 1990; Martin et al. 1995; Bissig et al. 2001; Litvak et al. 2005b; Litvak 2009; Winocur et al. 2015; Jones et al. 2015, 2016). A major unconformity separates both formations as the result of a period of deformation around 20 Ma, with a hiatus of volcanic activity of 3 Myr (Martin et al. 1995).

The late Oligocene arc sequences have been affected by varying degrees of phyllic to advanced argillic hydrothermal alteration, which overall comprises biotite-bearing dacitic lavas and crystalline and vitreous tuffs associated to the Cerro Doña Ana eruptive center. Early Miocene lavas are pyroxene-bearing porphyritic basaltic andesites and andesites, occasionally with propylitic alteration. The Doña Ana Group sequences also expanded towards the former retro-arc, cropping out in the eastern sector of the present Valle del Cura basin (Fig. 2), where they include pyroclastic and volcaniclastic deposits interbedded with clastic facies interpreted as river systems and alluvial fan deposits with associated ash-fall deposits due to the proximity of the magmatic vents (Limarino et al. 1999; Litvak et al. 2009; Winocur et al. 2015). Minor alkaline basalt with slab-derived input (Las Máquinas Basalts), exposed in volcanic necks in the Valle del Cura region are interpreted as back-arc lavas associated with the late Oligocene-early Miocene arc activity (Ramos et al. 1989; Kay et al. 1991; Litvak and Poma 2010).

Arc-magmatism by middle to late Miocene times is represented by the Cerro de las Tórtolas Formation, which is distributed along the Valle del Cura (Fig. 2), with the Cerro de las Tórtolas and Vacas Heladas volcanoes on the Argentinean-Chilean border preserved as partially eroded eruptive centers. Two main sections have been recognized in this formation: i) an andesitic to basaltic andesitic lower section, which is primarily comprised of porphyritic pyroxene to amphibole-bearing andesites within plagioclase-rich groundmass, with reported K-Ar, Ar-Ar and zircon U/Pb ages between 17 and 14 Ma; and, ii) An andesitic to dacitic upper section, with mostly porphyritic amphibole-bearing rocks within hyalopilitic to trydimite-rich groundmass, with ages ranging from 13 to 10 Ma (Maksaev et al. 1984; Ramos et al. 1989; Kay et al. 1991, 1999; Martin et al. 1995; Bissig et al. 2001; Litvak et al. 2007; Litvak and Poma 2014; Jones et al. 2015, 2016). The lower section is widespread and distributed across the Chilean-Argentinean border, particularly on the eastern side of the high Andes between 29° to

30°S, whereas the upper section is restricted to the highest altitudes, proximal to the Cerro de las Tórtolas volcano (Fig. 2). The Miocene lavas are generally subhorizontal, although in some cases they have been tilted by late Miocene reverse faulting. In contrast to the late Oligocene-early Miocene arc-rocks, the middle to late Miocene andesitic lavas are not particularly affected by hydrothermal alteration and appear fresh, preserving their primary textures and mineral assemblage. Further to the west, on the Chilean side of the high Andes, a series of high-K calc-alkaline, shallow level, intermediate intrusives (Infiernillo Unit, 18-15 Ma) have been interpreted as the subvolcanic equivalent of the Cerro de Las Tórtolas Formation (Kay et al. 1987, 1988, 1991; Bissig et al. 2001; Jones et al. 2016).

A limited number of exposures of dacitic crystalline tuffs with reported ages between 12 to 11 Ma (Tambo Formation, after Martin et al. 1995; Litvak et al. 2007) crop out in the southern Valle del Cura, but extends mostly to the north, near the Veladero ore deposit. These tuffs show distinctive petrographic features such as amphibole and titanite crystal fragments, and have been included as part of the middle to late Miocene volcanic sequences; however, nomenclature used for these sequences has been inconsistent and has changed through time (-also known as Vacas Heladas Formation- see Litvak et al. (2007) for further discussion on stratigraphy).

Late Miocene volcanism is volumetrically restricted in the area, as a consequence of the shallowing of the Nazca plate since ~20-18 Ma. The Vacas Heladas Ignimbrites are comprised of homogenous crystalline dacitic tuffs, derived from surge and pyroclastic flows and ash-deposits, and crop out on the eastern slope of the Vacas Heladas and Cerro de las Tórtolas volcanoes (Fig. 2), unconformably overlying Oligocene-Miocene sequences. These rocks represent the last significant volcanic activity in the region of the Valle del Cura on the Chilean-Pampean flat slab segment, with reported K-Ar, Ar-Ar and zircon U-Pb ages between 5.5 ± 0.1 Ma to 6.2 ± 0.19, and have been correlated with the Vallecito Formation in Chile (Ramos et al. 1989; Bissig et al. 2003; Jones et al. 2016).

Late Paleogene arc-related volcanism expanded into the foreland area associated with shallowing of the subduction regime. Andesitic to rhyolitic proximal block-and-ash pyroclastic flow deposits, ignimbrites, tuffs and minor dacitic lava flows, which crop out as N-S thin belts in the western Precordillera (Fig. 2), have been identified as coeval with the Tilito Formation (Las Trancas Formation, Poma et al. 2005, 2014). A zircon U-Pb age of 22.6 ± 0.33 Ma, obtained from a rhyolite, confirms the beginning of arc-related activity in the Precodillera by late Oligocene-early Miocene times (Jones et al. 2016). Minor granitic to granodioritic intrusive bodies have also been recognized along the eastern slope of the Colangüil Cordillera, cropping out around 30°S in the Valle del Iglesia (Miocene Intrusives). K-Ar ages between 22 to 13 Ma (Llambias et al. 1990; Cardó et al. 2007), and recently produced U-Pb zircon age (22.2 ± 0.23 to 20.43 ± 0.31 Ma) assign this magmatism to the early Miocene (Jones et al. 2016).

Further south (~30°45′S), in the Valle de Iglesia, pyroclastic rocks and dacitic subvolcanic bodies were also associated with arc volcanism during the Miocene. They comprise subvolcanic porphyritic amphibole-bearing andesites, ignimbrites, block and ash-deposits and minor lavas interbedded with epiclastic continental deposits (Tertiary Intrusives unit and Lomas del Campanario Formation, respectively; Cardó and Díaz 1999; Poma et al. 2014). The age of the intrusive equivalents were determined by K-Ar age dating and range between 18.3 ± 2.5 Ma and 17.5 ± 5 Ma (Cardó and Díaz 1999; Leveratto 1976), with one younger age of 8.8 ± 0.3 Ma reported (Wetten 2005). Recently reported U-Pb zircon ages suggest an age between 11.7 ± 0.21 to 9.4 ± 0.18 Ma (Jones et al. 2016), so overall age for this magmatism comprises 18 to 9 Ma.

3.2 The Payenia shallow subduction segment: calc-alkaline magmatism in the back-arc region

Late Oligocene-early Miocene main arc activity in the Payenia shallow subduction zone is represented by the Cura Mallín Formation, which developed as part of an intra-arc basin with pyroclastic and volcaniclastic deposits and minor basaltic andesitic lavas; reported Ar-Ar ages range between 24.6 ± 1.8 and 22.8 ± 0.7 (Jordan et al. 2001; Kay et al. 2006a), although younger K-Ar ages up to 11 Ma had been previously reported (Suarez and Emparan 1995). Volcanic rocks, dykes and intrusives bodies cropping out on the Chilean slope are also considered as part of the Miocene main volcanic arc activity (Trapa Trapa Formation; Niemeyer and Muñoz 1983), with reported K-Ar ages from 19 to 12 Ma (Niemeyer and Muñoz 1983; Muñoz and Niemeyer 1984; Suárez and Emparan 1995). To the east, on the Argentine side, west of the Cordillera del Viento, early to late Miocene arc-related volcanism is represented by andesite to dacitic lavas and agglomerates, andesitic dykes and stocks, and pyroclastic rocks to ash deposits, with an overall age range from 14 to 5 Ma, according to reported K-Ar and Ar-Ar ages. This includes several geological units including the Trapa Trapa, Cajón Negro, Quebrada Honda and Pichi Neuquén Formations (see Kay et al. 2006a and reference therein) (see Chapter 17).

However, changes in the geodynamic conditions of the Andean margin through time, and the associated consequences on arc volcanism are particularly reflected across the present-day Payenia retro-arc. Calc-alkaline products which crop out in the retro-arc region represent the eastward expansion of arc volcanism and have ages ranging from 20 to 4 Ma in the eastern foreland (Fig. 3) (Nullo et al. 2002; Baldauf, 1997; Giambiagi et al. 2005, 2008; Kay and Copeland 2006; Kay et al. 2006a, b; Sruoga et al., 2008; Spagnuolo et al. 2012; Litvak et al. 2015; Dyhr et al. 2013a, b; Ramos et al. 2014).

Early Miocene volcanism in the present-day Payenia back-arc is associated with alkaline magmatism. The lavas from Sierra de Huantraico (Fig. 3), in the Neuquén basin, provide the first evidence for the influence of the slab on a retro-arc position at around 20 Ma (Kay and Copeland 2006; Kay et al. 2006b; Dyhr et al. 2013b).

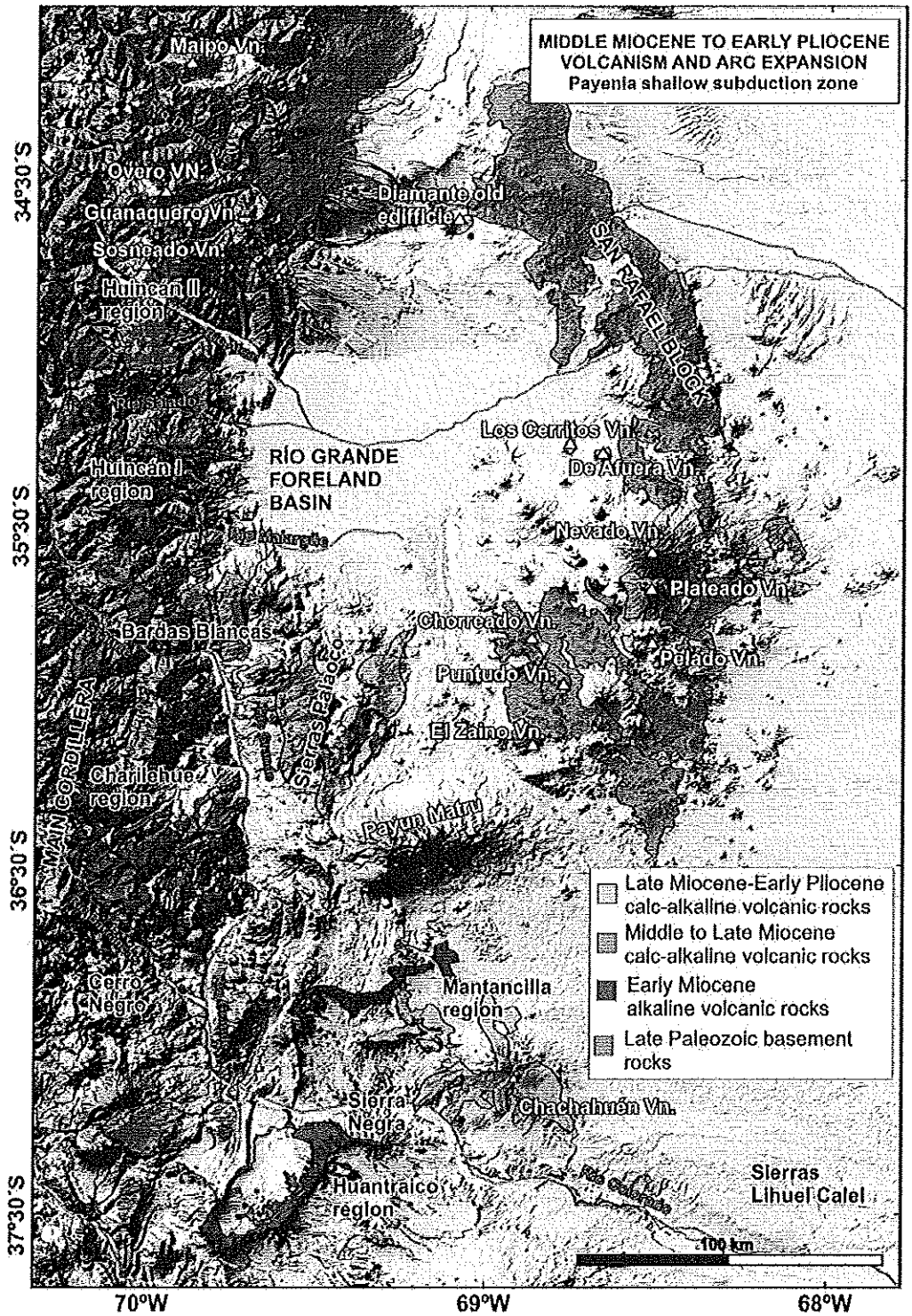

Fig. 3 Distribution of mesosilicic volcanic rocks from the eastern Main Andes to the San Rafael Block in the foreland area showing the eastward arc influence from middle Miocene to early Pliocene in the back-arc area. Modified from Litvak et al. (2015); (age compilation from Nullo et al. (1993, 1999, 2002), Ramos and Barbieri (1989), Ostera et al. (1999), Cobbold and Rossello (2003), Giambiagi et al. (2005),

Kay and Copeland (2006), Kay et al. (2006a,b), Folguera et al. (2009), Spagnuolo et al. (2012), Dyhr et al. (2013a,b) and Ramos et al. (2014)).

Middle Miocene to early Pliocene calc-alkaline mesosilicic volcanic sequences are exposed from the near back-arc to the far back-arc along the studied latitudes, between the eastern Malargüe fold and thrust belt in the west, and the San Rafael Block in the east (Fig. 3). These volcanic sequences can be divided into two main volcanic stages in Neogene times, based on their age distribution. The first stage, from the Middle to late Miocene (15 to 10 Ma), includes the Huincán I and part of the Huincán II andesites, Cerro Negro andesite, Charilehue volcanic rocks and eruptive centers located nearby the San Rafael Block (Fig. 3) (Nullo et al. 2002; Kay and Copeland 2006; Kay et al. 2006a; Spagnuolo et al. 2012; Ramos et al. 2014; Litvak et al. 2015;). These latter volcanic centers are mostly preserved as highly eroded stratovolcanoes, whose lava flows, pyroclastic deposits and subvolcanic bodies were originally named the Cortaderas Formation (Delpino and Bermúdez 1985; Llambías et al. 2010). They comprise fresh pyroxene to amphibole-bearing basalts and basaltic andesites to andesites, with plagioclase-rich groundmass, with interstitial tridymite commonly occurring in the more silica-rich compositions.

The second volcanic stage of calc-alkaline volcanism in the back-arc, includes late Miocene to early Pliocene (8 to 3.5 Ma) magmas represented by the younger Huincán II andesites, Palaoco volcanism, Chachahuén Volcanic Complex and younger San Rafael volcanic rocks (Nullo et al. 2002; Kay et al. 2006b; Dyhr et al. 2013a, Ramos et al., 2014; Litvak et al. 2015). These younger calc-alkaline andesites from the San Rafael volcanic associations are related to the easternmost volcanic centers in the area, such as the Nevado-Plateado Volcanic Complex, which also include alkaline trachytes, trachyandesites and basalts, grouped as the Nevado Formation by Bermúdez (1991), and considered to be Pliocene in age (Quidelleleur et al. 2009; Ramos et al. 2014). The Chachahuén Volcanic Complex includes an older sequence (Vizcachas Group, from 7.3 to 6.8 Ma) with dacitic dikes along with andesitic to dacitic ignimbrites and lava flows that display intraplate chemical affinities (Kay et al. 2006b). However, arc-like rocks comprise the younger Early Chachahuén unit (6.8 to 6.4 Ma) with intermediate to mafic lavas and dykes, while the Late Chachahuén sequence is composed of andesitic to dacitic pyroclastic rocks overlain by basaltic to basaltic andesite lava flows, and hornblende-rich andesites (6.3 to 4.9 Ma) (Kay et al. 2006b). The andesites and dacites of the San Rafael Block volcanism share common petrographical characteristics with the Early-Late Chachahuén Volcanic Complex rocks (Kay et al. 2006a, b; Litvak et al. 2015).

4 Geochemistry of late Oligocene to late Miocene arc magmas influenced by the Chilean-Pampean flat-slab regime

Overall, the geochemical features for the late Oligocene-late Miocene volcanic rocks cropping out in the high Andes (29°30"-30°30"S) indicate a calc-alkaline affinity with 'arc-like' signatures. Variations in trace element ratios and isotopic signatures indicate changes in residual mineral assemblages over time, which have been linked with crustal thickening due to the shallowing of the downgoing slab (Kay et al. 1991, 1999; Kay and Mpodozis 2002; Bissig et al. 2003; Litvak et al. 2007; Jones et al. 2015, 2016).

The late Oligocene-early Miocene Doña Ana Group is comprised of subalkaline rocks, with a continuous SiO_2 wt.% content ranging from basaltic to rhyolitic compositions. Despite large differences in silica content, all of these volcanic rocks show an arc-type trace element pattern on mantle and chondrite normalized multi-element diagrams, e.g. La/Ta > 25, as well as the reported Ba/La and Ba/Ta ratios for the unit (Fig. 4). REE patterns and ratios (La/Yb, La/Sm and Sm/Yb) suggest that this arc magmatism has variably equilibrated with a low to medium pressure residual mineral assemblage, including plagioclase and pyroxene (Kay et al. 1991, 1999; Bissig et al. 2003; Litvak et al. 2007; Jones et al. 2016).

Similar compositions, although less evolved and with lower Ba/Ta ratios, have been reported for the more eastern volcanic sequences, interbedded with epiclastic and volcanoclastic facies as part of the Doña Ana Group retro-arc basin infill (Litvak et al. 2007; Winocur et al. 2015; Jones et al. 2016). The partially contemporaneous early Miocene mafic volcanism (Las Máquinas Basalts) shows a more alkaline-like tendency and scarce slab-input, with the least enrichment in the LILE, consistent with emplacement in a back-arc setting. Geochemical modeling suggests that fractional crystallization of these mafic magmas can produce the less evolved sequences of the Tillito Formation (early Miocene) that also crop out in a more easterly position, further away from the Chile trench. However, the more evolved magmas located in the main volcanic arc also require the assimilation of the Permo-Triassic basement to produce their compositions or, alternatively, they could be derived from a different mantle source with a greater influence from subducting components (Jones et al. 2016).

Evidence for crustal contributions in the late Oligocene to early Miocene arc magmas is given by their gradual increase in $^{87}Sr/^{86}Sr$ ratios and decrease in Nd isotope ratios, reflecting an increase in radiogenic crustal contribution with time. This is in contrast to alkaline-like Paleocene and early Miocene basalts, which have an isotopically depleted nature (Fig. 4) (Kay et al. 1991; Litvak and Poma 2010; Litvak y Page 2010; Kay and Abruzzi 1996). Specific evidence for the assimilation of the Permo-Triassic basement by the Early Miocene silicic magmas (Tilito Formation) located in the main arc on Chilean slope comes from inherited zircon core ages (158.0±2.4, 241±2.7 and 388.1 ±5.3 Ma; Jones et al. 2016), and is consistent with the relatively high $^{87}Sr/^{86}Sr$ ratios of the Doña Ana Group volcanic rocks (Kay and Abbruzzi 1996). However, the more intermediate and mafic units of the Tilito Formation,

located further to the east, show no inherited zircon providing evidence for a more limited interaction with the local basement (Jones et al. 2015, 2016).

The first expression of early Miocene arc-related magmatism within the Precordillera is within the Valle de Iglesia (Miocene Intrusives) (Fig. 4). These magmatic rocks are more evolved and enriched in incompatible trace elements. Relatively high Nb/Zr ratios could be indicative of a relatively small degree of partial melting, consistent with their generation further away from the trench and therefore over a more dehydrated slab (Jones et al. 2016).

Arc-related volcanic activity was widespread during the early Miocene and throughout middle to late Miocene times in the location of the present Argentinean-Chilean border (Cerro de las Tórtolas and Tambo Formations) (Fig. 2). These lavas have calc-alkaline andesitic to dacitic compositions (Fig. 4) with typical arc-type trace element patterns (Kay et al. 1987, 1991, 1999; Ramos et al. 1989; Otamendi et al. 1994; Bissig et al. 2003; Litvak et al. 2007; Jones et al. 2016).

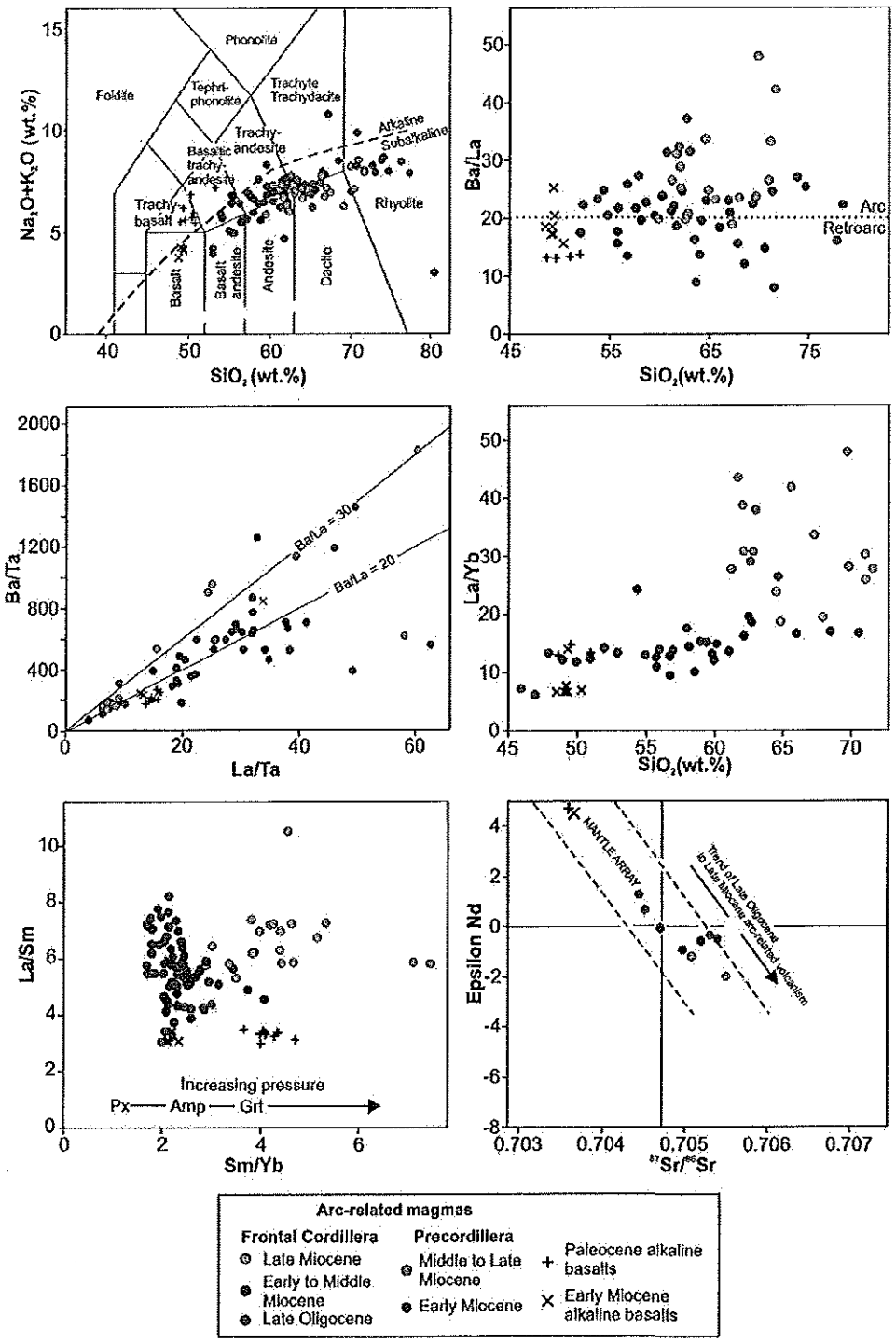

Fig. 4 Geochemical features of late Oligocene to late Miocene magmas over the Chilean-Pampean flat-slab segment, from the main arc (Cordillera Frontal) to its expansion to the east (western Precordillera). a) Chemical classification according to total alkali vs. silica content (Le Maitre et al. 1989); b) arc-like signature given by Ba/La vs. SiO_2; c) Ba/Ta vs. La/Ta show variable slab-input for the Oligo-Miocene sequences; d) REE behavior reflected in La/Yb vs. SiO_2; e) Variable HREE signature evidenced from the La/Sm vs. Sm/Yb ratios; f) Isotopic signatures that show an increase of crustal component towards the

late Miocene arc-magmas. Compiled data came from Bissig et al. (2003); Jones et al. (2016); Kay et al. (1987, 1988, 1991, 1999); Litvak et al. (2007), Litvak and Poma (2010) and Ramos et al. (1989).

Overall, the reported La/Ta, Ba/Ta, Ba/La for these Miocene magmas are indicative of mantle sources influenced by the slab (Fig. 4). An increase in the 'arc-like' signature (e.g. high Ba/La, Fig. 4) is seen in middle to late Miocene magmas, which have higher fluid mobile/immobile incompatible element ratios (e.g., Ba/Nb and U/Nb) suggesting a higher degree of partial melting of the mantle wedge due to an increase in fluids derived from the subducting slab, when compared to the late Oligocene magmas (Litvak et al. 2007; Jones et al. 2016).

Normalized REE patterns show evidence for a variable residual mineral assemblage throughout the Miocene arc magma evolution, as also seen in the La/Sm vs. Sm/Yb plots (Fig. 4). La/Yb values are generally between 5 and 20, however, a main break in La/Yb ratio evolution is seen in the intermediate middle to late Miocene arc rocks, with the late Miocene showing a remarkable increase in La/Yb ratios. The trace element composition of the early Miocene to middle Miocene lavas infer that the residual assemblage was dominated by amphibole and pyroxene, whereas by the late Miocene it was dominated by garnet. Mass balance calculations and melting models have been used to conclude that the addition of garnet to the fractionation of middle to late Miocene magmas could generate the steep and variable REE patterns (Kay et al. 1987, 1991).

Overall, the late Miocene arc rocks display adakitic signatures (Drummond and Defant 1990), given by their $SiO_2 > 56\%$, $Al_2O_3 > 15\%$, and $Sr > 400$ ppm, together with low values of Y (<18 ppm) high La/Yb ratios (>20) (Litvak et al. 2007; Kay and Mpodozis 2002; Jones et al. 2016). Although defining geochemical signatures and the origin of adakites remain controversial, there is consensus about the origin of this signal in the Chilean-Pampean flat-slab magmas (~30°S). The development of the adakitic signature in the late Miocene rocks is explained by arc magmas equilibrating with variable residual mineral assemblages in the lower crust related to increasing pressure conditions (Kay et al. 1991; 1999; Bissig et al. 2003; Kay et al. 2005; Litvak et al. 2007; Jones et al. 2016). The residual mineral assemblage develops from being pyroxene bearing in early-middle Miocene, to garnet bearing (higher pressure) by late Miocene times, reflecting an increase in crustal thickness (Kay et al. 1991; 1999; 2005; Bissig et al. 2003; Litvak et al. 2007; Goss et al. 2013; Jones et al. 2016). This is consistent with a more enriched isotopic signature; Nd and Sr isotope ratios are enriched and εNd decreases from the late Paleogene, suggesting a higher contribution of crustal derived components with time (Fig. 4).

The Miocene arc magmas (Cerro de las Tórtolas Formation) equilibrated at the base of the crust and evolved towards intermediate depth magma chambers. Equilibrium temperatures

for phenocrysts assemblages were estimated using two-pyroxene, amphibole-plagioclase and amphibole geothermometers and show a consistent temperature range between 970 to 850°C; while the equilibrium pressure estimated from amphibole compositions for the volcanic suites was close to 4 kbar (Litvak and Poma 2014). Thus, although the crustal thickness has increased from Early to Late Miocene no change in pressure conditions for crystallization of phenocrysts assemblages has been recorded. The latest Miocene volcanism (~8-6 Ma, Vacas Heladas Ignimbrites) is similar to the late Miocene intermediate magmas (Fig. 4), corresponding to high-K silicic rocks with arc-like geochemical signatures and high ratios of fluid-mobile/immobile incompatible trace elements (e.g., Ba/Nb, Pb/Ce, Ba/La), providing evidence for the influence of slab-derived fluids. Moreover, these arc magmas appear to have variably equilibrated with higher pressure assemblages, including amphibole, garnet, and lesser amounts of plagioclase (Fig. 4) (Litvak et al. 2007; Jones et al. 2016).

The highest $^{87}Sr/^{86}Sr$ values and lowest εNd within the entire late OligocenelLate Miocene arc magmas are observed in the Vacas Heladas Ignimbrites rocks (Fig. 4), indicating they received the highest crustal contribution. It is suggested that these magmas represent small volumes of lower crustal melts, generated due the influence of heat and fluids derived from the subducting slab (Litvak et al. 2007; Kay et al. 1991; Kay and Abruzzi 1996; Jones et al. 2016).

Middle to late Miocene arc-related volcanism is also developed in Argentina on the eastern side of the Cordillera del Colanguil, Valle de Iglesia and western Precordillera (Fig. 2, Miocene Intrusives unit, Lomas del Campanario and Las Trancas Formation). These magmatic rocks have mainly andestic to dacitic compositions and 'arc-like' Ba/La ratios (Fig. 4). Ultimately before cessation of magmatism, volcanism migrated almost 700 km to the east of the Chilean trench, to the Pocho volcanic field in the Sierras Pampeanas. This has been associated with the arrival of the shallowly dipping subducting slab at these latitudes in the Chilean-Pampean flat-slab segment (Kay and Gordillo 1994).

5 Variable crustal contributions in late Oligocene to late Miocene magmas over the Pampean flat-slab segment based on the O and Hf isotopic composition of zircon

Geochemical features of the arc-related Miocene magmatism over the Chilean-Pampean flat-slab region show a clear increase in crustal-derived contribution from the late Oligocene to late Miocene. A major question pertains to the origin of the crustal contaminants that have influenced the trace element and isotopic compositions of the arc magmas during petrogenesis and over time.

Kay et al. (1987, 1988, 1991) and Kay and Abruzzi (1996) first correlated the chemical changes in the El Indio belt (Fig. 2) with an increase in crustal thickness, as reflected by the residual mineral assemblages equilibrating with the magmas at depth. Therefore, the main

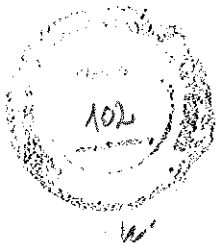

crustal contributions were related to crustal assimilation during magma ascent through the crust. On the other hand, geochemical variations in the Miocene to Pliocene volcanic suite of the El Teniente region, south of the Chilean-Pampean flat-slab (~34°), were explained by subducted sediment, along with continental crust entering the asthenospheric wedge from forearc subduction erosion (Stern and Skewes 2003; Skewes et al. 2002). Kay et al. (2005) concluded that both forearc erosion and crustal thickening are responsible for the geochemistry in the Oligocene-Miocene sequence of volcanic rocks at the latitude of the El Teniente deposit and in the northern SVZ. Moreover, trace element and isotopic ratios of Neogene andesitic magmatism in the Maricunga Belt, at the northern extreme of the Pampean flat-slab segment (~25.5°-28.2°S) were also attributed to magmas evolving under a thickened crust combined with a peak in forearc subduction erosion as the arc migrated east (Kay et al. 2013).

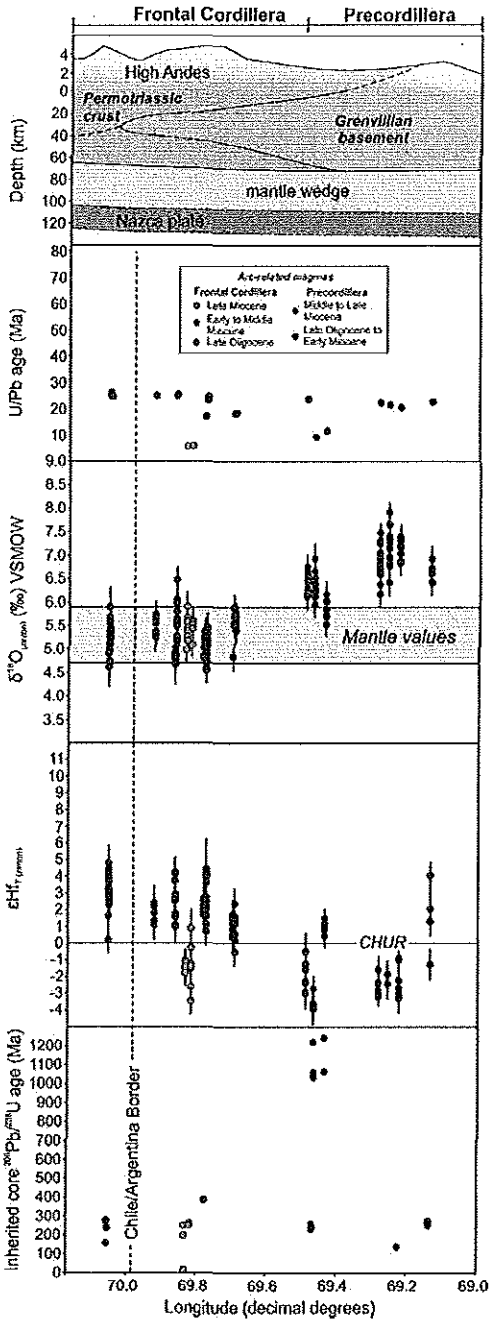

Fig. 5 Values of U-Pb crystallization ages, $\delta^{18}O_{(zircon)}$, $\varepsilon Hf_{(zircon)}$ from rims or zircons without inherited ages, and inherited $^{206}Pb/^{238}U$ core ages plotted against longitude. This demonstrates that the arc magmas have been affected by variable crustal contributions across the High Andes into the western Precodillera in the late Oligocene to late Miocene arc-related magmas over the Chilean-Pampean flat-slab segment (modified from Jones et al. 2015).

Similarly, crustal contributions in the Valle del Cura volcanic rocks have been related to both episodes of crustal thickening and increased crustal assimilation, and peaks in forearc

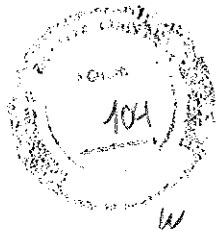

subduction erosion (Kay and Mpodozis 2002; Kay et al. 2005; Litvak et al. 2007; Jones et al. 2016).

Studies based on in-situ analysis of O and Hf isotopes in zircon combined with high resolution U-Pb dating show across arc variations in age and composition of the crustal components that influenced late Oligocene to late Miocene arc-volcanism (Jones et al. 2015). Late Oligocene to early Miocene volcanic rocks in the main arc, located in the Cordillera Frontal, show mantle-like $\delta^{18}O_{(zircon)}$ values (+4.8‰ (±0.2 (2σ)) to +5.8‰ (±0.5 (2σ))), but less radiogenic initial $\varepsilon Hf_{(zircon)}$ values than would be expected for recent mantle-derived melts (+1.0 (±1.1 (2σ)) to +4.0 (±0.6 (2σ))) compared to ~+13 (Dhuime et al. 2011). Mixing models suggest that these arc magmas are derived from the mantle and have assimilated up to ~20% Permo-Triassic basement (Jones et al. 2015). The same authors report that late Miocene rocks from the main arc in the Frontal Cordillera, together with the eastern sequences from late Oligocene to late Miocene times in the present Precordillera, require the assimilation of both the Permo-Triassic Andean crust and a Grenville-aged basement to produce the higher than mantle-like $\delta^{18}O_{(zircon)}$ values (+5.5‰ (±0.6 (2σ) to +7.2‰ (±0.4 (2σ))) and unradiogenic, initial $Hf_{(zircon)}$ values (-3.9 (±1.0 (2σ)) to +1.6 (±4.4 (2σ))) (Figure 5). It is important to notice that the isotopic variation correlates with the presence of Permo-Triassic and Grenville inherited zircon ages in the late Oligocene to late Miocene magmatic suites spanning the main Andes and Precordillera (Fig. 5). The observed isotopic changes appear to be related to their geographic position relative to the Chilean margin and the composition of the underlying basements, rather than the sample age (Fig. 5). Forearc subduction erosion might be an expected process during evolution of these arc-magmas. However, any effect derived from subducted continental material affecting the melt source region appears to have been overprinted by the assimilation of the overlying crust en route to the surface, as O and Hf isotopic across arc variations reflect the distinct basement terranes (Jones et al. 2015). Thus, at least two types of basement, that differ in age and composition, are required to generate the observed variability in the isotopic composition of the late Oligocene (~23 Ma) to late Miocene (~6 Ma) arc magmas, highlighting a period of significant crustal assimilation.

6 Geochemical signatures of back-arc magmas during middle Miocene to early Pliocene as evidence of the Payenia shallow subduction development

The geochemical evolution of calc-alkaline back-arc magmas in the present-day retro-arc of Payenia can be evaluated according to the two time intervals that reflect the expansion of arc magmatism due to the shallowing of the subducting slab: 1) the middle to late Miocene (15–10 Ma), with volcanic rocks located in the near to middle retro-arc position and 2) the latest Miocene to early Pliocene (9–3.5 Ma) middle to far retro-arc magmatic rocks.

Major element classifications show a range in composition from mid to high-K basaltic to dacitic calc-alkaline rocks (Fig. 6). Some of the rocks are rhyolitic in composition, primarily from the late Miocene Chachahuén Volcanic Complex (Kay et al. 2006a, b), conversely trachybasaltic to trachyandesitic composition have been reported for the late Miocene Palaoco volcanism (Dyhr et al. 2013b) (Fig. 6). Evidence for the influence of the subducting slab on the studied sequences is given by their Ba/Ta, La/Ta ratios, which are 'arc-like' regardless of silica content (Fig. 6). Normalized trace element patterns, also show depletions in HFSE (e.g., Nb, Ta, Zr) relative to LILE (e.g., Rb, Ba, Sr, Pb), suggesting that hydrous fluids coming from the subducted slab have enriched the melts in the asthenospheric mantle wedge. However, some geochemical differences are reported between the first volcanic stage (15–10 Ma) and the second one (9–3.5 Ma) that require changes in the geodynamic setting.

The middle to late Miocene arc-related sequences, representing the Payenia retro-arc, show lower SiO_2 vs. FeO/MgO ratios when compared to the younger sequences within this stage (particularly Charilehue samples, ~14 Ma; Spagnuolo et al. 2012), which have a more tholeiitic differentiation trend and the lowest Ba/La and La/Ta ratios (Fig. 6). Younger samples, within this older stage (Cerro Negro, Huincán I and part of II lavas, and older San Rafael volcanic rocks, ~15-10 Ma), are more 'arc-like' based on the same ratios (Fig. 6) (Nullo et al. 2002; Kay et al. 2006b; Litvak et al. 2015). Consistently, the late Miocene Palaoco volcanic sequences (Dyhr et al., 2013a) also exhibit a stronger arc-related geochemical signature when compared to the older volcanic events.

The late Miocene to early Pliocene sequences continue the general trend towards an increase in slab derived components in the retro-arc magmas with time. In particular, the youngest volcanic rocks within this stage (Early-Late Chachauhén and the younger San Rafael rocks), which represent the easternmost expression of the arc expansion, show the strongest arc-related signature when compared with earlier Miocene volcanism, based on their high Ba/Ta and La/Ta ratios (700-2000 and 27-50, respectively) (Fig. 6) (Kay et al. 2006a, b; Litvak et al. 2015).

Rare elements patterns from the whole series of middle Miocene to early Pliocene calc-alkaline back-arc magmas share a flattened overall REE pattern and similar La/Yb and Sm/Yb ratios, regardless of their silica content (Fig. 6). However, the late Miocene to early Pliocene samples show higher Sm/Yb, with the highest ratios reported for the youngest San Rafael volcanic sequences (Litvak et al. 2015; Fig. 6). This increase in Sm/Yb ratios for the arc-related retro-arc volcanism has been related to a period of back-arc crustal thickening between 12 and 10 Ma under the Neuquén Basin (Kay et al. 2006a, b; Nullo et al. 2002; Baldauf 1997). Despite this, all of the REE ratios are indicative of a low to intermediate pressure residual mineral assemblage, such as pyroxene and amphibole, in equilibrium with the Late Cenozoic magmas,

demonstrating no significant increase in crustal thickness and a garnet-free lower crust (Litvak et al. 2015).

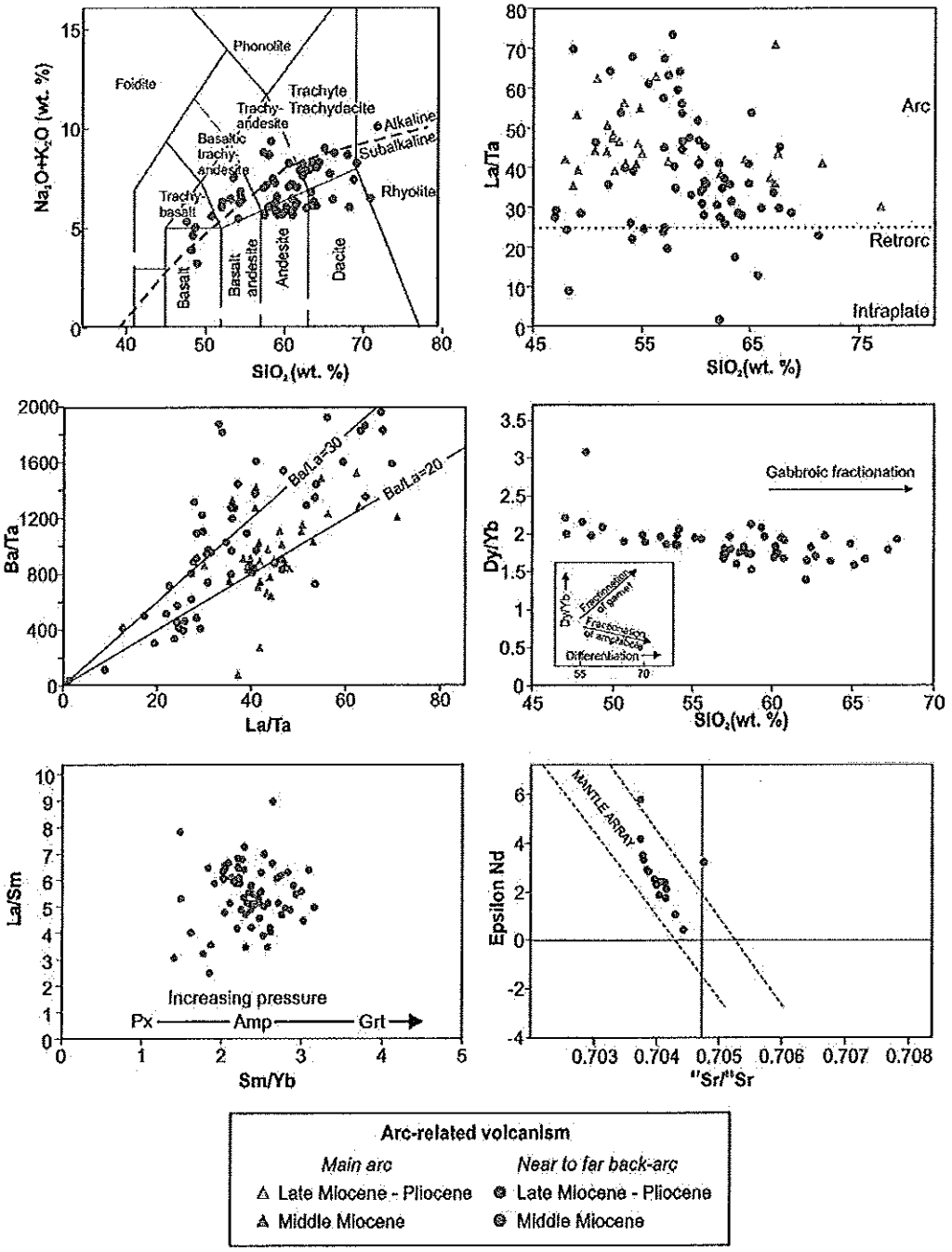

Fig. 6 Geochemical features of Late Cenozoic arc-related volcanism across the present-day Payenia retro-arc region. a) Chemical classification based on total alkali vs. silica content (Le Maitre et al. 1989); b) 'arc-like' signatures given by La/Ta vs. SiO_2; c) Ba/Ta vs. La/Ta for the Middle Miocene to Early Pliocene calc-alkaline sequences; c) REE behavior reflected in Dy/Yb vs. SiO_2; Middle Miocene to early Pliocene main arc volcanism is included (a-c) for comparison; d) Variable HREE signatures demonstrated

by La/Sm vs. Sm/Yb ratios; c) Isotopic signatures that show a limited contribution from a crustal component.. Compiled data came from Nullo et al. (2002), Kay et al. (2006a, b), Kay and Copeland (2006), Spagnuolo et al. (2012), Dyhr et al. (2013a ,b) and Litvak et al. (2015).

Lower crustal contamination was proposed as a plausible process that could explain the low REE, Cs, Rb, Th and U contents and high values of Sr and Ba, such as those seen in the more silica-rich lavas of the Late Miocene San Rafael Block, these also have Mg# similar to the more mafic lavas (Litvak et al. 2015). Kay et al. (2006b) proposed crustal contamination of the silicic samples from the early Miocene intraplate-like sequences within the Chachahuén Volcanic Complex (Vizcachas Group), based on whole rock chemistry and isotope composition. Isotopic data from the Miocene intermediate to silicic calc-alkaline retro-arc magmas show $^{87}Sr/^{86}Sr$ and εNd compositions (Fig. 6) relatively more radiogenic than the late Oligocene-early Miocene mafic back-arc alkaline-type volcanism (Kay et al. 2006a, b; Dyhr et al. 2013b). Overall, the Late Cenozoic magmas show an evolving trend with increasing $^{87}Sr/^{86}Sr$ ratios and decreasing εNd values as 'arc-like' signatures also increase. Contamination of the magmas may have occurred en route to the surface rather than by the addition of crust through forearc subduction erosion (Kay et al. 2006a, b). However, Dyhr et al. (2013) advocated a role for subduction erosion on the petrogenesis of the late Miocene arc-related rocks (Early Palaoco andesites) in the present Payenia back-arc.

7 Tectonic and geodynamic implications for the evolution of arc-related magmas over the Pampean flat-slab and Payenia shallow subduction regimes

Geochemical features of the arc-related magmatism, developed between the late Oligocene to early Pliocene in both the Chilean-Pampean flat-slab and Payenia shallow subduction segments, provide evidence to refine the geodynamic evolution of the Andean margin in the Southern Central Andes (Figs. 7 and 8).

7.1 Late Oligocene-early Miocene (~24-20 Ma)

A major tectonic reconfiguration of the Andean margin occurred in the late Oligocene (~25 Ma) by the breakup of the Farallón plate (see Chapter 14). This resulted in a change in convergence to an orthogonal direction at increased rates and a ~30° slab dip geometry (Pardo Casas and Molnar 1987; Somoza 1998; Somoza and Ghidella 2012).

In the present-day Chilean-Pampean flat-slab region, volcanic arc activity during this period (~27-18 Ma) is represented by the calc-alkaline Doña Ana Group whose parental magmas formed in the asthenospheric mantle wedge and erupted through a crust of normal thickness (30-35 km) (Fig. 7a, b). These sequences were developed in a subduction-related

setting, with an associated extensional tectonic regime, as reflected by the eruption of alkaline basalts in the retro-arc at ~21 Ma (Las Máquinas basalts; Ramos et al. 1989; Kay et al. 1991). Evidence for an extensional regime is also provided by the synextensional emplacement of volcaniclastic deposits in the former retro-arc, exposed in the Valle del Cura basin (Winocur et al. 2015).

The high-K, calc-alkaline silicic magmatism (Tillito Fm.), particularly those closer to the Chilean trench, have trace element signatures and inherited zircon grains/cores that suggest assimilation of the Permo-Triassic basement; however, this assimilation is shown to be more limited in the contemporaneous and easternmost andesitic deposits (Jones et al. 2015) (Fig. 7). Furthermore, these latter andesites show more negative $\delta^{11}B$ values (from pyroxene melt inclusions) relative to the younger Miocene arc rocks, which is consistent with a greater depth to the slab-mantle interface and is potentially related to the widening of the volcanic arc and their distal position from the trench (Jones et al. 2014). Emplacement of subvolcanic bodies associated with pyroclastic and lava flows in the western Precordillera (~22-20 Ma, Miocene Intrusives and Las Trancas Formation) provide evidence for contemporaneous, although limited, volcanic activity in the easternmost sector of the retro-arc (Fig. 7a). While volcanic arc magmas show evidence for interaction with the Permo-Triassic Andean crust, these easternmost magmas also show contributions from a Grenville-age basement, as suggested by inherited zircon ages and Hf-O isotopes (Jones et al. 2015, 2016) (Figs. 5 and 7a).

At the same time, further south in the Payenia segment, the slab dip geometry was also relatively steeply dipping due to the prevailing Andean tectonic configuration and the main arc was characterized by volcanic and volcaniclastic activity as part of the infill of the intra-arc Cura Mallín basin (Fig. 7c). Bimodal composition and trace element patterns obtained from these arc rocks reflect magmas evolving through a thin crust in an extensional setting (Kay et al. 2006a). Meanwhile, back-arc magmatism comprises a series of isotopically enriched intraplate, OIB-like basaltic flows (Kay and Copeland 2006; Dyhr et al. 2013b).

7.2 Early to middle Miocene (~19-16 Ma)

The first evidence of slab influence on the alkaline back-arc magmas in the present-day Payenia region is registered in the early to middle Miocene Huantrainco region lavas (~20-19 Ma; Fig. 7d). These show depletions in HFSE, higher La/Ta ratios and an excess of fluid-mobile elements, indicative of a more hydrous component, relative to the previously erupted lavas (Kay et al. 2006a; Dyhr et al. 2013a). As explained by these authors, the change in back-arc lava composition took place over a short period, from 23 to 18 Ma, in response to the initiation of a shallower subduction geometry, which in turn led to the cessation of extension.

By the early to middle Miocene (~19-15 Ma) in the present-day Chilean-Pampean flat-slab segment, the prevailing extensional regime was also ceasing due to the shallowing of the downgoing slab in response to the subduction of the Juan Fernandez Ridge, which arrived at the northern extreme of the segment at ~20-18 Ma (Yañez et al. 2001; Jones et al. 2014). Basaltic to andesitic lavas of early Miocene age (Escabroso Formation) were erupted along the main arc. The main arc-volcanic activity includes middle Miocene andesitic lavas (~16-14 Ma; Cerro de las Tórtolas Fm.) with clearer 'arc-like' signatures and REE ratios which indicate that they evolved through a crust of relatively normal thickness (30–35 km). The shallowing of the slab led to the migration of the volcanic front to the east and into present-day Argentina (Fig. 7b).

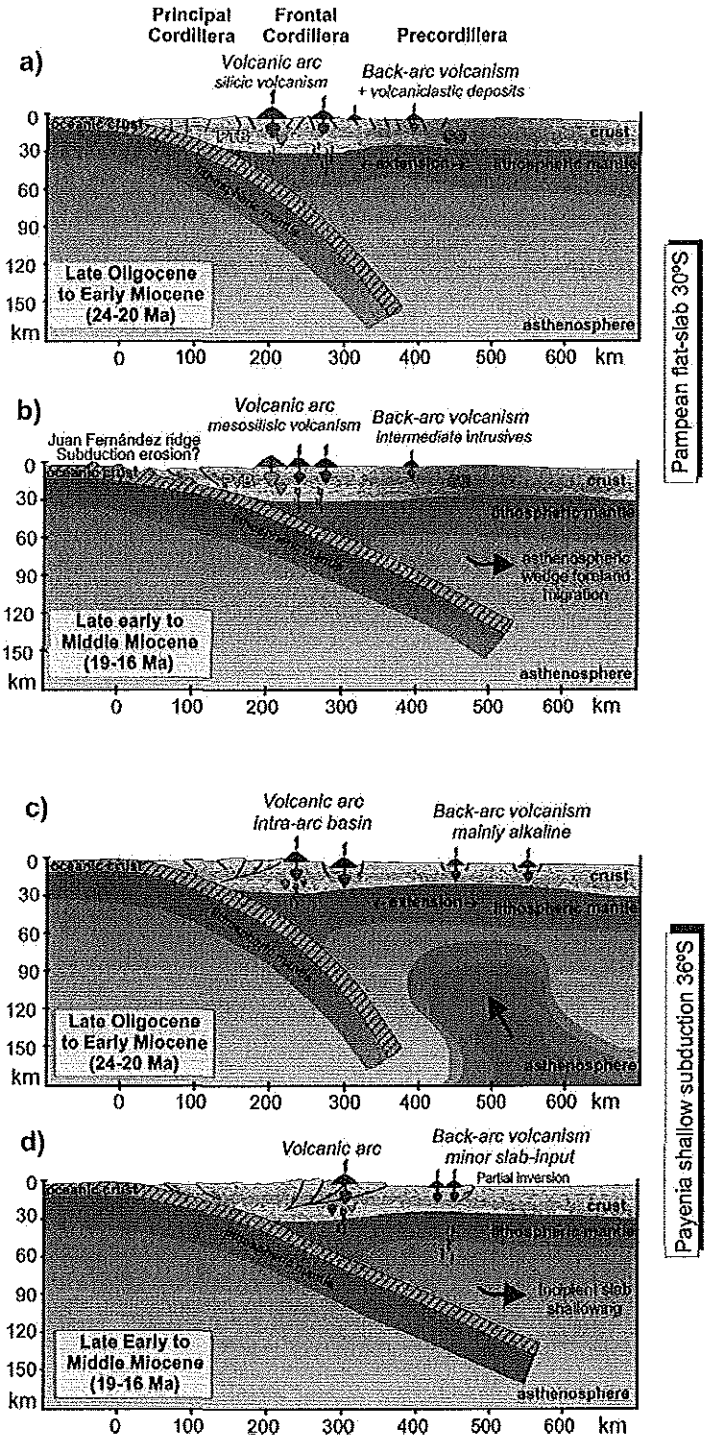

Fig. 7 Late Oligocene to middle Miocene geodynamic model and magmatic evolution for: a-b) Chilean-Pampean flat-slab segment; c-d) Payenia shallow subduction zone. PTB: Permian-Triassic basement, GB: Grenville basement (based on Kay et al. 2006a; Litvak et al. 2007, 2015; Spagnuolo et al. 2012; Jones et al. 2016).

Overall, this period of andesitic arc volcanism shows evidence for increased influence of slab-derived fluids on the melt source region and a higher degree of partial melting, in comparison to the late Oligocene. This is indicated by higher $\delta^{11}B$ values reported from Miocene melt inclusions, suggesting an increase in the influence of serpentinite-derived fluids on the source of arc magmas after ~19.5 Ma (Jones et al. 2014).

The Pampean and Payenia segments show a spatial continuity (Fig. 1), while timing of slab shallowing in both segments is contemporaneous. Thus, the collision of the Juan Fernandez Ridge is likely the cause of the progressive shallowing throughout both segments since early to middle Miocene times.

7.3 Middle to late Miocene (~10-15)

The gradual reduction of the subducted slab angle, in the present-day Chilean-Pampean flat-slab segment, led to the migration of arc magmatism to the east and the development of a compressional regime, which resulted in the main phase of uplift of the Andean range (Kurtz et al. 1997; Gregory-Wodzicki 2000). Arc volcanism is represented by the andesitic to dacitic lavas and minor dacitic pyroclastic flows (upper Cerro de las Tórtolas and Tambo Fms.) which have adakitic signatures, resulting from the equilibration of the melts with a garnet-bearing lower crust (Kay et al. 1991; Litvak et al. 2007; Jones et al. 2016). This is consistent with tectonic shortening and an increase of crustal thickness (>50 km). In addition, the asthenospheric wedge was restricted in volume below the main arc (Kay and Abruzzi 1996). Flattening of the slab is also evidenced by the eastwards migration of arc-related magmatism and the emplacement of shallow level, subvolcanic andesites and dacites in the eastern Frontal Cordillera and the western Precordillera (Tertiary Intrusives) (Fig. 8a).

Contemporaneously, arc magmatic rocks in the present-day Payenia back-arc region show an increase in slab-derived components at this time. While the main arc magmas show no significant geochemical differences to the early Miocene volcanic front (Kay et al. 2006a), retro-arc magmas from middle to late Miocene age (~15-10 Ma; Charilehue, Cerro Negro, Huincán I, part of Huincán II lavas, older San Rafael volcanic rocks and Palaoco volcanism) show a progression from initial tholeiitic to more pronounced calc-alkaline signatures (Kay et al. 2006; Dyhr et al. 2013a, b; Litvak et al. 2015). This eastern increase of slab derived components present in back-arc magmas is consistent with the progressive shallowing of the slab at these latitudes and the expansion of the arc-related activity (Fig. 8c).

7.4 Late Miocene to early Pliocene (~9-4 Ma)

As the subducting Nazca plate continued to shallow, the volcanic front and arc-related products gradually migrated to the east during the late Miocene and volcanism ceased in the flat-slab segment (e.g. Ramos et al. 1989; Kay et al. 1991; Kay and Gordillo 1994; Kay and Mpodozis 2002; Litvak et al. 2007). Minor dacitic volcanism marked the end of the main arc activity (~8-6 Ma; Vacas Heladas Ignimbrites) as the remaining fluids and heat favored the melting of the crust.

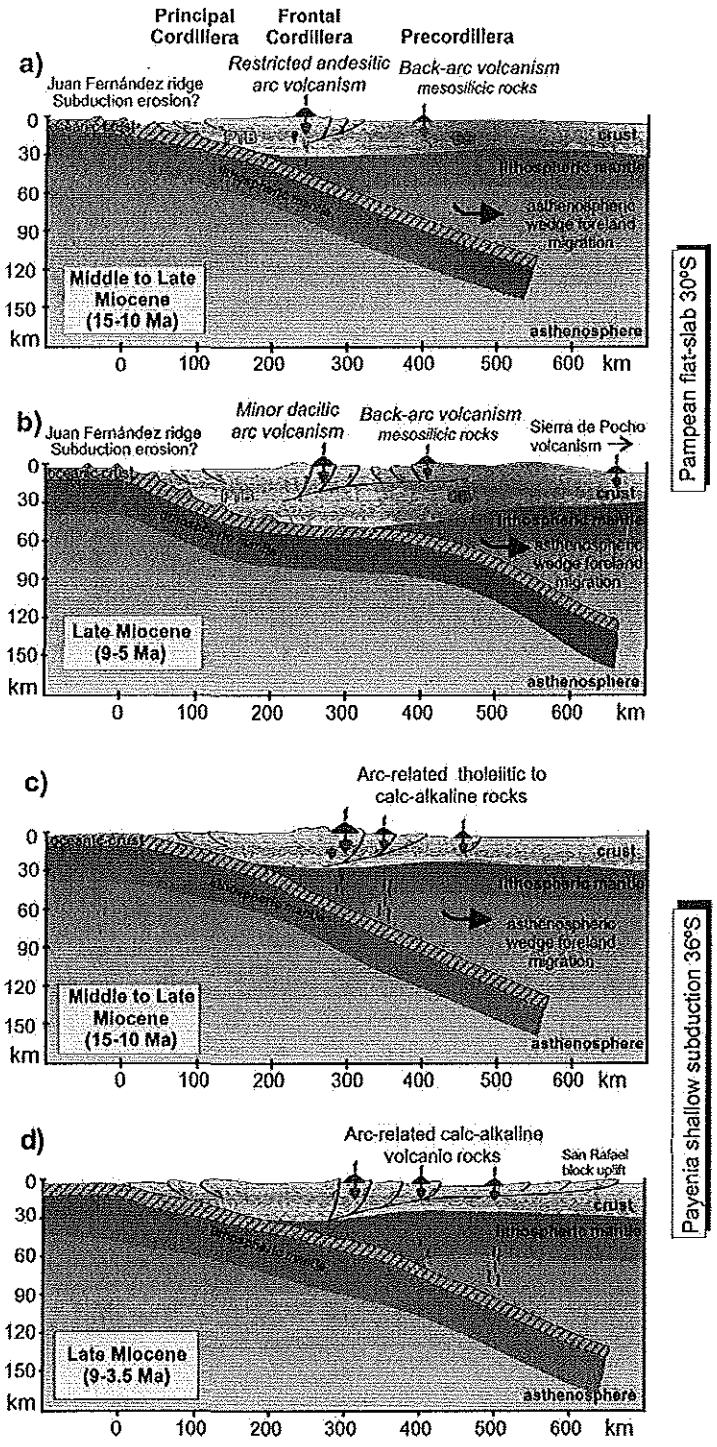

Fig. 8 Middle Miocene to early Pliocene geodynamic model and magmatic evolution over: a-b) The present-day Chilean-Pampean flat-slab segment; c-d) the Payenia shallow subduction zone. PTB: Permo-Triassic basement, GB: Grenville basement (based on Kay et al. 2006a; Litvak et al. 2007, 2015; Spagnuolo et al. 2012; Jones et al. 2016).

The O-Hf zircon isotopic compositions, together with inherited zircon ages, in these late Miocene rocks overlap the values from the magmatic rocks present in the Precordillera (Kay et al. 1991; Jones et al. 2015). This provides evidence for the presence of the Grenville-aged basement under theFrontal Cordillera in this sector of the Southern Central Andes (Jones et al. 2015) as a result of increased compression and crustal shortening in the latest Miocene, as proposed by several structural models (e.g. Allmendinger et al. 1990; Gans et al. 2011; Gilbert et al. 2006 Ramos et al. 2004). Progressive asthenospheric wedge retraction led to the migration of the arc-related products further east into the western Precordillera, and then to the Sierra de Pocho (Sierras Pampeanas, Fig. 8b), 700 km away from the Chile trench (Kay and Gordillo 1994).

The distribution of late Miocene to early Pliocene arc-related products was also progressively expanded to the east in the present-day Payenia back-arc, as consequence of the shallowing subduction regime (Fig. 8d). Arc expansion continued between 10 and 4 Ma with the extrusion of the back-arc Chachahuén Volcanic Complex and the younger San Rafael volcanic rocks; representing the easternmost expression of the calc-alkaline into the back-arc (Litvak et al. 2015; Kay et al. 2006a, b). After ~4 Ma no volcanism with clear arc-related signatures was developed in the back-arc at these latitudes. As the slab geometry changed drastically, late Pliocene to Recent back-arc volcanism comprised voluminous mafic eruptions with alkaline type geochemical fingerprints in a reinitiated extensional setting due to new steepening of the subducted Nazca plate (e.g. Ramos et al. 2014). The Juan Fernandez ridge collision with the Andean margin, and its variable influence from N to S along the Pampean and Payenia segments, could result in the subtle and progressive change in the angle of subduction around 33°S (Nacif et al. 2015). A re-steepening of the southern section of the slab might account for the different responses and evolutions of the two shallow subduction regimes in the Late Miocene to Early Pliocene times between both segments.

8 Conclusions

Arc-related magmatism in the Southern Central Andes is strongly controlled by changes in the geometry and composition of the subducted slab as reflected in the geochemical evolution of arc-related products over the late Miocene Payenia shallow subduction zone and the present-day Pampean flat-slab segment. Both segments show a progressive foreland expansion and migration of the volcanic arc, as shown by the geochemical signature of arc-related rocks, which is correlated to the more compressional style of deformation associated with the shallowing of the slab. Despite sharing this common general evolution, some differences can be appreciated between both the 'shallow' and 'flat' subduction regimes (Kay et al. 2006a, b; Litvak et al. 2015). Late Miocene shallow subduction is less pronounced in the Payenia segment, as the

easternmost expression of arc-volcanism are located 480-500 km away from the Chile trench, at ~36°S; while in the Chilean-Pampean zone, slab influence reaches almost 700 km away from the trench at ~30°S. A further and main difference between both segments is related to the increase in crustal thickness. Late Miocene magmas erupted in the main arc over the present-day Chilean-Pampean segment show geochemical features in their trace element compositions, which suggest magmas were equilibrating at the base of a thickened crust (> 50 km); however, in the Payenia shallow subduction segment the latest Miocene arc-rocks show a garnet-free residual mineral assemblages implying a crust of normal thickness (~40-45 km). Finally, while the re-steepening of the slab in the Payenia region promoted an increase of arc and retro-arc magmatism during late Neogene, the prevailing flat-slab geometry in the Chilean-Pampean segment defines the current volcanic arc gap in Southern Central Andes.

Acknowledgements

This work has been funded by grants from CONICET (grant 11220150100426CO) and University of Buenos Aires (grant UBACYT 20020150100166BA and 20020130100628BA). R. Jones was funded by a NERC CASE studentship awarded by the University of Edinburgh (NE/G524128/1), EIMF grants (IMF425/1010 and IMF450/1011), and the Derek and Maureen Moss Scholarship. L. Kirstein acknowledges the support from the Carnegie Trust for the Universities of Scotland. We thank Drs. S. Kay and P. Leal for fruitful discussion on the subject.

References

Allmenndinger R, Figueroa D, Snyder D, Beer J, Mpodozis C, Isacks B (1990) Foreland shortening and crustal balancing in the Andes at 30°S latitude. Tectonics 9: 789–809

Alonso S, Limarino CO, Litvak V, Poma S, Suriano J, Remesal M (2011) Paleogeographic, magmatic and paleoenviromental scenarios at 30°SL during the Andean Orogeny: Cross sections form the volcanic-arc to the orogenic front (San Juan province, Argentina). In: Salfity JA, Marquillas RA (eds) Cenozoic Geology of the Central Andes of Argentine. SGS Publisher, pp 23-45

Baldauf P (1997) Timing of the uplift of the Cordillera Principal, Mendoza Province, Argentina. M.S. thesis. George Washington University, p 356

Barckhausen U, Ranero CR, Cande SC, Engels M, Weinrebe W (2008) Birth of an intraoceanic spreading center. Geology 36(10): 767-770

Bermúdez A (1991) Sierra del Nevado. El límite oriental del arco volcánico del Neógeno entre los 35°30' y 36° L.S. Argentina. In: VI Congreso Geológico Chileno, Actas 1, Santiago de Chile, pp 318 – 322

Bermúdez A, Delpino D, Frey F, Saal A (1993) Los basaltos de retro-arcoextraandinos. In: Ramos VA (ed) Geología y Recursos Naturales de Mendoza, Asociación Geológica Argentina, Buenos Aires, pp 161-172

Bertotto GW, Cingolani CA, Bjerg EA (2009) Geochemical variations in Cenozoic back-arc basalts at the border of La Pampa and Mendoza provinces, Argentina. J South Am Earth Sci 28: 360-373

Bissig B, Clark AH, Rainbow A, Montgomery A (2015) Physiographic and tectonic settings of high-sulfidation epithermalgold–silver deposits of the Andes and their controls onmineralizing processes. Ore Geol Rev 65: 327-364

Bissig T, Clark AH, Lee JKW, Heather KB (2001) The Cenozoic history of volcanism and hydrothermal alteration in the Central Andean flat-slab region: New 40Ar-39Ar constrains from the El Indio-Pascua Au(-Ag, Cu) belt, 29°20-30°30" S. International Geology Review 43: 312-340

Bissig T, Clark AH, Lee JKW, von Quadt A (2003) Petrogenetic and metallogenetic responses to Miocene slab flattenig: New constrains from the El Indio-Pascua Au-Ag-Cu Belt, Chile/Argentina. Mineralium Deposita 38(7): 844-862

Burns WM, Jordan T, Copeland P, Kelley S (2006) Extensional tectonics in the Oligo-Miocene Southern Andes as recorded in the Cura-Mallín basin. In: Kay SM, Ramos VA (eds) Evolution of an Andean margin: a tectonic and magmatic view from the Andes to the Neuqén basin (35-39°S). Geological Society of America, Special paper 407, pp 163-184

Cardó R, Díaz IN (1999) Hoja Geológica 3169-I, Rodeo, Provincias de San Juan. Instituto de Geología y Recursos Minerales, Servicio Geológico Minero Argentino, Buenos Aires

Cardó R, Díaz IN, Limarino CO, Litvak VD, Poma S, Santamaria G (2007) Hoja Geológica 2969-III, Malimán, provincias de San Juan y La Rioja, Boletín 320 ed. Instituto de Geología y Recursos Minerales, Servicio Geológico Minero Argentino, Buenos Aires

Charrier R, Baeza O, Elgueta S, Flynn JJ, Gans P, Kay SM, Muñoz N, Wyss AR, Zurita E (2002) Evidence for Cenozoic extensional basin development and tectonic inversion south of the flat-slab segment, southern Central Andes, Chile (33°–36°S.L.). J South Am Earth Sci (15): 117-139

Charrier R, Pinto L, Rodríguez MP (2007) Tectonostratigraphic evolution of the Andean Orogen in Chile. In:Moreno T, Gibbons W (eds) The Geology of Chile. Geological Society of London, Special Publications pp 21–116

Chulick GS, Detweiler S, Mooney WD (2013) Seismic structure of the crust and uppermost mantle of South America and surrounding oceanic basins. J South Am Earth Sci 42: 260–276

Cobbold PR, Rosello EA (2003) Aptian to recent compressional deformation, foothills of the Neuquén Basin Argentina. Mar Petrol Geol 20:429–443

Delpino DH, Bermúdez A (1985) Volcán Plateado. Vulcanismo andesítico de retro-arco en el sector extrandino de la Provincia de Mendoza, 35°42' Lat. Sur. Argentina. In: IV Congreso Geológico Chileno, Actas 3, Antofagasta, 108-119

Dhuime B, Hawkesworth C., Cawood P (2011) When continents formed. Science 331: 154-155

Drummond MS, Defant MJ (1990) A model for trondjemite-tonalite-dacite genesis and crustal growth via slab melting: Archean to modern comparisons. J Geophys Res 95: 21503-21521

Dyhr CT, Holm PM, Llambías EJ (2013a). Geochemical constraints on the relationship between the Miocene–Pliocene volcanism and tectonics in the Palaoco and Fortunoso volcanic fields, Mendoza Region, Argentina: New insights from 40Ar/39Ar dating, Sr–Nd–Pb isotopes and trace elements. J Volcanol Geoth Res 266: 50-68

Dyhr CT, Holm PM, Llambías EJ, Scherstén A (2013b) Subduction controls on Miocene back-arc lavas from Sierra de Huantraico and La Matancilla and new 40Ar/39Ar dating from the Mendoza Region, Argentina. Lithos 179: 67-83

Folguera A, Naranjo JA, Orihashi Y, Sumino H, Nagzo K, Polanco E, Ramos VA (2009) Retro-arc volcanism in the northern San Rafael Block (34°–35°30'S), southern Central Andes: Occurrence, age, and tectonic setting. J Volcanol Geoth Res 186: 169-185

Folguera A, Orts D, Spagnuolo M, Rojas Vera E, Litvak VD, Sagripanti L, Ramos M, Ramos VA (2011) A review of Late Cretaceous to Quaternary paleogeography of the Southern Andes. Biol J Linn Soc 103: 250-268

Fromm R, Zandt G, Beck SL (2004) Crustal thickness beneath the Andes and Sierras Pampeanas at 30°S inferred from Pn apparent phase velocities. Geophys Res Lett 31: L06625

Gans CR, Beck SL, Zandt G, Gilbert H, Alvarado P, Anderson M, Linkimer L (2011) Continental and oceanic crustal structure of the Pampean flat slab region, western Argentina, using receiver function analysis: new high-resolution results. Geophys J Int 186: 45–58

Giambiagi LB, Bechis F, García V, Clark A (2005) Temporal and spatial relationship between thick- and thin-skinned deformation in the thrust front of the Malargüe fold and thrust belt, Southern Central Antes. In: VI International Symposium on Andean Geodynamics, Extended Abstracts, Niza, pp 315-318

Giambiagi L, Bechis F, García V, Clark A (2008) Temporal and spatial relationship between thick- and thin-skinned deformation in the Malargüe fold and thrust belt, Southern Central Andes. Tectonophysics 459: 123–139

Gilbert H, Beck S, Zandt G (2006) Lithospheric and upper mantle structure of central Chile and Argentina. Geophys J Int 165: 383–398

Goss AR, Kay SM, Mpodozis C (2013) Andean adakite-like high-Mg andesites on the northern margin of the Chilean–Pampean flat-slab (27–28.5° S) associated with frontal arc migration and fore-arc subduction erosion. J Petrol 54: 2193–2234

Gregory-Wodzicki KM (2000) Uplift history of the Central and Northern Andes: a review. Geol Soc Am Bulletin 112: 1091–1105

Gudnason J, Holm PM, Søager N, Llambías EJ (2012) Geochronology of the late Pliocene to recent volcanic activity in the Payenia back-arc volcanic province, Mendoza Argentina. J South Am Earth Sci 37: 191-201

Gutscher MA, Spakman W, Bijwaard H, Engdahl ER (2000) Geodynamics of flatsubduction: seismicity and tomographic constraints from the Andean margin. Tectonics190: 814–833

Hernando IR, Aragón E, Frei R, González PD, Spakman W (2014) Constrains on the origin and evolution of the magmas in the PayúnMatrú Volcanic Field, Quaternary Andean Back-arc of Western Argentina. J Petrol 55(1): 209-239

Jones RE, Hoog JC, Kirstein LA, Kasemann SA, Hinton R, Elliott T, Litvak VD, EIMF (2014) Temporal variations in the influence of the subducting slab on Central Andean arc magmas: evidence from boron isotope systematics. Earth Planet Sc Lett 408: 390-401

Jones RE, Kirstein LA, Kasemann SA, Dhuime BR, Elliott T, Litvak VD, Alsonso R, EIMF (2015) Geodynamic controls on the contamination of Cenozoic arc magmas in the southern Central Andes: Insigths from the O and Hf isotopic composition of zircon. Geochim Cosmochim Ac 164: 386-402

Jones RE, Kirstein LA, Kasemann SA, Litvak VD, Poma S, Elliott T, Alonso R, Hinton R, EIMF (2016) The role of changing geodynamics in the progressive contamination of Late Cretaceous to Late Miocene arc magmas in the southern Central Andes. Lithos 262: 169-191

Jordan TE, Isacks BL, Allmendinger RW, Brewer JA, Ramos VA, Ando CJ (1983) Andean tectonics related to geometry of subducted Nazca plate. Geol Soc Am Bull 94: 341–361

Jordan TE, Burns WM, Veiga R, Pangaro F, Copeland P, Mpodozis C (2001) Mid-Cenozoic intra-arc basins in the southern Andes. Tectonics 20. doi: 10.1029/1999TC001181

Kay SM, Abbruzzi JM (1996) Magmatic evidence for Neogene lithospheric evolution of the Central Andes "flat slab" between 30°S and 32°S.Tectonophysics 259: 15-28

Kay SM, Copeland P (2006) Early to middle Miocene back-arc magmas of the Neuquén Basin: Geochemical consequences of slab shallowing and the westward drift of South America. In: Kay SM, Ramos VA (eds) Late Cretaceous to Recent magmatism and tectonism of the Southern Andean margin at the latitude of the Neuquen basin (36-39°S). Geological Society of America, Special Paper 407, pp 185-214

Kay SM, Gordillo CE (1994) Pocho volcanic rocks and the melting of depleted continental lithosphere above a shallowly dipping subduction zone in the central Andes. Contrib Mineral Petr 117: 25-44

Kay SM, Mpodozis C (2002) Magmatism as a probe to Neogene shallowing of the Nazca plate beneath the modern Chilean flat-slab. J South Am Earth Sci 15(1): 39-57

Kay SM, Maksaev VA, Moscoso R, Mpodozis C, Nasi C (1987) Probing the evolving Andean lithosphere: Mid-late Tertiary Magmatism in Chile (29°-30°30'S) over the modern zone of subhorizontal subduction. J Geophys Res 92, 6173-6189.

Kay SM, Maksaev VA, Moscoso R, Mpodozis C, Nasi C, Gordillo CE (1988) Tertiary Andean Magmatism in Chile and Argentina between 28°S and 33°S: Correlation of magmatic chemistry with changing Benioff zone. J South Am Earth Sci 1: 21-38

Kay SM, Mpodozis C, Ramos VR, Munizaga F (1991) Magma source variations for mid-late Tertiary magmatic rocks associated with shallowing zone and thickening crust in the central Andes (28° to 33°S). In: Harmon RS, Rapela CW (eds). Andean magmatism and its tectonic setting. Geological Society of America, Special Paper 265, pp 113-137

Kay SM, Mpodozis C, Coira B (1999) Neogene magmatism, tectonism and mineral deposits of the Central Andes (22°-23° S Latitude). In: Skinner BJ (ed) Geology and Ore Deposits of the Central Andes. Soc of Economic Geol, Special Publication 7, pp 27-59

Kay SM, Godoy E, Kurtz A (2005) Episodic arc migration, crustal thickening, subduction erosion and magmatism in the South-Central Andes. Geol Soc Am Bulletin 117: 67-88.

Kay SM, Mancilla O, Copeland P (2006a) Evolution of the Back-arc Chachahuén volcanic complex at 37°S latitude over a transient Miocene shallow subduction zone under the Neuquén Basin. In: Kay SM, Ramos VA (eds) Late Cretaceous to Recent magmatism and tectonism of the Southern Andean margin at the latitude of the Neuquen basin (36-39°S). Geological Society of America, Special Paper 407, pp 215-246

Kay SM, Burns WM, Copeland P, Mancilla O (2006b) Upper Cretaceous to Holocene magmatism and evidence for transient Miocene shallowing of the Andean subduction zone under the northern Neuquén Basin. In: Kay SM, Ramos VA (eds) Late Cretaceous to Recent magmatism and tectonism of the Southern Andean margin at the latitude of the Neuquen basin (36-39°S). Geological Society of America, Special Paper 407, pp. 19-60

Kurtz AC, Kay SM, Charrier R, Farrar E (1997) Geochronology of Miocene plutons and exhumation history of the El Teniente region, Central Chile (34–35° 8). Andean Geol 24: 75–90

Le Maitre RW, Bateman P, Dudek A, Keller J, Lameyre MJ, Le Bas PA, Sabine R, Schmid H, Sorensen A, Streckeisen AR, Wooley Zanettin B (1989) A classification of igneous rocks and glossary of terms, pp. 193, Blackwell, Oxford.

Leveratto M (1976) Edad de intrusivos cenozoicos en la Precordillera de San Juan y su implicancia estratigráfica. Rev Asoc Geol Argent 31: 53–58

Limarino CO, Gutiérrez PR, Malizia D, Barreda V, Page S, Ostera H, Linares E (1999) Edad de las secuencias paleógenas y neógenas de las cordilleras de la Brea y Zancarrón, Valle del Cura, San Juan. Rev Asoc Geol Argent 54(2): 177-181

Litvak VD (2009) El volcanismo Oligoceno Superior – Mioceno Inferior del Grupo Doña Ana en la alta cordillera de San Juan. Rev Asoc Geol Argent 64(2): 200-212

Litvak VD, Page S (2002) Nueva evidencia cronológica en el Valle del Cura, provincia de San Juan. Rev Asoc Geol Argent 57(4): 483-486

Litvak VD, Poma S (2005) Estratigrafía y facies volcánicas y volcaniclásticas de la Formación Valle del Cura: magmatismo paleógeno en la Cordillera Frontal de San Juan. Rev Asoc Geol Argent 60 (2): 402-416

Litvak VD, Poma S (2010) Geochemistry of mafic Paleocene volcanic rocks in Valle del Cura region: Implications for the petrogenesis of primary mantle-derived melts over the Pampean flat-slab. J South Am Earth Sci 29(3): 705-716

Litvak VD, Poma S (2014) Petrogenesis of Miocene Volcanic arc rocks over the Chilean-Pampean flat-slab segment of the Central Andes constrained by mineral chemistry. Geologica Acta 12(2):151-171

Litvak VD, Poma S, K SM (2007) Paleogene and Neogene magmatism in the Valle del Cura region: a new perspective on the evolution of the Pampean flat slab, San Juan province, Argentina. J South Am Earth Sci 24(2-4): 117-137

Litvak VD, Spagnuolo MG, Folguera A, Poma S, Jones R, Ramos VA (2015) Late Cenozoic calc-alkaline volcanism over the Payenia shallow subduction zone, South-Central Andean back-arc (34°30-37′S), Argentina. J South Am Earth Sci 64: 365-380

Llambias EJ, Sato AM (1990) El Batolito de Colangüil (29–31° S) cordillera frontal de Argentina: estructura y marco tectonico. Andean Geol 17: 89–108

Llambías EJ, Bertotto GW, Risso C, Hernando I (2010) El volcanismo cuaternario en el retro-arco de Payenia: una revisión. Rev Asoc Geol Argent 67(2): 278-300

Maksaev V, Moscoso R, Mpodozis C, Nasi C (1984) Las unidades volcánicas y plutónicas del Cenozoico superior entre la Alta Cordillera del Norte Chico (29°-31° S), Geología, alteración hidrotermal y mineralización. Rev Geol Chile 21(1): 11-51

Martin MW, Clavero RJ, Mpodozis MC, Cuitiño L (1995) Estudio Geológico de la Franja El Indio, Cordillera de Coquimbo. Servicio Nacional de Geología y Minería, Santiago. Informe registrado IR-95-6, 1, 1-238.

McGlashan N, Brown L, Kay S (2008) Crustal thickness in the central Andes from teleseismically recorded depth phase precursors. Geophys J Int 175: 1013–1022

Mpodozis C, Kay SM (1990) Provincias magmáticas ácidas y evolucióntectónica de Gondwana: Andes chilenos (28-31°S). Andean Geol 17: 153–180

Muñoz J, Niemeyer RH (1984) Hoja Laguna del Maule, regiones del Maule y Biobio: Santiago, Chile. Servicio Nacional de Geología y Minería, Carta Geológica de Chile, no. 64, scale 1:250,000, 98 p

Muñoz Bravo J, Stern C, Bermúdez A, Delpino D, Dobbs MF, Frey FA (1989) El volcanismo plio-cuaternario a través de los 38° y 39°S de los Andes. Rev Asoc Geol Argent 44: 270–286

Muñoz M, Fuentes F, Vergara M, Aguirr L, OlovNyström J, Féraud G, Demant A (2006) Abanico East Formation: petrology and geochemistry of volcanic rocks behind the Cenozoic arc front in the Andean Cordillera, central Chile (33° 50'S). Rev Geol Chile 331: 109-140

Nacif S Triep E, Spagnotto S, Aragon E, Furlani R, Álvarez O (2015). The flat to normal subduction transition study to obtain the Nazca plate morphology using high resolution seismicity data fromthe Nazca plate in Central Chile. Tectonophysics 657: 102-112

Nasi CP, Moscoso RD, Maksaev VJ (1990) Hoja Guanta, Región de Coquimbo. Carta Geológica de Chile N° 67. Santiago de Chile, Servicio de Geología y Minería, 140 p

Niemeyer RH, Muñoz J (1983) Hoja Laguna de la Laja, Región del Bio Bio: Santiago, Chile. Servicio Nacional de Geología y Minería, Carta Geológica de Chile, no. 57, scale 1:250,000, 52 p

Nullo FE, Stephens G, Otamendi J, Baldauf P (2002) El volcanismo del Terciario superior del sur de Mendoza. Rev Asoc Geol Argent 57(2): 119-132

Nullo FE, Franchi M, González P, Herrero JC, Reinoso MS (1993). Mapa Geológico de la Provincia de Río Negro. Dirección Nacional del Servicio Geológico, Buenos Aires.

Nullo FE, Panza JL, Blasco G (1999) El Jurásico y Cretácico de la Cuenca Austral. In: Caminos R (ed) Geología Argentina. Servicio Geológico Minero Argentino, pp 528- 535

Ostera H, Linares E, Haller M (1999) Paramillos Altos intrusive belt, Southern Mendoza, Argentina. Ages, chemical and isotopic constraints. In: II South American Symposium on Isotope Geology, Actas 2, Córdoba, pp 256-260

Otamendi J, Nullo F, Godeas M, Pezzutti N (1994) Petrogenesis del volcanismo terciario del Valle del Cura, San Juan, Argentina. In: VII Congreso Geológico Chileno, Actas 2, Concepción, pp 1130-1135

Parada MA, Rivano S, Sepulveda P, Herve M, Herve F, Puig A, Munizaga F, Brook M, Pankhurst R, Snelling N (1988) Mesozoic and Cenozoic plutonic developmentin the Andes of central Chile (30°30′–32°30′S). J South Am Earth Sci 1: 249-260

Pardo Casas F, Molnar P (1987) Relative motion of the Nazca (Farallón) and South America plates since Late Cretaceous time. Tectonics 6: 233-248

Pilger RH (1981) Plate reconstructions, aseismic ridges, and low angle subduction beneath the Andes. Geol Soc Am Bulletin 92: 448-456

Pilger RH (1984) Cenozoic plate kinematics, subduction and magmatism: South American Andes. J Geol Soc Lond 141: 793-802.

Pineda G, Emparan C (2006) Geología del área Vicuña-Pichasca, Región de Coquimbo. Carta Geológica de Chile, Serie Geología Básica. Servicio Nacional de Geología y Minería, Santiago

Poma S, Limarino C, Litvak V (2005) Formación Las Trancas: expresión del arcomagmático terciario en el faldeo occidental de la Precordilera de San Juan. In: XVI Congreso Geológico Argentino Actas 1, La Plata, pp 331–334

Poma S, Ramos A, Litvak VD, Quenardelle S, Maisonnave B (2014). Tertiary volcanism from Iglesia Valley Basin, San Juan Province, Argentina. In: XIX Congreso Geológico Argentino, Actas CD, Córdoba, 2 p

Quidelleur X, Carlut J, Tchilinguirian P, Germa A, Gillot PY (2009) Paleomagnetic directions from mid-latitude sites in the southern hemisphere (Argentina): contribution to time averaged field models. Phys Earth Planet Inter 172: 199-209.

Radic JP, Rojas L, Carpinelli A, Zurita E (2002) Evolución Tectónica de la cuenca Terciaria de Cura-Mallín Región Cordillerana Chileno Argentina (36°30′-39°00′S). In: XIV Congreso Geológico Argentino, Actas 3, Calafate, pp 233-237

Ramos VA, Barbieri M (1989) El volcanismo cenozoico de Huantraico: edad y relaciones isotópicas iniciales, provincia del Neuquén. Rev Asoc Geol Argent 43: 210-223

Ramos VA, Folguera A (2005) Tectonic evolution of the Andes of Neuquén: Constraints derived from the magmatic arc and foreland deformation. In Veiga G, Spalletti L, Howell J, Schwarz E (eds) The Neuquén Basin: A case study in sequence stratigraphy and basin dynamics. Geological Society of London, Special Publication 252, pp 15-35

Ramos VA, Folguera A (2011) Payenia volcanic province in the Southern Andes: An appraisal of an exceptional Quaternary tectonic setting. J Volcanol Geoth Res 201: 53-64

Ramos VA, Page R, Kay S, Lapido O, Delpino D (1987) Geología de la región del Volcán Tórtolas, Valle del Cura, provincia de San Juan. In: X° Congreso Geológico Argentino, Actas IV, Tucumán, pp 260- 263

Ramos VA, Kay SM, Page R, Munizaga F (1989). La Ignimbrita Vacas Heladas y el cese del volcanismo en el Valle del Cura, provincia de San Juan. Rev Asoc Geol Argent 44(1-2): 336-352

Ramos VA, Cristallini EO, Pérez DJ (2002) The Pampean flat-slab of the Central Andes. J South Am Earth Sci 15(1): 59-78

Ramos VA, Zapata T, Cristallini E, Introcaso A (2004) The Andean thrust system—latitudinal variations in structural styles and orogenic shortening. Thrust Tectonics and Hydrocarbon Systems 82: 30-50

Ramos VA, Folguera A, Litvak VD, Spagnuolo M (2014) Andean tectonic cycle: From crustal thickening to extension in a thin crust (34°-37°SL). Geoscience Frontiers 5: 351-367

Skewes MA, Arévalo A, Floody R, Zuñiga H, Stern CR (2002) The giant El Teniente breccia deposit: hypogene copper distribution and emplacement. Society of Economic Geologists Special Publication 9: 299-332

Søager N, Holm PM, Llambías EJ (2013) Payenia volcanic province, southern Mendoza, Argentina: OIB mantle upwelling in a back-arc environment. Chem Geol 349-350:36-53

Somoza R (1998) Updated azca (Farallon)—South America relative motions during the last 40 My: implications for mountain building in the central Andean region. J South Am Earth Sci 11: 211–215

Somoza R, Ghidella ME (2012) Late Cretaceous to recent platemotions in western South America revisited. Earth Planet Sc Lett 331–332: 152–163

Spagnuolo M, Litvak VD, Folguera A, Ramos VA (2012) Neogene magmatic expansion and mountain building at the southern Central Andes, 36°-37°S, Argentina. J Geodyn 53: 81-94

Sruoga P, Rubinstein NA, Etcheverría MP, Cegarra M, Kay SM, Singer B, Lee J (2008) Estadio inicial del arco volcánico neógeno en la Cordillera Principal de Mendoza (35°S). Rev Asoc Geol Argent 63 (3): 454-469

Stern CR, Skewes MA (2003) Generation of giant Miocene and Pliocene copper deposits in Central Chile: Role of ridge subduction, decreased subduction angle, increased subduction erosion, crustal thickening, and mafic and adakite-like dacitic magma within long-lived, batholith size, open system magma chambers. In: X Congreso Geológico Chileno, Actas CD, Concepción.

Suárez M, Emparan C (1995) The stratigraphy, geochronologyand paleophysiography of a Miocenefreshwater interarc basin, Southern Chile. J. S. Am. Earth Sci. 8: 17-31

Wetten AF (2005) Andesita Cerro Bola: Nueva unidad vinculada al magmatismo mioceno de la Cordillera de Olivares, San Juan, Argentina (30° 35′ S; 69° 30′ O). Rev Asoc Geol Argent 60: 003-008

Winocur DA, Litvak V, Ramos VA (2015) Magmatic and tectonic evolution of the Oligocene Valle del Cura basin, Main Andes of Argentina and Chile: Evidence for generalized extension. Geological Society of London, Special Publications 399, pp 109-130

Yañez GA, Ranero CR, von Huene R, Díaz J (2001) Magnetic anomaly interpretation across the southern central Andes (32°–34°): the role of the Juan Fernández Ridge in the late Tertiary evolution of the margin. J Geophys Res106(B4): 6325-6345

Yañez GA, Cembrano J, Pardo M, Ranero CR, Selles D (2002) The Challenger–Juan Fernández–Maipo major tectonic transition of the Nazca–Andean subduction system at 33–34°S: geodynamic evidence and implications. J South Am Earth Sci 15: 28-38

GRANITOIDES Y DEFORMACION DURANTE LA OROGENIA TRANSAMAZONIANA EN TANDILIA, PROVINCIA DE BUENOS AIRES, ARGENTINA

Ramos, A.[1] y Poma, S.[2]

[1] *IGEBA (UBA-CONICET) Departamento de Geología, FCEyN-UBA. Buenos Aires. amramos@gl.fcen.uba.ar*
[2] *IGEBA (UBA-CONICET) Departamento de Geología, FCEyN-UBA. Buenos Aires. stella@gl.fcen.uba.ar*

El objetivo de este trabajo es destacar la importancia de la deformación en la evolución del basamento cristalino de Tandilia, provincia de Buenos Aires, Argentina (Fig.1). El basamento está constituido principalmente por migmatitas, gneises, esquistos, granitoides, diques ácidos, pegmatíticos, diques máficos y ultramáficos y escasos mármoles. Estas rocas fueron afectadas por eventos de metamorfismo y deformación durante distintos pulsos de la Orogenia Transamazoniana (2300-1700 Ma). Fueron reconocidas importantes zonas o fajas de cizalla con formación de milonitas y ultramilonitas (González Bonorino et al. 1956; Teruggi et al. 1973; Dalla Salda et al. 1981, 1992 y Frisicale et al. 1999). Gran parte del basamento cristalino de este extremo sur del cratón del Río de la Plata está cubierto por rocas sedimentarias del Neoproterozoico. Una síntesis completa de la geología fue publicada por Dalla Salda et al. (2006) y Cingolani (2011) presentó una actualización del conocimiento geológico de Tandilia. El área estudiada comprende la zona de las antiguas canteras Villa Mónica, Sierra Chica, Cerro Sotuyo. San Nicolás y Cerro El Peregrino, en los alrededores de la ciudad de Olavarría, región occidental de las Sierras de Tandilia. En los frentes de canteras se observan gneises deformados con bandeamiento y pasaje transicional a migmatitas y granitoides. Estudios previos de Pankhurst et al. (2003) determinaron edades Sm-Nd de 2100-2200 Ma para el emplazamiento de granitoides sincolisionales a postorogénicos, con edades modelo promedio de 2600 Ma. En un diagrama geoquímico de discriminación tectónica, las composiciones de estas rocas se ubican dentro de la zona que corresponde a un ambiente relacionado con subducción, pudiéndose establecer una secuencia de eventos que culminaron con deformación y anatexis durante la fase colisional y postorogénica (Pankhurst et al. 2003). Durante la evolución orogénica, los gneises fueron afectados por metamorfismo de facies anfibolita y granulita asociado con procesos de fusión parcial, acumulación y migración de fundidos leucocráticos cuarzo-feldespáticos, con progresiva generación de migmatitas y granitoides anatécticos (Ramos y Poma, 2013). Los gneises presentan bandeamiento discontinuo, acentuado por diferencias de color (rosado a gris verdoso) vinculado con la mineralogía dominante (feldespato alcalino y/o plagioclasa, anfíbol y biotita). Están atravesados por venas y diques de composición leucogranítica. El espesor de las bandas varía desde mm hasta pocos metros.

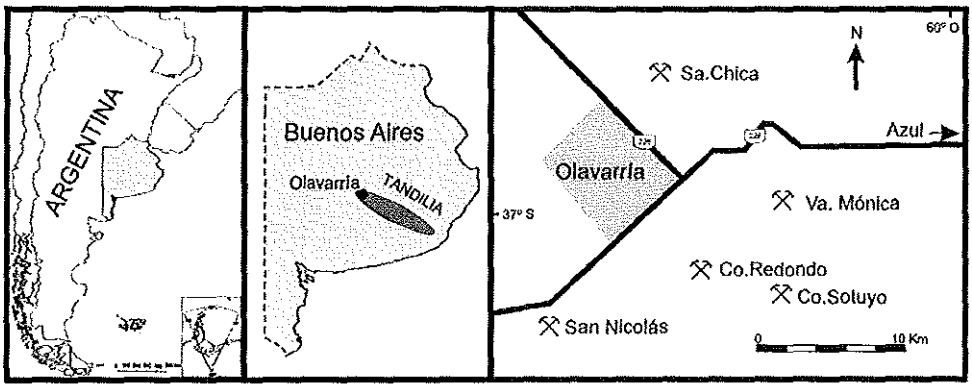

Figura 1. Ubicación de la zona de estudio

Las migmatitas son metatexitas, diatexitas con schlieren y estructuras nebulíticas y diatexitas masivas. En las metatexitas se distinguen bandas de leucosomas cuarzo-feldespáticos que alternan con delgadas bandas de melanosomas con anfíbol y biotita y ocasionales relictos de paleosoma, remanentes de la granulita original modificada, con piroxeno reemplazado por anfíbol y biotita y gran cantidad de nódulos de magnetita (Ramos y Poma, 2013). Estos enclaves máficos (restitas) son generalmente elipsoidales, están parcialmente disgregados y sus minerales se encuentran dispersos en el leucosoma. Las diatexitas evolucionan a partir de las metatexitas, con lentes o parches irregulares y venas de leucosomas cuarzo-feldespáticos; es común el desarrollo de estructuras nebulíticas y schlieren con delgadas bandas ricas en anfíbol y biotita. Las diatexitas masivas son texturalmente más homogéneas y presentan contactos transicionales con venas y diques de granitoides anatécticos leucocráticos de espesores irregulares y composición promedio granodiorítica. Se observan algunos

delgados diques discordantes de pegmatitas. A escala microscópica se reconoce una transición entre textura granoblástica y granosa con texturas de deformación cataclástica, milonitica y blastomilonítica, marcada recristalización y retrogresión mineralógica en granulitas y migmatitas. La presencia de texturas miloníticas relícticas y texturas cataclásticas sobreimpuestas a deformaciones y recristalizaciones mineralógicas previas, son evidencia de más de un evento de deformación (Ramos y Poma, 2013).

La zona de estudio está localizada en el extremo occidental de la Mega Cizalla de Azul, faja de cizalla de dirección E-O (Frisicale et al. 1999). En las zonas de cizalla se desarrollan estructuras que favorecen la infiltración de grandes volúmenes de fluidos acuosos que promueven recristalización y metasomatismo con enriquecimiento en sílice (Doyle y Cartwright, 2000). El sucesivo pasaje ó retrogresión metamórfica de piroxeno a anfíbol y a biotita estaría facilitado por la incorporación de fluidos acuosos. Por lo tanto, los relictos de piroxeno entre parches de anfíbol o biotita son evidencia de la mineralogía previa, hidratada por fluidos expulsados durante la cristalización del magma leucogranitico invasivo (Morfin et al., 2013). Por otro lado, estudios sobre granitoides archeanos sin o post-tectónicos sugieren que su origen podría ser consecuencia del metasomatismo asociado con migración de fluidos en zonas de cizalla (López et al. 2005).

Existe una transformación progresiva desde gneises, metatexitas y diatexitas hacia los granitoides. La principal diferencia entre las metatexitas y las diatexitas es estructural y la transición entre ambas es consecuencia del aumento en la participación de fundidos leucocráticos. Este aumento en la contribución de fundidos pudo ser originado por la mayor circulación de fluidos acuosos a través de zonas de cizalla, dando origen a diatexitas masivas leucocráticas, sin relictos de estructuras schlieren (White et al., 2005; Maki et al., 2014 y referencias). Estas características estructurales permiten interpretar que la deformación favoreció la segregación y migración de fundidos durante la evolución orogénica (Toe, et al., 2013).

Durante la orogenia Transamazoniana los procesos de fusión parcial, acompañados por acumulación y/o movilidad de fundidos leucocráticos intervinieron en la evolución de migmatitas y dieron origen al conjunto de granitoides heterogéneos y de leucogranitos emplazados en distintos niveles estructurales de las Sierras de Tandilia (Ramos y Poma, 2013 y referencias). Observaciones similares fueron realizadas en otras localidades de Tandilia, en afloramientos preservados de la explotación en canteras y en los que se han distinguido estructuras de domos de granitoides que pasan sucesivamente a diatexitas y luego a metatexitas en franjas milonitizadas, indicando la evolución progresiva entre migmatitas y granitoides en zonas de intensa deformación orogénica.

TRABAJOS CITADOS EN EL TEXTO

Cingolani, C.A. 2011. The Tandilia System of Argentina as a southern extension of the Río de la Plata craton: an overview. International Journal Earth Sciences (Geologische Rundschau) 100: 221-242.

Dalla Salda, L. 1981. Tandilia, un ejemplo de tectónica de transcurrencia en basamento. Revista de la Asociación Geológica Argentina 43, 2: 198-209.

Dalla Salda, L.H., Franzese, J.R., Posadas, V.G. 1992. The 1800 Ma Mylonite-Anatectic Granitoid Association in Tandilia, Argentina. Basement Tectonics 7. Proceedings of the International Conferences on Basement Tectonics. 1: 161-174.

Dalla Salda, L., Spalletti, L., Poiré, D., De Barrio, R., Echeveste, H., Benialgo, A. 2006. Tandilia. Temas de Geología Argentina I. INSUGEO, Serie Correlación Geológica 21: 17-46. Tucumán.

Doyle, C., Cartwright, I. 2000. The role of fluids in retrograde shearing: Broken Hill, Australia. Journal of Geochemical Exploration 69-70: 575-579.

Frisicale, M.C., Dimieri, L.V., Dristas, J.A. 1999. Megacizalla en Boca de la Sierra, Tandilia: Convergencia normal? XIV Congreso Geológico Argentino 1, 168–171.

González Bonorino, F., Zardini, R., Figueroa, M., Limousin, T. 1956. Estudio geológico de las Sierras de Olavarría y Azul (Provincia de Buenos Aires). Lemit, Serie 2, 63: 1-22.

López, S. A., Castro, A. García-Casco, 2005. Production of granodiorite melt by interaction between hydrous mafic magma and tonalitic crust. Experimental constraints and implications for the generation of Archaean TTG complexes. Lithos 79: 229-250.

Maki, K., Yui, T-F., Miyazaki, K., Fukuyama, M., Wang, K-L., Martens, U., Grove, M. and Liou, J. G. 2014. Petrogenesis of metatexite and diatexite migmatites determined using zircon U–Pb age, trace element and Hf isotope data, Higo metamorphic terrane, central Kyushu, Japan. Journal of Metamorphic Geology 32: 301-323.

Morfin, S., Sawyer, E.W., Bandyayera, D. 2013. Large volumes of anatectic melt retained in granulite facies migmatites: An injection complex in northern Quebec. Lithos 168-169: 200-218.

Pankhurst, R.J., Ramos, A., Linares, E. 2003. Antiquity of the Rio de la Plata craton in Tandilia, southern Buenos Aires province, Argentina. Journal of South American Earth Sciences 16, 1: 5-13.

Ramos, A., Poma, S. 2013. Evidencias de mezcla de magmas en migmatitas de Tandilia, Provincia de Buenos Aires, Argentina. 11° Congreso de Mineralogía y Metalogenia. Facultad de Ciencias Exactas, Físicas y Naturales. UNSJ. Actas: 341-346.

Teruggi, M.E., Kilmurray, J.O., Dalla Salda, L. 1973. Los dominios tectónicos de la región de Tandil. Anales de la Sociedad Científica Argentina 95, 1-2: 81-96.

Toe, W., Vanderhaeghe, O., André-Mayer, A.-S., Feybesse, J.-L., Milési, J. P. 2013. From migmatites to granites in the Pan-African Damara orogenic belt, Namibia. Journal of African Earth Sciences 85: 62-74.

White, R., W., N. E. Pomroy and R. Powell, 2005. An in situ metatexite diatexite transition in upper amphibolite facies rocks from Broken Hill, Australia. Journal of Metamorphic Geology 23, 7: 579-602.

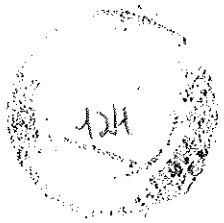

Soraya Amar Nimer **andeangeology@sernageomin.cl**

20/1
2/16

para mí

inglés
español

Traducir mensaje

Desactivar para: inglés

Dra Stella Poma:

Thank you for submitting the manuscript, "Southern Central Andes Neogene Back Arc Magmatism Over the Pampean Flat Slab: Implications on Crustal and Slab Melts Contribution to Magma Generation in Precordillera, Western Argentina" to Andean Geology. With the online journal management system that we are using, you will be able to track its progress through the editorial process by logging in to the journal web site:

Manuscript URL:
http://www.andeangeology.cl/index.php/revista1/author/submission/3025
Username: stellapoma

If you have any questions, please contact me. Thank you for considering this journal as a venue for your work.

Paper en arbitraje

Stella Poma

Soraya Amar Nimer andeangeology@sernageomin.cl a través de biblioteca.ucv.cl 20/12/16
para mí

inglés español Traducir mensaje Desactivar para: inglés

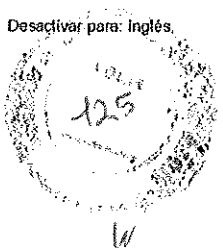

Dra Stella Poma:

Thank you for submitting the manuscript, "Southern Central Andes Neogene Back Arc Magmatism Over the Pampean Flat Slab: Implications on Crustal and Slab Melts Contribution to Magma Generation in Precordillera, Western Argentina" to Andean Geology. With the online journal management system that we are using, you will be able to track its progress through the editorial process by logging in to the journal web site:

Manuscript URL:
http://www.andeangeology.cl/index.php/revista1/author/submission/3025
Username: stellapoma

If you have any questions, please contact me. Thank you for considering this journal as a venue for your work.

Carátula de la tesis

126

UNIVERSIDAD DE BUENOS AIRES

Facultad de Ciencias Exactas y Naturales

Departamento de Ciencias Geológicas

Petrología y evolución del volcanismo Neógeno y Cuaternario al sur de 24° LS y al Oeste de 67°30'O, Puna, Provincia de Salta, Argentina

Tesis presentada para optar al título de Doctor de la Universidad de Buenos Aires en el área de Ciencias Geológicas

Emma Beatriz Maisonnave

Directora de Tesis: Dra. Stella Poma

Consejera de Estudios: Dra. Stella Poma

Buenos Aires, octubre de 2015

Fecha de Defensa: 8 de abril de 2016

Ref.: Exp. (FCEN) Nº 505.103/15

Ciudad de Buenos Aires, 10 ABR 2017

VISTO lo dispuesto en el artículo 50º del Estatuto Universitario que instituye el Año Sabático para profesores regulares de la Universidad,

CONSIDERANDO:

Que por Resolución CD Nº 1716/15 se solicitó al Consejo Superior se autorice a la Dra. Stella Maris Norma Poma, Profesora Regular Asociada con dedicación exclusiva del Departamento de Ciencias Geológicas a hacer uso del Año Sabático,

Que por Resolución CS Nº 3596/15 se aprobó dicha solicitud otorgando licencia entre el 1 de febrero de 2016 y hasta el 31 de diciembre de 2016,

Que en cumplimiento con el Art. 12º de la Resolución CS Nº 4518/93, la Dra. Stella Maris Norma Poma presentó su informe de actividades,

Que es necesario cumplir con lo establecido por los Art. 13º y 14º de la citada resolución,

Lo aconsejado por la Comisión de Enseñanza, Programas y Planes de Estudio,

Lo actuado por este cuerpo en la sesión realizada en el día de la fecha,

En uso de las atribuciones que le confiere el art. 113º del Estatuto Universitario,

EL CONSEJO DIRECTIVO DE LA FACULTAD DE CIENCIAS EXACTAS Y NATURALES
RESUELVE:

Artículo 1º: Aprobar el informe correspondiente a las actividades desempeñadas por la Dra. Stella Maris Norma Poma durante su Año Sabático.

Artículo 2º: : Enviar un ejemplar del informe a la Biblioteca de esta Facultad.

Artículo 3º: Regístrese, notifíquese a quienes corresponda, elévese al Consejo Superior y cumplido, archívese.

RESOLUCIÓN CD Nº 0565

Dr. JORGE ZILBER
SECRETARIO ACADEMICO ADJUNTO

Dr. JUAN CARLOS REBOREDA
DECANO